The Vascular and Anti-inflammatory Activity of Cyanidin-3-Glucoside and its Metabolites in Human Vascular Endothelial Cells

A Thesis Presented to

Norwich Medical School

In Fulfilment of the Requirement for the Degree of

Doctor of Philosophy

By

Hiren P. Amin (MSc)

June 2015

Abstract

High dietary consumption of anthocyanins has been associated with a reduced risk of cardiovascular disease (CVD), which is supported by evidence from human, animal and *in vitro* studies. However, owing to anthocyanins' poor bioavailability and extensive metabolism, it is likely their metabolites are responsible for their reported health effects; yet the bioactivity of anthocyanin metabolites remains largely unknown. This thesis aimed to address this deficiency in current scientific literature by investigating the vascular and anti-inflammatory activity of cyanidin-3-glucoside (C3G), the most abundant anthocyanin in the UK diet, and 11 of its recently identified metabolites (including six synthetic metabolites) at physiological concentrations (0.1 – 10 μM) in a human endothelial cell model. Here protein and mRNA levels were established using ELISA and RT-qPCR, superoxide levels were quantified by spectrophotometric measure of cytochrome c reduction and electron paramagnetic resonancespectroscopy, and nuclear factor kappa B (NF-κB) activation was established by flow cytometry. The data indicate that C3G, its A-ring degradant, phloroglucinaldehyde (PGA), and its phase II metabolite vanillic acid (VA) increased the basal expression of endothelial nitric oxide synthase (eNOS) by between 1.5-to-3 fold ($p<0.05$). In contrast, none of the compounds tested modulated angiotensin II (Ang II)-stimulated superoxide production and basal endothelin-1 expression in endothelial cells. Anti-inflammatory activity of the treatments was characterised by their effects upon oxidised low density lipoprotein (oxLDL) and cluster of differentiation 40 ligand (CD40L) stimulated expression of vascular cell adhesion molecule-1 (VCAM-1) and interleukin-6 (IL-6) in endothelial cells. Here, significant bioactivity of C3G metabolites was observed, as 7 out of 12 of the tested treatments reduced CD40L-induced VCAM-1 expression up to 65% (relative to control, $p<0.05$), eight compounds reduced CD40L-induced IL-6 production up to 95% (relative to control, $p<0.05$), and nine compounds reduced oxLDL-induced IL-6 protein secretion up to 99% of control incubations ($p<0.05$). Protocatechuic acid (PCA) and VA reduced VCAM-1 and IL-6 protein and mRNA levels under both stimulation conditions, and were therefore selected for further targeted investigation of transcription factor activity. Here IL-1β-induced activation of nuclear factor-kappa B (NF-κB) was significantly reduced by both PCA and VA ($p<0.05$). Therefore, anthocyanin metabolites appear to exert their effects on inflammatory chemokines through attenuation of NF-κB p65 phosphorylation in endothelial cells. In summary, the beneficial effects of anthocyanins *in*

vivo may arise, in part, from the anti-inflammatory activity of their metabolites, as the metabolites displayed significant anti-inflammatory activity and are found in the circulation at considerably higher concentrations than their unmetabolised precursor structures, hence likely contributing to the observed vascular activity in humans. These findings provide novel insight to bioactivity of anthocyanins and extend current knowledge in the field of anthocyanin research.

Table of contents

List of Tables

List of Figures

List of Abbreviations

ADMA	Asymmetric dimethylarginine
ANOVA	Analysis of variance
ATP	Adenosine triphosphate
BAEC	Bovine aortic endothelial cells
BCA	Bicinchoninic acid
BH4	Tetrahydrobiopterin
BSA	Bovine serum albumin
cGMP	Cyclic guanosine monophosphate
C3G	Cyanidin-3-glucoside
CBG	Cytosolic B-glucosidase
CD40	Cluster of differentiation 40
CD40L	CD40 ligand
CHD	Coronary heart disease
COX-2	Cyclo-oxygenase-2
CPH	1-Hydroxy-3-carboxy- 2,2,5,5-tetramethylpyrrolidine
CVD	Cardiovascular disease
CVS	Cardiovascular system
DMSO	Dimethyl sulphoxide
(c)DNA	(complementary) deoxyribonucleic acid
DNase	Deoxyribonuclease
dNTP	Deoxyribonucleotide triphosphate
DUOX	Dual oxidases
EC	Endothelial cell
EDRF	Endothelium-derived relaxing factor
EDTA	Ethylene diamine tetra acetate
ELISA	Enzyme-linked immunosorbent assay
EPR	Electron paramagnetic resonance
ERK	extracellular-signal-regulated kinases
ET-1	Endothelin-1
eNOS	Endothelial nitric oxide synthase

FAD	Flavin adenine dinucleotide
FBS	Foetal bovine serum
FCS	Foetal calf serum
FMN	Flavin mononucleotide
GTP	Guanosine triphosphate
HO	Haem oxygenase
HCAEC	Human coronary artery endothelial cell
HUVEC	Human umbilical vein endothelial cell
ICAM-1	Intercellular adhesion molecule-1
IL-1β	Interleukin-1 beta
IL-6	Interleukin – 6
IκB	Inhibitor of κB (inhibitory protein)
IκK	IκB kinase
iNOS	Inducible nitric oxide synthase
IVA	Isovanillic acid
JNK	c-Jun N-terminal kinase
LDL	Low density lipoprotein
LOX-1	Lectin-like low-density lipoprotein receptor-1
LPH	Lactase phloridzin hydrolase
LPS	Lipopolysaccharide
MAEC	Mouse aortic endothelial cell
MAPK	Mitogen-activated protein kinase
mRNA	Messenger ribonucleic acid
NADH	Nicotinamide adenine dinucleotide
NADPH	Nicotinamide adenine dinucleotide phosphate
NF-κB	Nuclear factor kappa B
NO	Nitric oxide
nNOS	Neuronal nitric oxide synthase
NOX	NAD(P)H oxidase
PBS	Phosphate buffered saline
PGA	Phloroglucinaldehyde
PCA	Protocatechuic acid
Pg3G	Pelargonidin-3-glucoside

Pn3G	Peonidin-3-glucoside
Pt3G	Petunidin-3-glucoside
RNase	Ribonuclease
RNS	Reactive nitrogen species
ROS	Reactive oxygen species
RT-qPCR	Quantitative reverse transcription polymerasechainreaction
SD	Standard deviation
SGLT	Sodium-dependent glucose transporter 1
SOD	Superoxide dismutase
TNF-α	Tumour necrosis factor-alpha
TRAF	TNF-α receptor associated factor
UEA	University of East Anglia
UK	United Kingdom
USA	United States of America
VA	Vanillic acid
VCAM-1	Vascular cell adhesion molecule-1
VEGF	Vascular endothelial growth factor
WST1	4-[3-(4-Iodophenyle)-2-(4-nitrophenyl)-2H-5-tetrazolio]-1,3-benzene disulphonate

Acknowledgement

I am grateful to my primary supervisor, Dr Colin Kay and secondary supervisors Professor Aedin Cassidy for their invaluable help and support throughout my PhD research and thesis preparations, without their guidance this work would have not been possible. I would like to take this opportunity to thank my wife, Dipika for her support throughout PhD. It was her love and support that allowed me to leave GSK, start PhD and kept me going through this incredible experience and I cannot imagine completing this PhD without her support, thanks a ton Dipika. The journey became even more interesting when Dipika and I had best possible stress buster in our lives –Kiaan, our son. After a long day of lab work, it was excitement to spend time with Kiaan that kept me refreshed and added an interesting flavour to this PhD. I cannot thank my parents enough for making me a person that I am today and made me capable of pursuing my dreams. It was their support and sacrifice that fuelled my desire to become successful in whatever I pursue, so thank you mom and dad. I also want to thank my sister Nirali for her love and support throughout PhD, the best sister I could ever have, thank you! I would like to extend my thanks to Nikunj and Jigna, whose support during my stay in Norwich was incredible. I felt that it was those social occasions that helped me keep work/life balance.

I would like to thank past and present members of analytical laboratory group, especially Michael Edwards, Rachel de Ferrars, Mike Smith, Dr Charles Czank, Jess di Gesso, Dr Jason Kerr. I had many interesting conversation relating to PhD and personal life with Michael and Rachel on many occasions and it was their support as fellow PhD students that helped me immensely to develop not only as a researcher but also as a person. I also want to thank Jess, Sandy, Sara and Manual for sharing their experiences with me throughout the PhD and helping me along the way along. I would like to extend my thanks to Dr Rosemary Davidson and Dr Darren Sexton for their inputs in finalising mRNA and flow cytometry work In addition, I would also like to thank Dr Christopher Ford and Professor Malcom Jackson at University of Liverpool for their support in setting up electron paramagnetic resonance method and analysing samples. I am extremely grateful to Biotechnology and Biological Sciences Research Council for the financial support which made this novel research project possible. Finally, I would like to thank the God for giving me strength and will power to work hard during my PhD.

Chapter 1. Anthocyanins: review of the scientific literature

1.1 Introduction

There are six main anthocyanins, a subclass of flavonoid, commonly found within the plant kingdom, which differ according to their degree of hydroxy- and methoxylation of the B ring (**Figure 1.1**) (Wallace 2011). They are considered to be secondary metabolites and are responsible for the dark red and purple colouration of many plants and commonly used as pigments in the food industry. However more recently, their potential health-related benefits (Cassidy, O'Reilly et al. 2010, Jennings, Welch et al. 2012, Cassidy, Mukamal et al. 2013) have drawn the attention of researchers. Epidemiological data suggest that anthocyanin consumption is associated with reduced incidence of cardiovascular disease (CVD) and particularly reduces the risk of hypertension, atherosclerosis and myocardial infarction (Mink, Scrafford et al. 2007, Cassidy, O'Reilly et al. 2010, Jennings, Welch et al. 2012).

Figure 1.1 Flavonoid skeleton and structures of anthocyanins

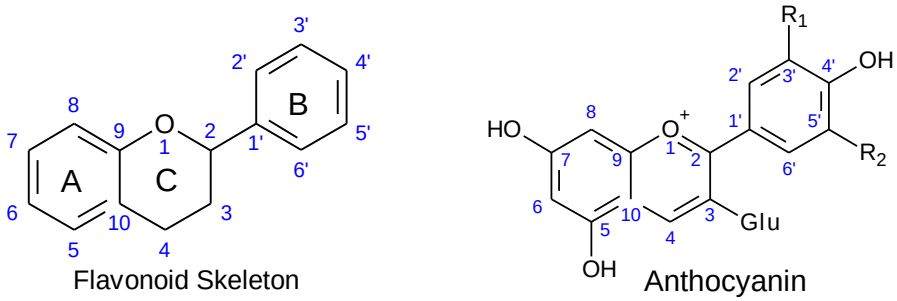

Anthocyanin	R_1	R_2
Cyanidin-3-glucoside (C3G)	OH	H
Malvidin-3-glucoside (M3G)	OCH_3	OCH_3
Delphinidin-3-glucoside (D3G)	OH	OH
Pelargonidin-3-glucoside (Pg3G)	H	H
Petunidin-3-glucoside (Pt3G)	OCH_3	OH
Peonidin-3-glucoside(Pn3G)	OCH_3	H

Glu, glucose.

Anthocyanins are consumed in appreciable amounts as a part of healthy diet high in fruits and vegetables. Anthocyanin consumption varies across populations and depends on the

type of food consumed (**Table 1.1**) (Zamora-Ros, Andres-Lacueva et al. 2010, Zamora-Ros, Knaze et al. 2011). For example, a single serving of berries and aubergine could provide up to several hundred milligrams of anthocyanins (Manach, Williamson et al. 2005, Zamora-Ros, Knaze et al. 2011).

Table 1.1 Anthocyanin content in common berries, juices and vegetables (Zamora-Ros, Knaze et al. 2011)

Foods	Anthocyanidins (mg) per 100 gm of fresh weght						
	Cyanidin	Delphinidin	Malvidin	Pelargonidin	Peonidin	Petunidin	Total
Fruits							
Elderberries, raw	758.48	-	61.35	1.13	-	-	820.96
Chokeberry, raw	435.78	-	-	1.44	-	-	437.22
Bilberry, raw	112.59	161.93	54.37	-	51.01	51.01	430.91
Raspberries, black	323.47	-	-	0.15	0.55	-	324.17
Blueberries, wild, raw	42.47	92.71	103.80	-	23.49	58.23	320.70
Vegetables							
Chicory red, raw	232.28	13.93	-	-	-	-	246.21
Cabbage, red, raw	72.86	0.10	-	0.02	-	-	72.98
Eggplant, raw	0.02	13.76	-	0.02	-	-	13.80
Onions, red, raw	6.16	2.28	-	0.02	1.22	-	9.68
Beverages							
Crowberry juice	16.97	47.40	61.35	-	11.38	26.42	163.52
Cranberry juice, raw	41.81	7.66	0.31	-	42.10	-	91.88
Grapes, black, juice	1.18	3.17	58.0	0.02	6.14	2.81	72.12
Black Currant Juice	16.05	27.80	-	1.17	0.66	3.87	49.55

A significant body of epidemiological evidence suggests that increased consumption of foods rich in flavonoids reduces the risk of CVD (Erdman, Balentine et al. 2007, Geleijnse and Hollman 2008, Grassi, Desideri et al. 2009, Jennings, Welch et al. 2012) but not all studies have shown this association (Curtis, Kroon et al. 2009, Wallace 2011). A 16 year follow-up study involving 34,489 post-menopausal women showed a significant inverse relationship between increased dietary anthocyanin intake and coronary heart disease mortality (CHD) (Mink, Scrafford et al. 2007). Data from more recent studies, for example a 14 year follow-up study which involved participants from the Nurse's Health Study (NHS) cross-sectional study, and a study involving 1898 women participants from the TwinsUK registry, both reported inverse association between the risk of hypertension and consumption of foods rich in anthocyanins (Cassidy, O'Reilly et al. 2010, Jennings, Welch et al. 2012); thereby suggesting that consumption of anthocyanin may reduce the relative risk of developing CVD.

Chemistry of anthocyanins. Anthocyanins have a similar skeletal structure (C_6-C_3-C_6) to other flavonoids, with the main difference being the presence of the unique flavylium cation on the C- ring (Figure 1.1) which is most stable in acidic conditions (Asenstorfer, Iland et al. 2003, Fleschhut, Kratzer et al. 2006, Crozier, Jaganath et al. 2009). More than 635 anthocyanins have been reported, and vary depending on numbers and positions of hydroxyl groups, methoxy groups and degree of glycosylation (de Pascual-Teresa, Moreno et al. 2010, Wallace 2011). The increased number of hydroxyl- and methoxy- groups increases the water solubility due to polarity change; however, it decreases their stability, for example, Pg3G (no hydroxyl group) is more stable compared to D3G (two hydroxyl groups) (Fleschhut, Kratzer et al. 2006, Crozier, Jaganath et al. 2009, Wallace 2011). Anthocyanins are predominantly mono glycosylated at position three of the C-ring (3-*O*-glucoside); however, mono and diglycosides at other positions are also reported (de Pascual-Teresa, Moreno et al. 2010).

The chemistry of anthocyanins is more complex when compared to the other flavonoid subclasses, owing to the presence of the flavylium cation. The cation stabilises anthocyanins under acidic conditions, however, it is extremely unstable under physiological pH and degrades to form acid and aldehyde (Seeram, Bourquin et al. 2001, Fleschhut, Kratzer et al. 2006, Castañeda-Ovando, Pacheco-Hernández et al. 2009). Anthocyanins can be present in four different forms depending upon the pH of their environment (**Figure 1.2**) (Asenstorfer, Iland et al. 2003, Castañeda-Ovando, Pacheco-Hernández et al. 2009). The flavylium cation (red colour) is the most stable form (stable at pH≤2) of the molecule under acidic conditions (Figure 1.2A) (McGhie and Walton 2007, Castañeda-Ovando, Pacheco-Hernández et al. 2009). However, as acidity decreases (pH 2-4) this form undergoes proton loss to give the quinonoid form (blue colour) (McGhie and Walton 2007). Under neutral pH conditions, the hemiketal and chalcone forms are predominant (both forms are colourless)(Del Rio, Borges et al. 2010).

1.2 Bioavailability of anthocyanins

1.2.1 Absorption

Anthocyanins are generally considered to have low human bioavailability and their absorption is poorly understood. Previous studies have reported low recoveries of anthocyanins, where the total plasma concentration and urinary excretion ranges from

14nM – 120nM which is equivalent to 0.004% – 5.1% of the total intake (Table 1.2) (Milbury, Cao et al. 2002, Kay, Mazza et al. 2005, Manach, Williamson et al. 2005, McGhie and Walton 2007, Milbury, Vita et al. 2010). A possible reason for the low recovery of anthocyanins may be that the majority of bioavailability studies conducted to date have generally attempted to detect aglycones, or intact or conjugated anthocyanins (Felgines, Talavera et al. 2005, Kay, Mazza et al. 2005) and failed to identify lower molecular weight metabolites such as phenolic acids.

Figure 1.2 pH dependent forms of anthocyanins and degradation products

A. pH dependent form of anthocyanins

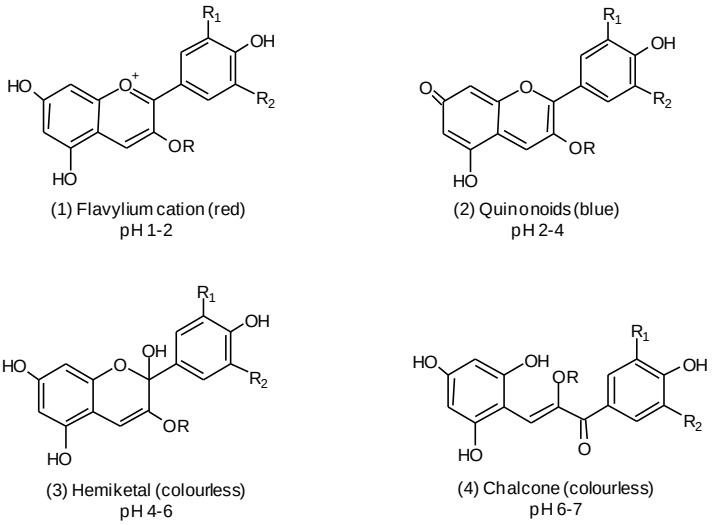

A. Degradation products of anthocyanins at neutral pH

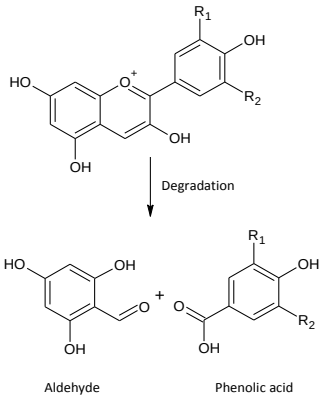

Anthocyanidin	R_1	R_2	Phenolic acid
Cyanidin	OH	H	Protocatechuic Acid
Malvidin	OCH_3	OCH_3	Syringic Acid (SA)
Delphinidin	OH	OH	Gallic Acid (GA)
Pelargonidin	H	H	4 - Hydroxybenzoic Acid (4HA)
Petunidin	OCH_3	OH	3 – Methylgallic Acid (3MGA)
Peonidin	OCH_3	H	Vanillic Acid (VA)

pHdependent forms of anthocyanin (A) and its degradation products (B). A – Derived from (Asenstorfer et al., 2003; McGhie et al., 2007; (Castañeda-Ovando, Pacheco-Hernández et al. 2009)). Flavylium cation form (1), the most stable form under acidic condition; quinonoids form (2) exists in mildly acidic conditions; hemiketal (3) and chalcone (4) forms are present under neutral pH. B – Degradation products of anthocyanins at neutral pH, derived from (Woodward et al., 2009).

It has been hypothesized that the apparent low levels of anthocyanins in biological samples may be due to rapid degradation and metabolism of anthocyanins associated with pH changes within the gastrointestinal tract (GIT) (Kulling, Honig et al. 2001, Manach, Williamson et al. 2005, McGhie and Walton 2007). In addition, the majority of the studies examining absorption and metabolism *in vivo* haveused anthocyanin rich extracts from fruits, which may have an influence on absorption, and production of degradants and metabolites in the body due to the complex mixture of various anthocyanins present (Crozier, Jaganath et al. 2009). However, recently Czank et al (2013) reported a C_{max} of 0.14 µM for cyanidin-3-glucoside (C3G) at 1.8 hours following ingestion of a ^{13}C isotope labelled C3G bolus (500 mg), in a study involving eight healthy participants where blood, urine, faeces and breath samples were collected at various time points up to 48 hours post bolus (Czank, Cassidy et al. 2013).

Table 1.2 Concentrations of anthocyanins in plasma and urine reported in human studies

Material consumed	Anthocyanin dose (total intake)	Plasma maximum concentration/C_{max}	Time to maximum Plasma concentration t_{max}(h)	Urinary excretion % of total intake – (time of sample collection)	References
^{13}C isotope labelled C3G	500 mg	0.14 µmol/L	1.8	5 (48h)	(Czank, Cassidy et al. 2013)
Chokeberry extract (7.1g)	721mg	96.08±6.04nmol/L	2.8	0.001 (24h)	(Kay, Mazza et al. 2005)
Red wine (500mL)	68mg	1.4nmol/L	0.8	0.016 (6h)	(Manach, Williamson et al. 2005)
Red wine (300mL)	218mg			1.5-5.1 (12h)	
Black currant juice (330mL)	1000mg	3.5-51nmol/L	1	0.0.032-0.046	
Red grape juice (500mL)	Malvidin-3-glucoside 117mg	2.8nmol/L	2	0.019 (6h)	
Cranberry extract (480mL)	Cyanidin-3-glucoside 1.58mg	0.93±1.04 nmol/L	1.1	0.007 (4h)	(Milbury, Vita et al. 2010)
Red wine anthocyanins extract (12g)	Peonidin-3-glucoside 15.2±1.5mg	0.8±0.2nmol/L	1.4±0.8	0.05(24h)	(Milbury, Cao et al. 2002)
Red wine anthocyanins extract (12g)	Malvidin-3-glucoside 80.2±3.1mg	4.2±1.3nmol/L	1.8±0.6	0.05(24h)	

As anthocyanins have a similar structural configuration to other flavonoid subclasses, their overall absorption and metabolism may be similar to other flavonoids. Current evidence suggests that flavonoids are fairly stable in the stomach and remain intact; owing to

attached glycoside groups. Once flavonoids enter the small intestine there are two potential pathways by which they may be absorbed into epithelial cells. Firstly, hydrolysis of flavonoids by lactase phloridizin hydrolase (LPH) on the brush border of the small intestine to produce aglycones, which then enter epithelial cells by passive diffusion (Kay 2006, He, Wallace et al. 2009, Del Rio, Borges et al. 2010). Secondly, intact flavonoids enter epithelial cells via active transport systems such as the sodium-dependent glucose transporter (SGLT), where they may be hydrolysed by cytosolic β-glucosidase to produce aglycones (**Figure 1.3**) (Kay 2006, McGhie and Walton 2007, Wang and Ho 2009, Del Rio, Borges et al. 2010).

Figure 1.3 Potential mechanisms of intestinal absorption of anthocyanins in humans

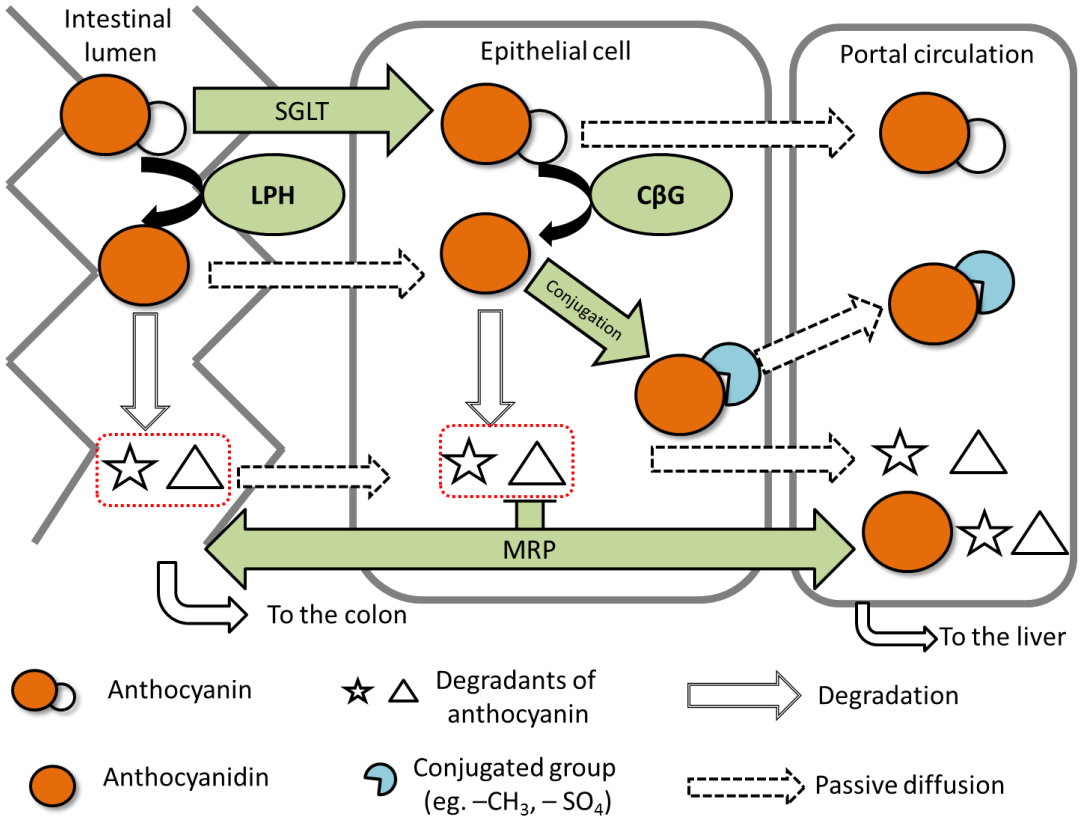

Mechanism of intestinal absorption of anthocyanins in human, based on(Kay 2006, McGhie and Walton 2007, Del Rio, Borges et al. 2010). SGLT, sodium-glucose transporter; LPH, lactase phloridizin hydrolase; CβG, cytosolic-β-glycosidase; MRP, multi-drug resistance protein

It is possible that the absorption and metabolism pathways in the small intestine could become saturated, and the remaining flavonoids enter large intestine as intact glycosides (Kay 2006). The degradation of anthocyanins has been reported at physiological pH resulting in formation of phenolic acids and aldehydes, which may then be absorbed in the small intestine or enter the large intestine where they may undergo further metabolism (Figure 1.3) (Fleschhut, Kratzer et al. 2006). For example, protocatechuic acid, which is a degradant

of C3G, has been identified as a metabolite present following consumption of red blood orange juice or ^{13}C-C3Gby healthy volunteers (Vitaglione, Donnarumma et al. 2007, Czank, Cassidy et al. 2013).

1.2.2 Metabolism

The metabolism of anthocyanins may have a major role in explaining the reported low bioavailability of the parent compounds. Recently, Czank et al(2013) reported 24 metabolites identified from a ^{13}C labelled C3G human feeding study, which included phase II conjugates of cyanidin and C3G, degradants of cyanidin [protocatechuic acid (PCA) and phloroglucinol aldehyde (PGA)], and phase II metabolites of PCA [including vanillic acid (VA), isovanillic acid (IVA), glucuronides and sulphates of PCA, and glucuronides and sulphates of VA and IVA] (Czank, Cassidy et al. 2013). Furthermore, Czank et al also described elimination of C3G in detail, where ~5% of total ^{13}C excretion was detected in urine, ~32% in faeces and ~7% in breath over a 48 hour period; with a minimum bioavailability of ^{13}C-C3G reaching ~12% of total ingested dose (Czank, Cassidy et al. 2013). Owing to structural similarities, the metabolism of flavonoids can also be extrapolated to anthocyanins, and may be divided into three stages. Firstly, Phase II metabolism: conjugation reactions; secondly, Phase I metabolism: hydroxylation and demethylation reactions; and thirdly, colonic microfloral metabolism in the large intestine (Kay 2006, Wang and Ho 2009, Del Rio, Borges et al. 2010). The metabolism of anthocyanins begins following absorption in the small intestine where they undergo conjugation, catalysed by the enzymes catechol-O-methyltransferase, sulphotransferase and UDP-glucuronosyltransferase present in epithelial cells, to produce methylated, glucuronidated and sulphated products respectively (Kay 2006, McGhie and Walton 2007, Del Rio, Borges et al. 2010). These conjugated metabolites then enter the hepatic portal circulation and ultimately the liver, where they are further metabolised. Intact anthocyanins and their conjugated metabolites which have reached the liver are subject to Phase I metabolism reactions such as hydroxylation and demethylation, resulting in mono- and di- hydroxyl metabolites. Mono- and di- hydroxy metabolites of isoflavones have been reported as metabolic products of liver microsomes (Wang and Ho 2009). Anthocyanins which are not absorbed in the small intestine may enter the large intestine, where they may undergo Phase II metabolism as described above and catabolism by colonic microflora. Colonic microflora may play a significant role in the metabolism of anthocyanins

(Williamson and Clifford 2010, Del Rio, Rodriguez-Mateos et al. 2013). A study involving human volunteers who had undergone ileostomy reported up to 85% of blueberry anthocyanins appearing in ileostomy bags depending on sugar moiety and attached methoxy groups (Kahle, Kraus et al. 2006).

In a blood orange juice feeding study (Vitaglione, Donnarumma et al. 2007) PCA was reported as a major anthocyanin metabolite. There is a potential for further metabolism of these metabolites, to produce hydroxybenzoic acids (Williamson and Clifford 2010). Such hydroxybenzoic acids (4 hydroxybenzoic acid, PCA, vanillic acid and genistic acid) have been reported in a strawberry feeding study by Russel et al(Russell, Scobbie et al. 2009). Complete dehydroxylation of phenolic acids can occur, as benzoic acid has been reported as a dehydroxylated metabolite of quinic acid (Williamson and Clifford 2010). Non-aromatic compounds can also be produced, such as oxaloacetate which is further metabolised to yield CO_2.

Phenolic acids and degradation products formed in the large intestine can be reabsorbed through the intestinal wall and undergo conjugation reactions, prior to excretion via urine (Kay 2006, Wang and Ho 2009). For example, C3G degradation to PCA and PGA, and phase II conjugation of PCA resulting in the formation of VA, IVA and glucuronic acid conjugates has been reported recently (Czank, Cassidy et al. 2013). All of these metabolites may then undergo demethoxylation, dehydroxylation and deglucuronidation by colonic microflora as described above.

1.3 Anthocyanins and cardiovascular disease

Cardiovascular disease (CVD) is the predominant cause of mortality globally (WHO 2011), resulting in the death of approximately 17 million people annually and this number is expected to reach 23.6 million by 2030 (WHO 2011). CVD includes hypertension (elevated blood pressure), coronary heart disease (CHD), cerebrovascular disease (stroke), peripheral artery disease, congenital heart disease, rheumatic heart disease, and heart failure (Wallace 2011, WHO 2011). An unhealthy diet, physical inactivity and smoking are believed to be the main causes of CVD (WHO 2011). With regard to the role of a healthy diet, anthocyanins have been linked with reduced incidence of CVD (Erdman, Balentine et al. 2007, Mink, Scrafford et al. 2007, Cassidy, O'Reilly et al. 2010);for example Cassidy et al(2010) recently

reported on a prospective study involving 156,957 participants from the Nurse's Health Society and Health Professionals Study and concluded that the relative risk of hypertension was reduced by 8% in the highest quintile of anthocyanin consumption compared to the lowest (Cassidy, O'Reilly et al. 2010). Mink et al (2007) have also described a correlation between consumption of foods rich in anthocyanins and a reduced mortality rate due to CVD (Mink, Scrafford et al. 2007); although not all studies support this correlation (Curtis, Kroon et al. 2009). Animal data support the hypothesis that anthocyanins are beneficial in the prevention of CVD (Elks, Reed et al. 2011, Zhu, Xia et al. 2011), however, once believed to be primarily radical scavengers (Wang 1997, Zheng and Wang 2003), anthocyanins are now thought to influence cell signalling pathways to reduce the detrimental effects of oxidative stress and therefore prevent CVD. Although several modes of action have been proposed and investigated *in vitro* (Xu, Ikeda et al. 2004a, Lazze, Pizzala et al. 2006), bioactivity of anthocyanins is still incompletely understood.

1.3.1 Endothelial dysfunction

Endothelial dysfunction is the hallmark of all conditions associated with CVD (Brunner, Cockcroft et al. 2005, Versari, Daghini et al. 2009). Endothelium-derived relaxing factors (EDRFs) such as nitric oxide (NO), prostacyclin (PGI_2) and endothelial hyperpolarising factors (EDHFs) are mainly responsible for endothelium-dependent vasorelaxation (Flammer and Luscher 2010). These factors are released in response to increased calcium levels in endothelial cells due to shear stress and cause smooth muscle relaxation (Flammer and Luscher 2010). Endothelium dependent vasorelaxation in response to stimuli is mainly driven by the generation of NO, which activates soluble guanyl cyclase to increase the production of cyclic guanosine monophosphate (cGMP) and subsequent relaxation of smooth muscle cells (Brunner, Cockcroft et al. 2005). NO is also responsible for maintaining endothelial homeostasis by inhibiting vascular smooth muscle cell proliferation, platelet adhesion/aggregation, neutrophil activation/adhesion, and expression of proinflammatory factors such as endothelial cell adhesion molecules and cytokines (Naseem 2005, Bian, Doursout et al. 2008). The bioavailability of NO can be diminished by various factors including increased production of radical species [eg reactive oxygen species (ROS) and reactive nitrogen species (RNS)], smoking, dyslipidemia, diabetes and hyperhomocysteinaemia (Li, Yi et al. 2002, Brunner, Cockcroft et al. 2005, Versari, Daghini et al. 2009) which cause disruption in the homeostatic environment of endothelium to

promote endothelial dysfunction. Flow mediated dilatation (FMD), a technique which measures NO-mediated brachial artery dilatation in response to endothelial shear stress, was significantly improved in a placebo controlled cross over study involving consumption of anthocyanins by 12 hypercholesterolemic volunteers (Zhu, Xia et al. 2011). Animal data also support the beneficial effect of anthocyanins in spontaneously hypertensive rats (SHR), which showed decreases in glutathione peroxidise, an enzyme expressed in response to oxidative stress, and improved endothelial dependent relaxation when SHR were fed red wine polyphenols including cyanidin-3-glucoside, peonidin-3-glucoside and malvidin-3-glucoside (Chan, Tabellion et al. 2008). Anthocyanins appear to act upon NO mediated endothelial relaxation as confirmed recently when rat aortic rings showed no relaxation, in the presence of NO and cGMP inhibitors when treated with anthocyanins, but showed significant relaxation in the absence of these inhibitors (Zhu, Xia et al. 2011). Anthocyanins may elicit this protective effect either by abolishing NAD(P)H oxidase (NOX) expression/activity hence reducing ROS production, or by increasing NO production [via endothelial nitric oxide synthase (eNOS), discussed later in section 1.4].

A. Endothelial nitric oxide synthase and anthocyanins

Endothelial nitric oxide synthase (eNOS) is expressed in most endothelial cells and is activated by various factors such as growth factors, bradykinin, histamine, hormones and thrombin (Michel and P.M.Vanhoutte 2010). The enzyme produces NO by oxidation of L-arginine to L-citrulline, where the cofactor tetrahydrobiopterin (BH_4) plays an important role (Michel and P.M.Vanhoutte 2010) by transferring the electrons to the guanidine nitrogen part of L-arginine to produce NO (Hobbs, Higgs et al. 1999, Michel and P.M.Vanhoutte 2010). In the absence of L-arginine or with reduced levels of cofactor BH_4 due to increased oxidative stress, uncoupling of eNOS occurs and $O_2^{\cdot -}$ and H_2O_2 are produced instead of NO (**Figure 1.4**) (Kawashima and Yokoyama 2004). It is believed that if partial uncoupling of eNOS occurs owing to lack of BH_4 then superoxide and NO both are produced, and as an outcome superoxide reacts with NO to produce $ONOO^-$ (Bonomini, Tengattini et al. 2008) which is a potent radical species and promotes endothelial dysfunction. In addition, ROS-induced inhibition of dimethylarginine dimethylaminohydrolase [DDAH, an inhibitor of asymmetric dimethylarginine (ADMA)], causes increased endogenous ADMA levels, this in turn reduces NO bioavailabiity by inhibiting of eNOS.

Figure 1.4 Uncoupling of eNOS due to elevated oxidative stress

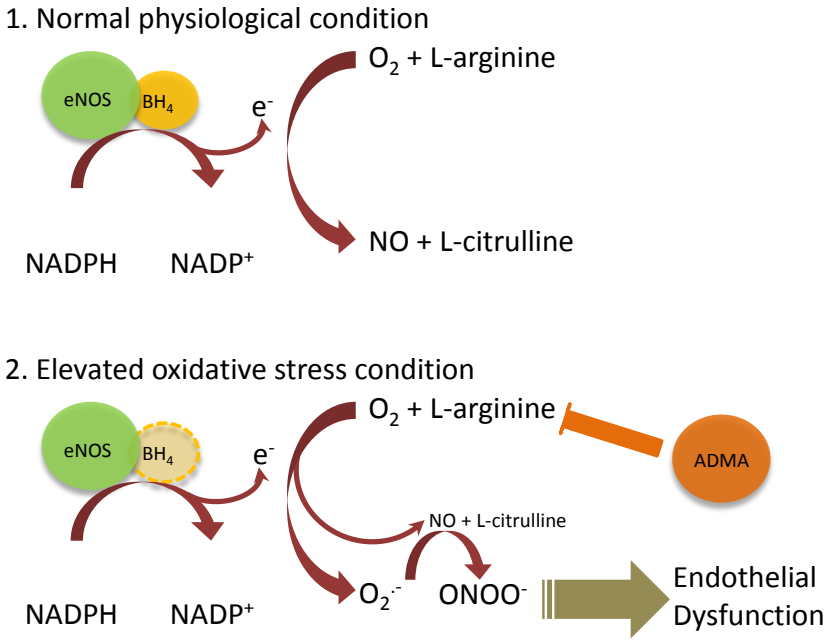

eNOS with co-factor BH_4 produces NO under normal physiological condition (1); however, elevated oxidative stress uncouples eNOS by reducing the levels of BH_4 which results in $O_2^{\cdot-}$ production and in turn increased production of $OONO^-$ (2). ADMA, assymetric dimethylargenine; eNOS, endothelial nitric oxide synthase, NADPH, nicotinamide adenine dinucleotide phosphate; BH_4, tetrahydrobiopterin.

An increased NO-dependent vasorelaxation in response to anthocyanins has been shown in rat thoracic aortic and porcine coronary arterial rings (Bell and Gochenaur 2006, Ziberna, Lunder et al. 2010). Cyanidin-3-glucoside has also been shown to increase eNOS expression and activity in bovine artery endothelial cells by phosphorylation of Src, ERK1/2 and eNOS at Ser1179 (Xu, Ikeda et al. 2004a, Xu, Ikeda et al. 2004b). With regards to human cells, treatment of human umbilical vein endothelial cells (HUVECs) with anthocyaninsdemonstrated that anthocyanins decrease the production of endothelin-1 (Lazze, Pizzala et al. 2006) and induce eNOS expression (Lazze, Pizzala et al. 2006, Edirisinghe, Banaszewski et al. 2011). Therefore, cyanidin-3-glucoside, and/or its degradation products and metabolites, may influence eNOS and NO levels to induce endothelial protective effects.

B. NAD(P)H oxidase and anthocyanins

The NAD(P)H oxidase (NOX) enzyme family is a major source of ROS in the vasculature (Griendling, Sorescu et al. 2000, Kuroda and Sadoshima 2010). There are seven types of NOX reported to date, NOX1 to NOX5, DUOX1 and DUOX2 (dual oxidases) (Bedard and Krause

2007, Brandes, Weissmann et al. 2010). Expression of NOX1, NOX2, NOX4 and NOX5 has been reported in the vasculature (Lyle and Griendling 2006, Brown and Griendling 2009). NOX1, NOX2 and NOX5 produce $O_2^{\cdot-}$ whilst NOX4 predominantly produces H_2O_2(Brandes, Weissmann et al. 2010). NOX1 and 2 require the transmembrane subunit $p22^{phox}$ for stabilisation, which then associates with the cytosolic subunit $p47^{phox}$ (**Figure 1.5**) ('organiser' subunit). NOX2 then initiates association with the 'activator' subunit $p67^{phox}$, followed by $p40^{phox}$(Bedard and Krause 2007, Drummond, Selemidis et al. 2011). With NOX1, association with $p47^{phox}$ initiates the translocation of NOXA1 towards the cell membrane, and associates with $p47^{phox}$ to activate the enzyme; however, NOX5 does not require cytosolic subunits for activity but rather is activated by Ca^{+2} in endothelial cells (Brown and Griendling 2009). NOX4 requires $p22^{phox}$ to be stabilised and a substantial amount of evidences suggest that it is constitutively active, however, recently it has been suggested that NOX4 activity is regulated by polymerase δ-interacting protein 2 (POLDIP2) (Figure 1.5) (Drummond, Selemidis et al. 2011).

Figure 1.5 NOX isoforms expressed in human endothelial cells

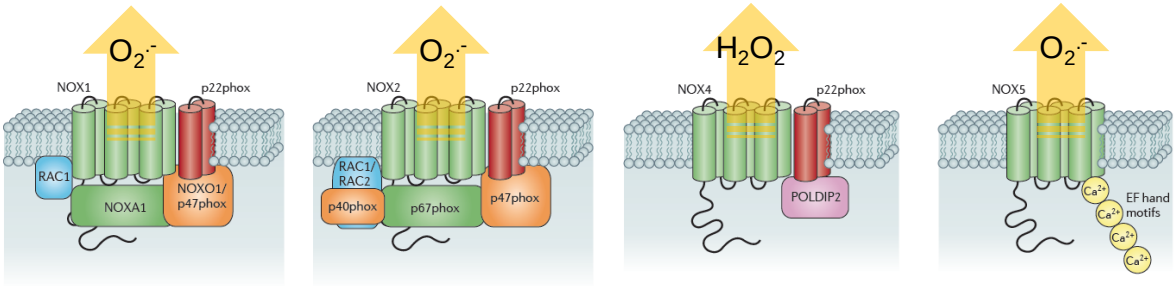

NOX1, NOX2, NOX4 and NOX5 are expressed in endothelial cells. NOX1, 2 and 4 require $p22^{phox}$ to be stabilised. NOX1 and 2 both produce $O_2^{\cdot-}$ by employing organiser unit $p47^{phox}$ which initiates the localisation of other cytosolic subunits such as NOXA1 (for NOX1) and $p67^{phox}$and $p40^{phox}$ (for NOX2) to the membrane. Polymerase δ-interacting protein 2 (POLDIP2) may activate NOX4 to produce H_2O_2 whilst only Ca^{+2} is required to activate NOX5 and produce $O_2^{\cdot-}$. Figure adapted from (Drummond, Selemidis et al. 2011)

Whilst there are no reported studies involving NOX and anthocyanins, the structurally similar flavonoid -(-)epicatechin and its metabolites have been explored in angiotensin II (Ang II) stimulated HUVECs for effects on superoxide production and NOX activity, and showed significant reductions in superoxide production and the expression of NOX4 (Steffen, Schewe et al. 2007b, Steffen, Gruber et al. 2008). Quercetin also induced decreased superoxide production and downregulation of $p47^{phox}$ in SHR and rat aortic rings (Sánchez, Galisteo et al. 2006, Romero, Jiménez et al. 2009). In addition, apocynin is a known vasoactive compound (Johnson, Schillinger et al. 2002) and has a similar structure to vanillic acid, a secondary

metabolite of C3G, thus these data indicate that anthocyanins and their degradants and metabolites may influence NOX activity to reduce oxidative stress and improve endothelial function.

1.3.2 Atherosclerosis

Atherosclerosis is one of the most common classes of cardiovascular disease (George and Johnson 2010). It is characterised by arterial stiffening and plaque build-up of medium and large sized arteries, leading to plaque rapture which in turn can lead to myocardial infarction and stroke (Hirooka, Gotoh et al. 2001, Nishi, Nanto et al. 2001). The formation of arterial plaques in atherosclerosis is more complex than simply accumulation of lipids on the arterial wall. During endothelial dysfunction, alterations to the homeostatic properties of endothelium occurs leading it to exhibit procoagulant rather than anticoagulant properties as the permeability and adhesiveness towards inflammatory agents such as platelets, monocytes, leukocytes, cytokines, vasoactive molecules and growth factors increases (**Figure 1.6**) (Ross 1999). If the inflammatory response is not deactivated, it continues indefinitely leading to migration and proliferation of smooth muscle cells and formation of an intermediate lesion (Bonomini, Tengattini et al. 2008). There are several factors that affect the process of continuous inflammatory response, including hypercholesterolemia, modified low density lipoprotein (LDL), hyperhomocysteinemia, hypertension and infection at the site of endothelial dysfunction (Eberhardt, Forgione et al. 2000). Post lesion formation, the process of artery dilation, called remodelling, occurs in order to compensate for artery thickening and to prevent obstruction to the blood flow due to lesions and proliferation of smooth muscle cells (George and Johnson 2010). At this stage the lesion is covered by a fibrous cap to protect it from rupturing and obstructing the lumen (Nishi, Nanto et al. 2001). Further inflammation leads to recruitment of increased numbers of macrophages and lymphocytes integrating within an intermediate lesion and produce high numbers of cytokines, chemokines, growth factors and hydrolytic enzymes. This process converts intermediate lesions to more complex and advanced lesions called focal necrosis. The vicious cycle of inflammatory response, migration and proliferation of smooth muscle cells leads to progression and restructuring of the focal necrosis to produce advanced and complex lesion covered by a fibrous cap (Gamkrelidze, Mamamtavrishvili et al. 2008). After a certain point the artery wall can no longer compensate for this extensive chronic inflammation process and the complex lesion intrudes the lumen, obstructing the blood flow

(Figure 1.6). The complex lesion is susceptible to rupture and causes complete blockage of the artery by formation of a thrombus or blood clot resulting in myocardial infarction and stroke (Hirooka, Gotoh et al. 2001, Nishi, Nanto et al. 2001).

Figure 1.6 Pathogenesis of atherosclerosis

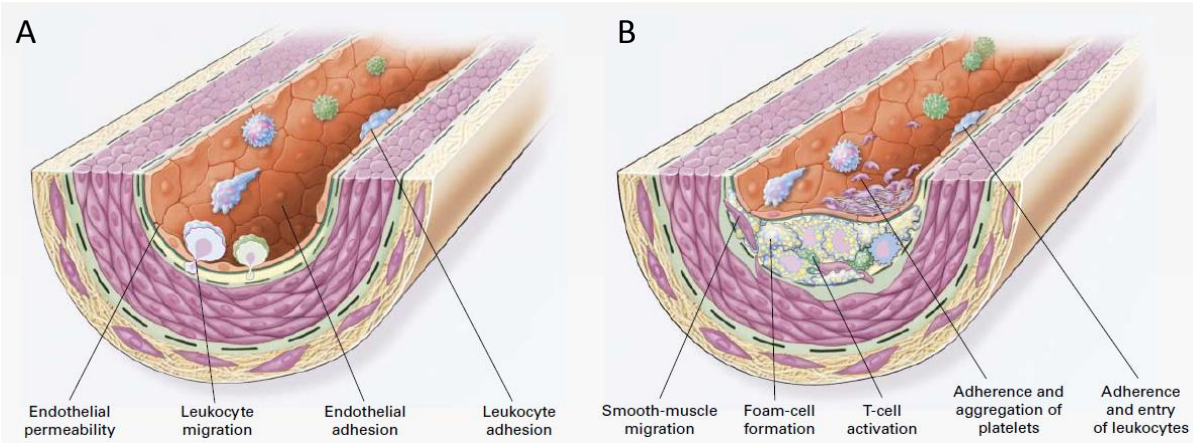

The contribution of various inflammatory factors in the progression of lesion formation from initiation of cell adhesion (A) to development of a complex lesion which intrudes into the lumen (B) to obstruct blood flow and becomes susceptible to rupture which leads to complete blockage of the artery. Figure adapted from (Ross 1999)

A. Vascular adhesion molecules and anthocyanins

The expression of adhesion molecules for tethering, arrest and transmigration of leukocytes into endothelium is one of the earliest and most important events in the pathogenesis of chronic inflammation (Ross 1999, García-Lafuente, Guillamón et al. 2009). This involvement of adhesion molecules occurs when endothelium is exposed to pro-atherogenic stimuli such as oxidised low density lipoprotein (oxLDL) and cluster of differentiation 40 ligand (CD40L) resulting in expression of selectins and cell adhesion molecules by endothelial cells (Pamukcu, Lip et al. 2011, Greig, Kennedy et al. 2012). The selectins and cell adhesion molecules then ensure tethering of leukocytes (expressing L-selectins) to the surface of endothelial cells (via P- and E-selectins) followed by firm adhesion to the endothelial cells aided mainly by intercellular adhesion molecule-1 (ICAM-1) and vascular cell adhesion molecule-1 (VCAM-1) **(Figure 1.7)**(Blankenberg, Barbaux et al. 2003, Fotis, Giannakopoulos et al. 2012). Platelet endothelial cellular adhesion molecule-1 (PECAM-1) and ICAM-1 support transmigration of leukocytes across endothelium. However, VCAM-1 plays an important role in the transmigration as it interacts with integrin α4β1 resulting in NOX activation to produce superoxide which changes the shape of endothelial cells allowing

leukocytes to transmigrate (Figure 1.7) (Matheny, Deem et al. 2000). The transmigration initiates chronic inflammation and eventually results in clinically significant events. VCAM-1 is a transmembrane glycoprotein member of the immunoglobulin superfamily and consists 6 or 7 immunoglobulin particles. It is expressed by vascular endothelial cells when stimulated by pro-atherogenic stimuli and in the endothelium of the modula. However, other cell types such as fibroblast, chondrocytes, epithelial cells, pericytes, macrophages and dendritic cells also express VCAM-1. In addition soluble VCAM-1 (sVCAM-1) has emerged as a biomarker of cardiovascular disease as it has been observed in high concentrations in blood serum of diabetic patients (Blankenberg, Barbaux et al. 2003). However, it remains unclear that how sVCAM-1 is produced from membrane bound VCAM-1 as the contributing factors can be changes in mRNA stability, increased transcription of genes, changes in translation or most hypothesised –increased proteolytic cleavage of membrane bound VCAM-1 to produce sVCAM-1.Vedem et al., reported that amongst the cell adhesion molecules VCAM-1 has better correlation between sVCAM-1 and mRNA levels in HUVECs and therefore is preferred form when investigating modulation of VCAM-1*in vitro* and *in vivo*(Videm and Albrigtsen 2008). The consumption of anthocyanins has been associated with reduced plasma levels of VCAM-1. For example, plasma levels of VCAM-1 were significantly reduced in subjects with hypercholesterolemia when 320 mg/day anthocyanins were consumed (Zhu, Ling et al. 2013). In addition, purple potato fed mice also showed significant reduction in plasma levels of VCAM-1 (Miyazaki, Makino et al. 2008). *In vitro* studies also support these observations, as anthocyanins from black soy beans reduced VCAM-1 production in tumor necrosis factor–α (TNF-α) induced HUVECs and bovine aortic endothelial cells (BAECs) (Kim, Tsoy et al. 2006, Nizamutdinova, Kim et al. 2009). Cyanidin-3-glucoside (C3G) at 1, 10 and 100μM, reduced VCAM-1 production in CD40L-stimulated HUVECs in a dose-dependent manner (Xia, Ling et al. 2009).

Figure 1.7 Diagram of leukocytes and endothelial interactions and roles of adhesion molecules during early stages of atherosclerosis

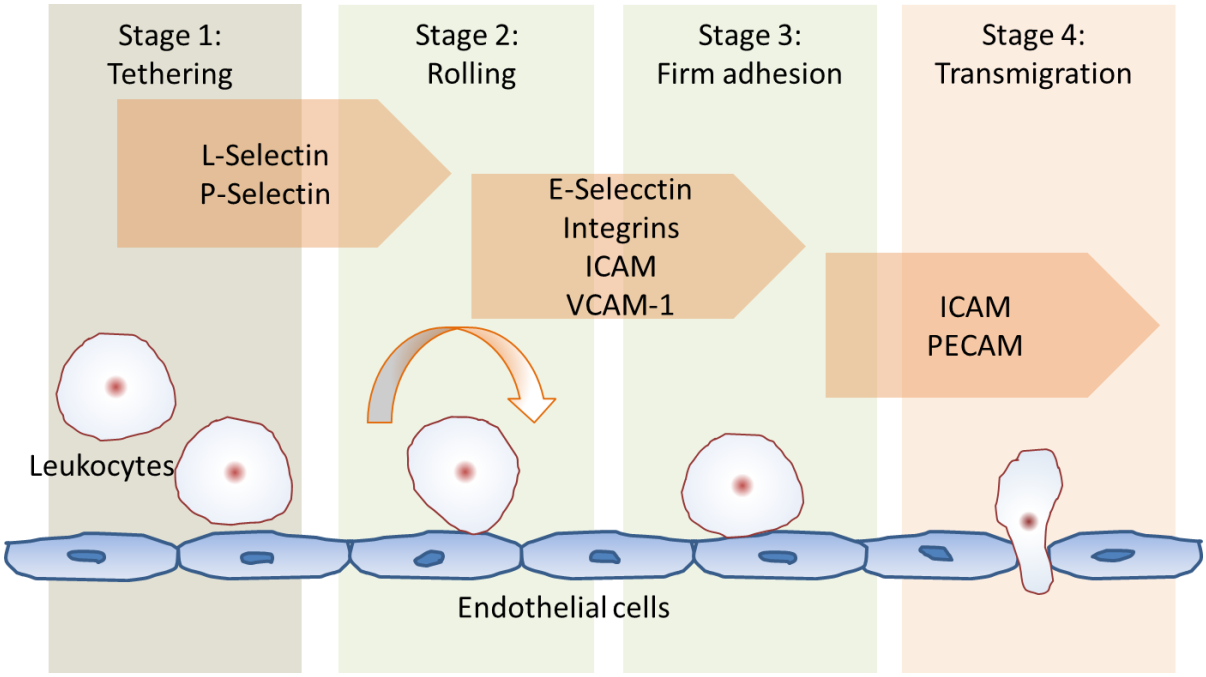

ICAM, intercellular adhesion molecule; PECAM platelet endothelial cellular adhesion molecule; VCAM-1, vascular cell adhesion molecule-1. Adapted from ((Blankenberg, Barbaux et al. 2003, Fotis, Giannakopoulos et al. 2012)

B. Interleukin-6 and anthocyanins

Pro-inflammatory mediators such as cytokines and chemokines play pivotal roles in pathogenesis of atherosclerosis (Ross 1999). In response to chronic inflammation, macrophages and T-cells are activated and produce pro-inflammatory cytokines and chemokines such as TNF-α, interleukin-1β (IL-1β), IL-6 and monocyte chemoattractant protein-1 (MCP-1) (Baud and Karin 2001, García-Lafuente, Guillamón et al. 2009). Post transmigration, these pro-inflammatory activators promote chronic inflammation by inducing proliferation of smooth muscle cells (García-Lafuente, Guillamón et al. 2009). In addition, cytokines also activate pro-inflammatory signalling pathways including nuclear factor-κB (NF-κB) and mitogen activated protein kinases (MAPK) which as a result up-regulate other pro-inflammatory mediators (Terasaka, Miyazaki et al. 2010) to promotea vicious cycle of chronic inflammation. Recently, IL-6 has emerged as a key cytokine involved in chronic inflammation as it has been shown to contribute to the development of atherosclerotic plaques and their instability leading to critical clinical endpoints such as myocardial infarction and stroke (Schuett, Luchtefeld et al. 2009). A significant association between IL-6 and coronary artery calcium (an indicator of plaque build-up) has been

reported in patients with type 2 diabetes (Saremi, Anderson et al. 2009). High levels of IL-6 cause over-production of other pro-inflammatory cytokines, matrix metalloproteinase and oxidation of lipoprotein to propagate the inflammation further (Yudkin, Kumari et al. 2000, Song and Schindler 2004, Saremi, Anderson et al. 2009). Anthocyanins have been reported to reduce the production of IL-6 both *in vivo* and *in vitro* (Xia, Ling et al. 2007, Karlsen, Paur et al. 2010, Edirisinghe, Banaszewski et al. 2011, Xie, Kang et al. 2011). In randomised controlled trials Karlsen et alshowed that chronic (Karlsen, Paur et al. 2010, Kolehmainen, Mykkänen et al. 2012) and acute (Edirisinghe, Banaszewski et al. 2011) consumption of anthocyanin-containing juice reduced plasma levels of IL-6 significantly in subjects at elevated risk of CVD compared to the control group. In addition, IL-6 expression was significantly lower in mice fed bilberry extract for 5 weeks compared to a control diet (Xie, Kang et al. 2011). *In vitro* data have also demonstrated that C3G significantly reduced cluster of differentiation ligand (CD40L)-induced IL-6 production in endothelial cells (Xia, Ling et al. 2007).

C. NF-κB and anthocyanins

As described above, pro-inflammatory mediators such as VCAM-1 and IL-6 play a vital role in the progression of atherosclerosis and both VCAM-1 and IL-6 are regulated by the NF-κB transcription factor; therefore, NF-κB is also crucial in the pathogenesis of atherosclerosis (Siomek 2012). Under normal conditions, NF-κB resides in the cytoplasm bound to an inhibitory protein, NF-κB inhibitory protein (IκB). Pro-atherogenic stimuli such as oxLDL and CD40L activate NF-κB by stimulating IκB kinase (IKK), which phosphorylates IκB. The phosphorylated form of IκB then undergoes poly-ubiquitination, following which phosphorylation of NF-κB p65 and nuclear translocation occurs resulting in increased production of IL-6 and VCAM-1 (**Figure 1. 8**). Anthocyanins have been shown to inhibit the activation of lipopolysaccharide- and CD40L-stimulated NF-κB activity (Xia, Ling et al. 2007, Min, Ryu et al. 2010, Xie, Kang et al. 2011). In addition, C3G metabolites (namely PCA and VA) have also been reported to reduce NF-κB activation by blocking the translocation of the p65 subunit to the nucleus in *ex vivo* mouse models (Kim, Kim et al. 2010, Wang, Wei et al. 2010, Kim, Kim et al. 2011, Wei, Chu et al. 2013).

Figure 1. 8 Schematic diagram of NF-κB activation following oxLDL and CD40L-stimulation

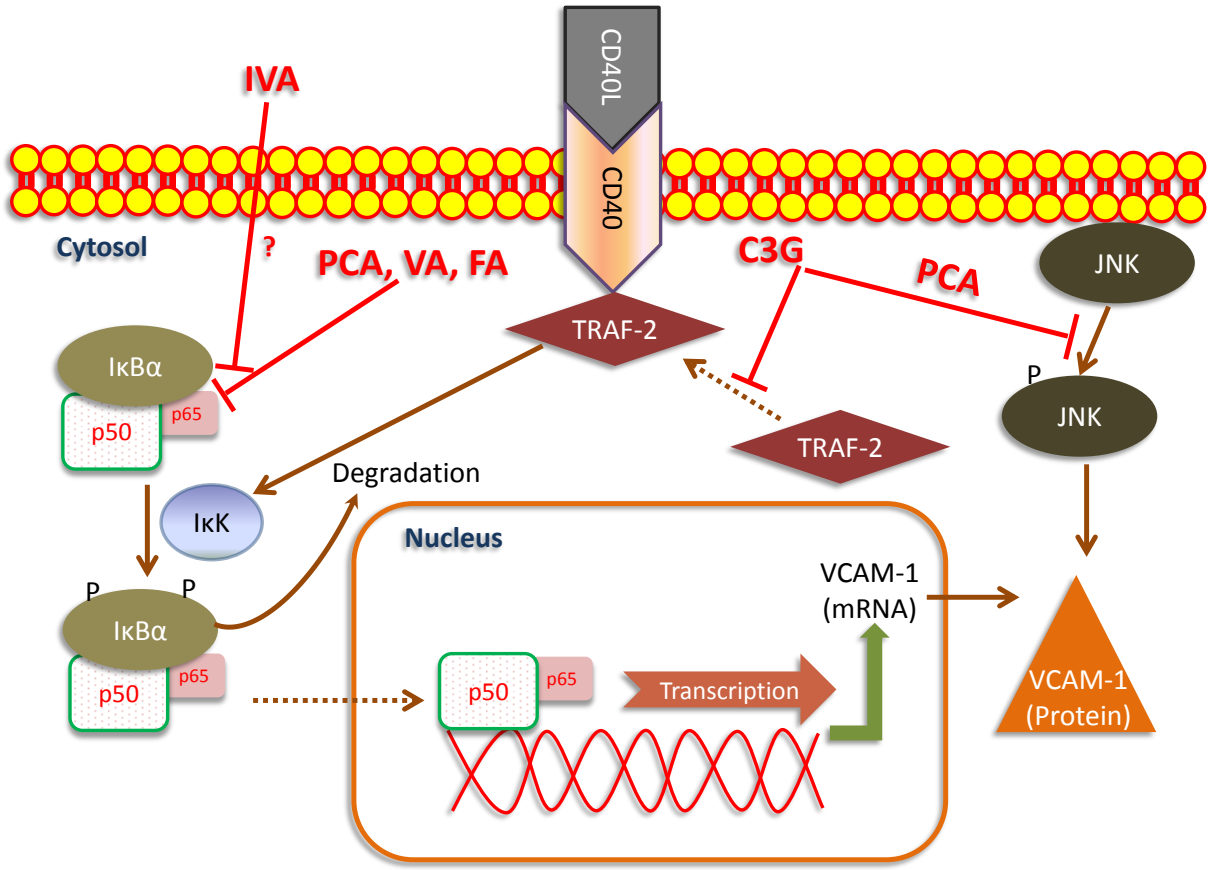

CD40L, cluster of differentiation 40 ligand; IκB, inhibitory nuclear kappa B; IκK, IκB kinase; LOX-1, lectine-type oxidise LDL receptor-1; oxLDL, oxidised low density lipoprotein; TRAF-2, tumor necrosis factor receptor associated factor-2; VCAM-1, vascular cell adhesion molecule-1. Adapted from (Xia, Ling et al. 2007, Siomek 2012)

1.4 Concluding remarks

Although evidence from epidemiological studies and randomised control trials suggest that a high intake of anthocyanins is associated with a reduced risk of CVD, and these data are supported by observations from animal and *in vitro* studies (Xu, Ikeda et al. 2004a, Bell and Gochenaur 2006, Mink, Scrafford et al. 2007, Cassidy, O'Reilly et al. 2010, Ziberna, Lunder et al. 2010), the lack of bioavailability of anthocyanins is a major obstacle in exploring their mechanisms of bioactivity. The apparent low bioavailability of anthocyanins may be attributed to their rapid degradation, resulting in the formation of corresponding phenolic acid and aldehyde counterparts. *In vitro* studies investigating the beneficial effects of

anthocyanins reported to date have been performed using only parent compounds and very few studies have attempted to demonstrate bioactivity of metabolites of anthocyanins. Therefore, these metabolites should be used to explore their influence on the activity and expression of key vascular proteins such as eNOS, ET-1, NOX and inflammatory targets such as IL-6, VCAM-1 and NF-κB.

1.5 Hypothesis and aims of current thesis

It is postulated that the beneficial effects of anthocyanins may arise from their *in vivo* degradants and metabolites, which may act by modulating key vascular proteins and anti-inflammatory activity. Therefore the aims of the present thesis were to examine the effects of C3G and 11 recently identified metabolites (including six synthesised metabolites) at physiological concentrations (0.1, 1 and 10 μM) in endothelial cells on:

1. Modulation of key vascular proteins such as up-regulation of basal eNOS production and Inhibition of stimulated superoxide and basal ET-1 production (Chapter 2)
2. Expression of key inflammatory agents such as stimulated VCAM-1 and IL-6 (Chapters 3 and 4)
3. Modulation of stimulated NF-κB activation (Chapter 5).

Up-regulation of eNOS, in conjunction with inhibition of superoxide production, can improve the bioavailability of NO and therefore maintain endothelial homeostasis (Chapter 2). In addition, inhibition of pro-inflammatory mediators, VCAM-1 (Chapter 3) and IL-6 (Chapter 4) under pro-atherogenic conditions may retard the build-up of atherosclerotic plaques and therefore clinical events such as myocardial infarction. Finally, the molecular and cellular mechanism of actions of metabolites can be explored by examining their effects on the key pro-inflammatory transcription factor NF-κB under stimulated conditions (Chapter 5).

Chapter 2. General Methods & Materials

2.1 Methods and materials

Standards and reagents. Cyanidin-3-glucoside was purchased from Extrasynthese (Genay Cedex, France). Protocatechuic acid (PCA), phloroglucinaldehyde (PGA), vanillic acid (VA), isovanillic acid (IVA), ferulic acid (FA), pyrogallol, catalase from bovine liver, superoxide dismutase, bovine heart cytochrome c, Medium 199, simvastatin and fibronectin were purchased from Sigma Aldrich (Paisley, UK). Phase II conjugates of phenolic acids [PCA-3-glucuronide (PCA-3-Gluc), PCA-4-glucuronide (PCA-4-Gluc), IVA-3-sulfate (IVA-3-Sulf), PCA-4-sulfate (PCA-4-Sulf), VA-4-sulfate (VA-4-Sulf), PCA-3-sulfate (PCA-3-Sulf)] were synthesised by the University of St Andrews, St Andrews (Fife, UK) as described previously (Zhang, Raheem et al. 2012). Human umbilical vein endothelial cells (HUVEC), large vessel endothelial cell growth medium, growth factors and antibiotic supplements (amphotericin B/gentamycin 1000x concentrated) were obtained from TCS Cell Works (Buckingham, UK) whilst 75 cm^2 flasks, foetal bovine serum (FBS), glutamine and penicillin/streptomycin were from PAA [A&E Scientific of PAA Laboratories (Kent, UK)]. ELISA quantification was performed using an Omega BMG plate reader (BMG Labtech, Aylesbury, UK). TRIzol® reagent, SuperScript® II Reverse Transcriptase, first strand buffer and dithiothreitol (DTT, 100 mM) were purchased from Invitrogen (Paisley, UK). RiboLock, RNase inhibitor, DNase reaction buffer (with $MgCl_2$), DNase I (RNase free), and EDTA (50 mM) were purchased from Fisher Scientific (Loughborough, UK). Chloroform (molecular biology grade), isopropanol/propan-2-ol and dNTP PCR mix (ready mixed 10 mM) were obtained from Fisher Scientific. Primers for real-time polymerase chain reaction (PCR), geNorm reference genes kit, and Real Time PCR master mix with SYBR® green were supplied by Primer Design (Southampton, UK); and oligo (dT) primers and nuclease-free DEPC-treated water were purchased from Ambion, Life Technologies (Paisley, UK). Quantitative PCR (qPCR) was performed using an ABIS7500 system (Life Technologies) using MicroAmp™ 96-well plates purchased from Applied Biosystems (Paisley, UK). All other chemicals were from Sigma-Aldrich. Milli-Q grade (18.2 MΩ cm^{-1}) water was used during all experiments except reverse transcription (RT)-qPCR.

Preparation of cell treatments. C3G, PCA, PGA, VA, IVA, PCA-4-Gluc, PCA-3-Gluc, PCA-4-Sulf, PCA-3-Sulf, VA-4-Sulf, IVA-3-Sulf and FA were assessed at concentrations of 0.1, 1 and 10 µM in cell culture media. Standard solutions were initially prepared in 100% dimethyl sulfoxide (DMSO) at concentrations of 40 mM for C3G and 25 mM for all other metabolites. The standards were then diluted to their final concentrations immediately prior to application to cells. Final treatment concentration of DMSO was <0.05%.

HUVEC Cell culture. Early-passage, cryo-preserved pooled HUVECs were used between passages two to four. HUVECs were routinely cultured on fibronectin-coated (0.25 µg/cm^2) 75 cm^2 flasks in large vessel endothelial cell growth medium. Once confluent (90% - 95%), HUVECs were sub-cultured using trypsin (0.025%) and 0.01% EDTA, and seeded in fibronectin-coated (0.25µg/cm^2) 24-well plates (PAA) at 60,000 cells/well. Cells were incubated for 24 hours at 37°C, 5% CO_2 before treatment.

RNA extraction and reverse transcription. HUVEC cultured in 24-well plates were homogenised using TRIzol® (500 µL/well), and RNA extracted using chloroform (100 µL/well). After centrifugation (12000 × *g* for 15 minutes at 4°C), the aqueous layer was transferred into eppendorf tubes, where RNA was precipitated by incubating the aqueous layer with propan-2-ol (250 µL/well) for 10 minutes at room temperature. Samples were then shaken vigorously and centrifuged (12000 × *g* for 10 minutes at 4°C) before supernatants were discarded. RNA pellets were allowed to air dry at room temperature and washed with 75% ethanol (500 µL/well) followed by air drying for 10 minutes before re-suspension in 20 µL of DEPC-treated nuclease-free water. After quantification [by Nanodrop (Thermo Scientific)], 1 µg of RNA was reverse transcribed by incubating RNA solution with DNase buffer (1 µL/reaction) and DNase (1 µL/reaction) at 37°C for 30 minutes with RiboLock (0.25 µL/reaction) to inhibit RNase activity and eliminate any genomic DNA contamination. RNA solutions were then incubated with EDTA (50 mM, 1 µL/reaction), oligo (dT) primers (1 µL/reaction) and dNTP PCR mix (1 µL/reaction) at 65°C for 10 minutes. Annealing of oligo (dT) primers was performed during incubation of reaction mixtures with first strand buffer (4 µL/reaction), RiboLock (1 µL/reaction) and DTT (100 mM, 1 µL/reaction) for 2 minutes at 42°C. Reverse transcription of mRNA was then initiated by addition of SuperScript® II (1 µL/reaction) and incubation at 42°C for 50 minutes, followed by 15 minutes at 70°C to

inactivate SuperScript® II. The resulting cDNA solutions were diluted in DEPC-treated nuclease-free water (1/10 dilution) and stored at 4°C until required for real-time PCR.

Real-time PCR. Five microliters (25 ng) of cDNA solution from each sample was used to perform real time PCR. eNOS, VCAM-1 or IL-6 primers (1 µL/reaction), real time PCR master mix with SYBR® green (8.33 µL/reaction) and nuclease-free water (5.67 µL/reaction) were added to micro-plate wells containing cDNA solution to achieve a final reaction volume of 20 µL per well. Real time PCR was performed using ABIS7500 (7500 software version 2.0.5), with enzyme activation at 95°C for 10 minutes, followed by 50 cycles of denaturation for 15 s/cycle at 95°C and data collection for 1 minute/cycle at 60°C.

Statistical Analysis. Analysis of variance (ANOVA) with Tukey post-hoc tests were performed using SPSS software (IBM, New York, USA) version 18 for Windows. Significance was determined at the level of 5%. Three biological replicates for each of the controls and treatments (plated in technical duplicates) were used for analysis unless otherwise stated, and means of biological replicates were represented graphically. Error bars in figures represent standard deviation.

Chapter 3. Relative vascular bioactivity of cyanidin-3-glucoside and its metabolites in human primary endothelial cells

3.1 Introduction

Endothelium-derived relaxing factors (EDRFs), including nitric oxide (NO), are responsible for mediating endothelium-dependent vasorelaxation (Flammer and Luscher 2010). In addition to inducing vasorelaxation, NO also has other key vasoprotective properties such as preventing aggregation of platelets, activation/adhesion of neutrophils, expression of cell adhesion molecules and oxidation of low density lipoprotein (oxLDL) (Naseem 2005, Bian, Doursout et al. 2008). Nitric oxide is generated by endothelial nitric oxide synthase (eNOS), which is constitutively expressed by vascular endothelial cells, in response to shear stress or agonist stimulation (Fleming and Busse 2003). Reduced NO bioavailability underlies the development of endothelial dysfunction, and a key factor limiting NO availability is increased production of superoxide anion ($O_2^{\cdot -}$) ; which reacts with NO to produce the unstable radical and potent oxidant peroxynitrite ($OONO^{\cdot -}$) (Bonomini, Tengattini et al. 2008), which is a radical species that promotes endothelial dysfunction.

Multiple anthocyanins have been shown to increase NO-dependent vasorelaxation in rat thoracic aortic and porcine coronary arterial ring models (Bell and Gochenaur 2006, Ziberna, Lunder et al. 2010) and cyanidin-3-glucoside (C3G) has been shown to increase eNOS expression and activity in bovine artery endothelial cells (Xu, Ikeda et al. 2004a, Xu, Ikeda et al. 2004b). In addition, anthocyanins have demonstrated similar activity in human endothelial cell models (Lazze, Pizzala et al. 2006, Edirisinghe, Banaszewski et al. 2011). The flavanol epicatechin, which is structurally similar to cyanidin, has also been shown to reduce $O_2^{\cdot -}$ production in endothelial cells, (Steffen, Schewe et al. 2007b, Steffen, Gruber et al. 2008), thus preserving NO bioavailability in the vasculature (Cassidy, O'Reilly et al. 2010). The present study aims to establish if anthocyanin metabolites have similar effects on vascular function as reported previously for anthocyanins and flavanols.

In the present study, C3G and its recently identified phenolic metabolites (Czank, Cassidy et al. 2013) (**Figure 3.1**) were screened for their effects on the production of stimulated $O_2^{\cdot -}$ and eNOS expression in human umbilical vein endothelial cells (HUVECs), to assess relative vascular bioactivity. In addition, the activity of the selected treatment compounds on endothelin-1 (ET-1) expression was explored, as ET-1 is a known biomarker of endothelial dysfunction which elicits vasoconstriction thus counteracting the vasodilator activity of NO (Lazze, Pizzala et al. 2006). The cytotoxicity of selected compounds was previously established in-house using WST-1 method at 0.05, 0.1, 10 and 100 µM (refer to Appendix 1 for cytotoxicity data).

Figure 3.1 C3G and its phenolic metabolites screened for vascular activity[1]

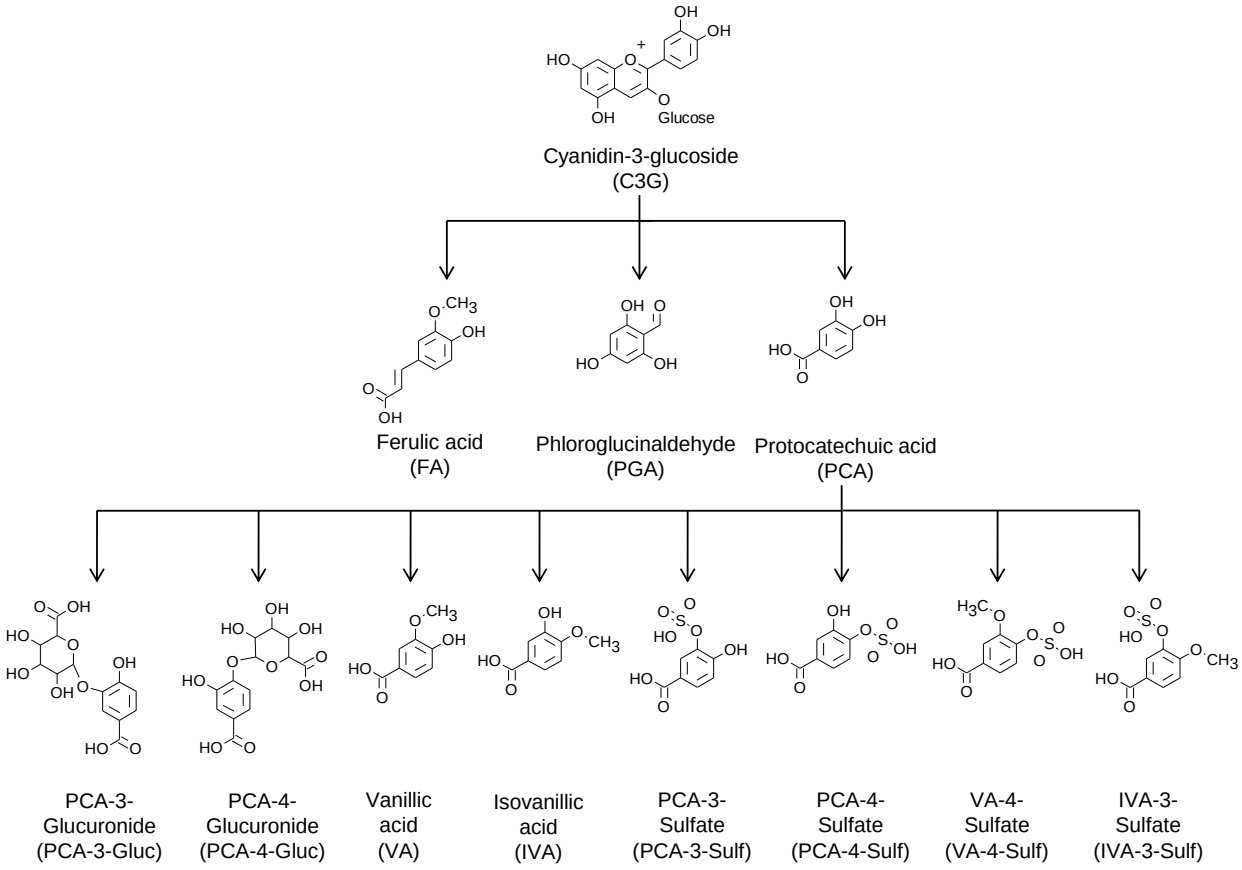

[1]Recently identified C3G phenolic metabolites (Czank, Cassidy et al. 2013).

3.2 Methods and materials

Standards and reagents. Angiotensin II was obtained from Tocris (Bristol, UK) and VAS2870 from Enzo Life Sciences [Exeter, United Kingdom (UK)]. Quantikine® enzyme-linked immunosorbent assay (ELISA) kits for eNOS (R&D, DEN000) and ET-1 (R&D DET100) were

purchased from R&D Systems (Abingdon, UK). ELISA quantification was performed using an Omega BMG plate reader (BMG Labtech, Aylesbury, UK). CPH probe (1-hydroxy-3-carboxy-2,2,5,5-tetramethylpyrrolidine), electron spin resonance (ESR)-Krebs-HEPES buffer, chelators DF (deferoxamine methanesulfonate) and DETC (diethyldithiocarbamic acid sodium) were purchased from Noxygen (Elzach, Germany).

Stimulated superoxide ($O_2^{\cdot -}$) production [cytochrome c assay, (Steffen, Gruber et al. 2008)]. As described in methods chapter (chapter 2), HUVEC were cultured in fibronectin coated 24-well plates were stimulated with angiotensin II (Ang II; 0.1µM) and co-incubated with 0.1, 1 and 10µM of treatment compounds for 6 hours in medium 199. Cytochrome c reduction by generated superoxide was established by parallel incubations with or without 100U superoxide dismutase (SOD). The specificity of the assay was confirmed by incubating HUVECs with 5 µM of VAS2870, a selective NOX inhibitor (Stielow, Catar et al. 2006, ten Freyhaus, Huntgeburth et al. 2006, Altenhofer, Kleikers et al. 2012). Supernatants were transferred to 96-well plates and cytochrome c reduction was measured at 550 nm (reference wavelength 620 nm) using micro plate reader [Fluostar Omega or Polarstar Optima, BMG Labtech (Aylesbury, UK)]. Plates containing HUVECs were stored at -80°C until cell harvesting for protein quantification and normalisation of absorbance data The cells were thawed and incubated with 150µL lysis buffer (1% IGEPAL® CA-630, 10% glycerol, 150mM NaCl, and 20mM Tris, pH 8.0) for 30 minutes at 4°C.

Thereafter, cells were removed from culture plates by scraping, and cell disruption performed by oscillation with acid washed glass beads at 50Hz for 5 minutes (Qiagen Tissue Lyser) followed by centrifugation of lysates for 15 minutes (4°C, 13,000 rpm). Protein quantification of supernatants was performed using the Pierce BCA Protein Assay Kit according to the manufacturer's instructions.

Stimulated O_2^{-} production (EPR probe assay). Confluent HUVECs were incubated with HUVEC media (untreated) or treatment compounds (PCA or VA) at 0.1, 1 or 10 µM for 24 hours in 24 well plates; followed by washing with chelators in ESR-Krebs-HEPES buffer solution. HUVECs were then incubated with CPH probe and Ang II (0.1 µM), Ang II + SOD (100 U/mL), pyrogallol (400 µM) or pyrogallol + SOD for 30 minutes, after which supernatants were collected and centrifuged at 300 x *g* for 5 minutes before storage in liquid

nitrogen. All samples were shipped on dry ice to Prof Malcom Jackson's Laboratory, at the Institute of Ageing and Chronic Disease, University of Liverpool (Liverpool, UK) and were analysed by electron paramagnetic resonance (EPR) spectroscopy (Bailey, Davies et al. 2003)for measurement of superoxide radical production using E-Scan(Bruker, Coventry, UK) according to in-house procedures.

Cell treatments for eNOS and ET-1 expression assay. Confluent HUVECs, cultured on fibronectin (0.25µg/cm^2) coated 24-well plates, were incubated with culture media (untreated), vehicle control (0.05% DMSO in cell media) or treatment compounds at 0.1, 1 or 10 µM for 24 hours. Supernatants were collected, and cells harvested in 500 µL of trypsin/EDTA:trypsin-blocking solution (1:1 ratio) before storage at -80°C until assay for ET-1 or eNOS expression by ELISA. Simvastatin was used as a positive control for ET-1 expression.

eNOS enzyme-linked immunosorbent assay (ELISA). eNOS protein quantification in HUVEC lysates was performed with a commercially available ELISA (Quantikine, R&D Systems), using a microplate pre-coated with monoclonal anti-eNOS. Briefly, harvested HUVECs were thawed, prior to centrifugation at 10,000 rpm for 10 minutes and discarding of supernatants. Cells were then lysed at 2-8°C using assay lysis buffer, and centrifuged at 5000 rpm for five minutes; the resulting supernatants were subsequently assayed in duplicate (100 µL/well). Assay diluent (100 µL) was added to each well, and plates incubated for two hours at room temperature with agitation (500 rpm). Polyclonal anti-eNOS (conjugated to horseradish peroxidase) was then added to each well (200 µL/well), and plates were incubated for a further two hours. Any unbound antibody was removed by washing; and 200 µL/well substrate solution was added prior to a 30 minute incubation. After addition of 50 µL/well stop solution, end-point absorbance was measured at 450 nm (reference 540 nm) with a micro plate reader [Fluostar Omega, BMG Labtech (Aylesbury, UK)]; and eNOS quantified based upon a standard curve generated using a recombinant human eNOS standard. The intra-assay coefficient of variation (CV) was 4.27% ± 1.15% [mean ± standard deviation (SD), n=3] and the inter-assay CV was 5.90% (n=3, refer to appendix 2 for standard curve).

ET-1 ELISA. ET-1 protein production was quantified with a commercially available ELISA kit (Quantikine, R&D Systems), using a microplate pre-coated with rat monoclonal anti-ET-1.

Briefly, supernatants were thawed, prior to centrifugation at 10,000 rpm for 10 minutes, and then used as samples for ET-1 quantification. Assay diluent (150 µL) was added to each microplate well used, followed by samples (75 µL/well) of supernatants, and plates incubated for one hour at room temperature with agitation (500 rpm). Mouse monoclonal anti-ET-1 conjugate (conjugated to horseradish peroxidase) was added to each well (200 µL/well), and plates incubated for a further three hours. Any unbound antibody was removed by washing; and 200 µL/well substrate solution was added prior to a 30 minute incubation. After addition of 50 µL/well stop solution, end-point absorbance was measured at 450 nm (reference 540 nm) with a microplate reader [Fluostar Omega, BMG Labtech (Aylesbury, UK)]; and ET-1 quantified based upon a standard curve generated using a synthetic ET-1 standard. Simvastatin (20 ng/ml) was screened as a positive control for ET-1 expression(Mraiche, Cena et al. 2005). The intra-assay CV was 5.15% ± 1.86% (n=3) and the inter-assay CV was 4.99% (n=3, refer to appendix 3 for standard curve).

RT-qPCR reference gene validation. RT-qPCR method validation was conducted to establish the optimal endogenous reference genes for normalisation of C_t data for genes of interest using a geNorm^{PLUS} kit (PrimerDesign Ltd). Primer sets for six stably expressed human reference genes used for this validation were designed (pre-validated) and provided by PrimerDesign Ltd. RNA extraction and real-time PCR were performed as described in the general methods chapter.

Confluent HUVECs were incubated with culture medium only (untreated), PCA, VA, PCA-3-Gluc or PCA-3-Sulf (at 10µM) for 24 hours. Following RNA extraction and cDNA synthesis, real time PCR was utilised to evaluate reference gene expression. C_t values generated by real time PCR were analysed using the geNorm function in qbase^{PLUS} software (version 2.3, Biogazelle NV, Zwinaarde, Belgium) to examine the optimal number of reference genes, **Table 3.1** and **Figure 3.2**) and stability of reference genes across various treatments (**Figure 3.3**) (Vandesompele, De Preter et al. 2002). Based on geNorm V values (Figure 3.2) it was apparent that there was no additional benefit gained by using more than two reference genes, as the geNorm V value for using two reference genes or more was below 0.15. UBE2D2 and PRDM4 were identified as the most stable reference genes (Figure 3.3) and were used in the final methodology.

Table 3.1 List of geNorm reference genes evaluated for their relative stability

Gene	Description
VIPAR	VPS33B interacting protein
TYW1	tRNA-γW synthesizing protein 1 homologue (*S. Cerevisiae*)
UBE4A	Ubiquitination factorE4A
PIPA	Peptidylprolyl isomerase A (cyclophilin A)
UBE2D2	Ubiquitin-conjugating enzyme E2D 2
PRDM4	PR domain containing 4

Figure 3.2 Determination of optimal number of reference genes for untreated HUVECs.

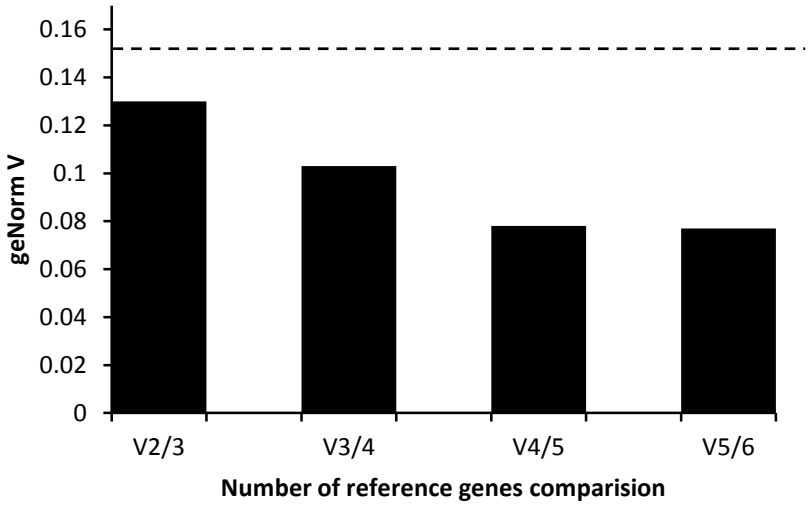

geNorm V chart demonstrating optimal number of reference genes. "V2/3" indicates comparison between use of 2 reference genes vs 3 reference genes (V3/4 indicates comparison between 3 and 4 genes, etc) across various treatments (unstimulated, or incubation with 10μM of PCA, VA, PCA-3-Gluc or PCA-3-Sulf). geNorm V value below 0.15 (dotted line) indicates no additional benefit from using a higher number of reference genes.

Figure 3.3 Average reference gene expression stability in untreated HUVECs or following incubation with phenolic metabolites for 24 hours

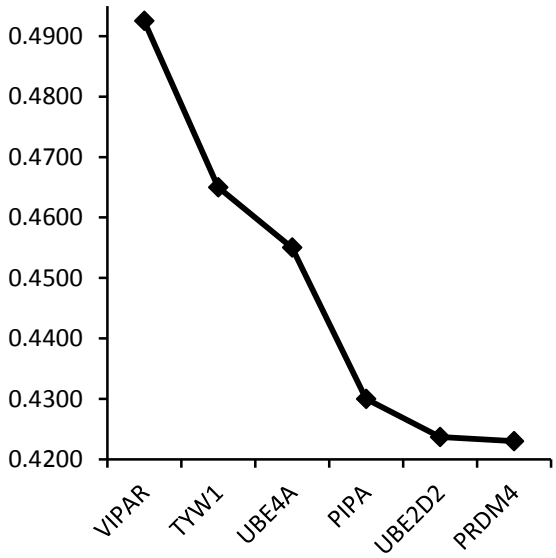

geNorm M chart illustrating average stability of reference genes (y-axis – geNorm M value) following various cell treatments (unstimulated, or incubation with 10 µM of PCA, VA, PCA-3-Gluc or PCA-3-Sulf).

The target gene (eNOS) was normalised against two geNorm reference genes, UBE2D2 and PRDM4, validated based on their expression stability (as established above) following exposure to the treatment compounds used for screening. Gene expression was quantified using the comparative C_t method (Schmittgen and Livak 2008) incorporating the geometric mean of reference genes as the normalisation factor. The forward and reverse primer sequences for eNOS were ACA AGA GTT ATA AGA TCC GCT TCA A and CCT GCA CTG TCT GTG TTA CTG respectively.

3.3 Results

Ang II-induced superoxide production in HUVECs

Stimulation of HUVECs with Ang II did not produce quantifiable increases in $O_2^{\cdot-}$ relative to basal un-stimulated cells (p=0.69, n=4, **Figure 3.4A**). In addition, there was no significant difference observed between untreated and vehicle control (0.05% DMSO, 102±3.1% relative to untreated control, p>0.05 – data not shown) HUVECs. However, when HUVECs were pre-incubated with VAS2870, an established NOX inhibitor (Stielow, Catar et al. 2006, Altenhofer, Kleikers et al. 2012), 80.5±3.2% of Ang IIstimulated $O_2^{\cdot-}$ production was

decreased. None of the selected compounds were cytotoxic, as established previously in house, at any concentration tested (refer to Appendix 1).

Figure 3.4 Production of superoxide measured by cytochrome c reduction in HUVECs following incubation with Ang II or Ang II and VAS2870

A)

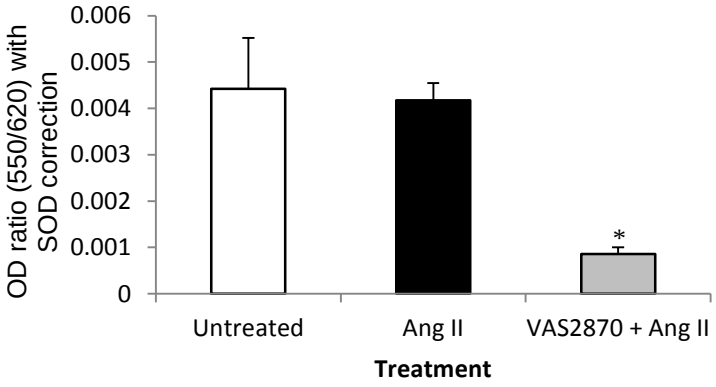

B)

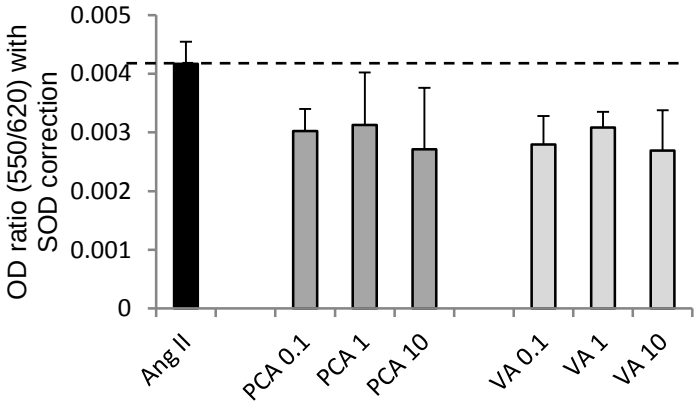

Superoxide production in cultured HUVEC following incubation with cell media untreated (basal), Ang II (100 nM/mL), or Ang II + VAS2870 (5 µM) for 6 hours (A), and with Ang II + PCA or VA at 0.1, 1 and 10 µM. Supernatants were used to quantify reduction of cytochrome c by generated superoxide, using parallel incubations with or without SOD (100 U/mL). All data are expressed relative to Ang II-induced superoxide production as SOD-corrected mean OD ratio (n=4). *p < 0.05 relative to Ang II control. Ang II, angiotensin II; PCA, protocatechuic acid, VA, vanillic acid

The screened treatment compounds were unable to alter superoxide ($O_2^{\cdot-}$)levels following stimulation of HUVEC with Ang II (p=0.91, Figure 3.4B). A representative graph (Figure 3.4B) summarising effects of PCA and VA on Ang II-stimulated $O_2^{\cdot-}$ shows no effect due to treatment compounds.In addition, Ang II-induced $O_2^{\cdot-}$ production was also measured through quantification of $CP^{\cdot}$ion, the direct oxidation product of the CPH probe by $O_2^{\cdot-}$, using electron paramagnetic resonance (EPR) spectroscopy. Again, no increase in $O_2^{\cdot-}$production was detected (p=0.81, n=4, **Figure 3.5**) following Ang II stimulation or vehicle control (0.05% DMSO+ESR-Krebs-HEPES buffer solution, 102±4.0% of untreated p>0.05 – data not shown).

The specificity of the assay was confirmed by using pyrogallol as an external oxidising agent (Bell and Gochenaur 2006)to generate CP ion, which resulted in ≈17 fold higher (42.2±1.3 µM) levels of CP ion as compared to the Ang II-stimulated HUVECs ($p<0.001$, n=4, Figure 3.5). Therefore the absence of a discernible endothelial response to Ang II stimulation substantiates the lack of response by the screened treatments.

Figure 3.5 Production of superoxide measured by EPR probe in HUVECs following incubation with Ang II or pyrogallol

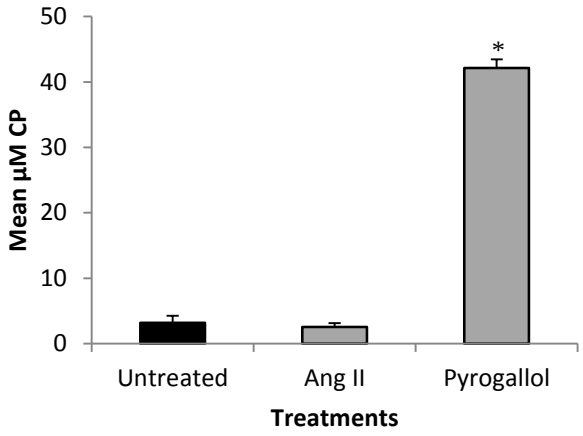

Superoxide production following incubation of HUVEC with Ang II (100 nM/mL) or pyrogallol (400 µM) and CPH probe for 30 minutes. Supernatants were used to quantify oxidation of CPH probe by measuring CP ion concentration. All data are expressed relative to Ang II-induced superoxide as mean concentration of CP (n=4). *$p<0.05$ relative to untreated. Ang II, angiotensin II.

eNOS expression in HUVECs

eNOS expression in vehicle control (0.05% DMSO, 98.4±3.1% of untreated, $p>0.05$, data not shown) was non-significant to the production in untreated HUVECs. Of the 12 treatment compounds tested, 3 compounds significantly increased basal eNOS protein production [by >153.4±23.2% ($p<0.001$)] relative to untreated (basal) HUVEC, and 3 significantly decreased eNOS levels by >51.4±4.3% of basal ($p<0.001$). C3G, PGA and VA all increased eNOS expression, with the maximum increase elicited by VA (357.1±2.0%, $p<0.001$, **Figure 3.6**). In contrast, PCA, PCA-4-Sulf and PCA-3-Sulf reduced eNOS protein expression, with the maximal observed reduction induced by PCA-3-Sulf (59.1±5.3%, $p<0.001$, Figure 3.6).

Figure 3.6 Effect of C3G and its metabolites on basal eNOS expression in HUVECs.

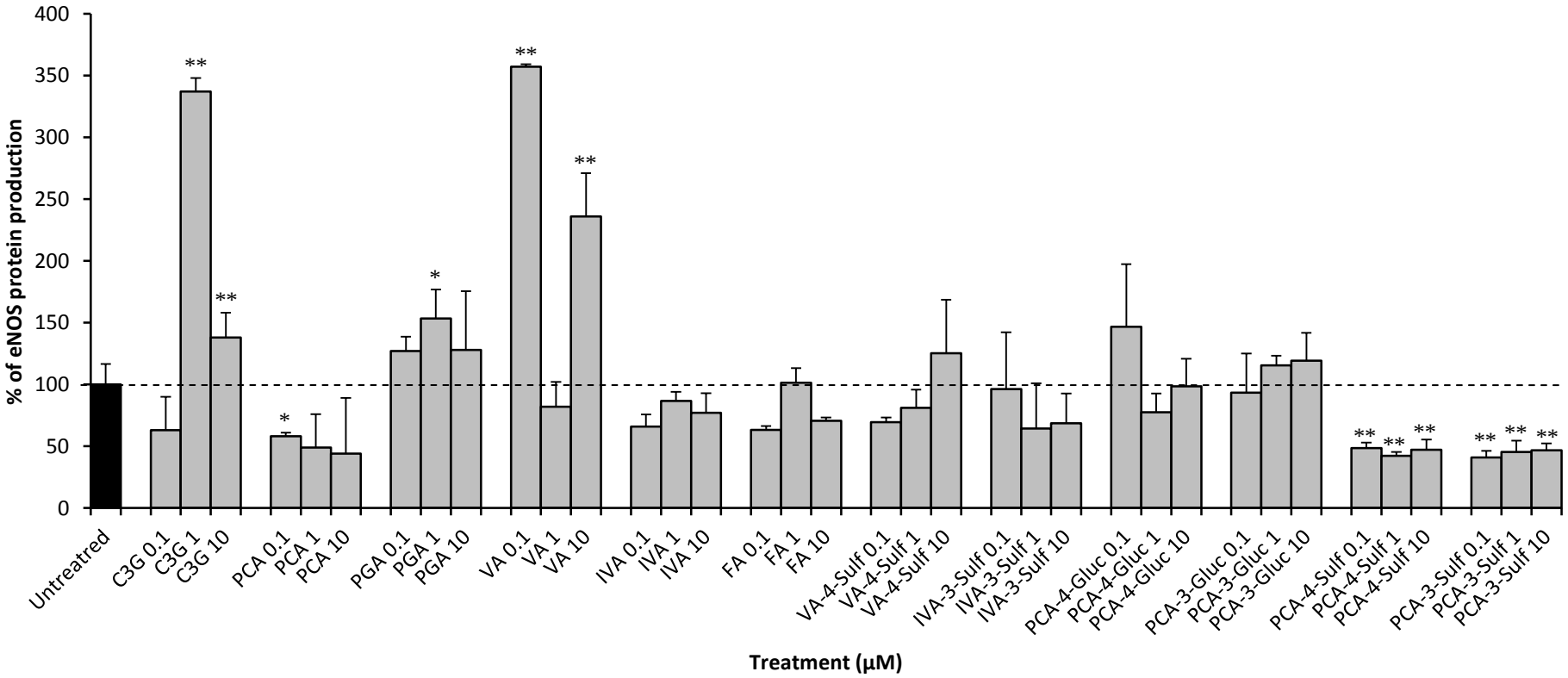

HUVECs incubated with C3G or phenolic metabolites for 24 hours at 0.1, 1, 10 µM. All data expressed as mean percentage (± SD, n=3) of untreated (basal) HUVECs. Absolute eNOS protein value in untreated HUVECs - 126.0 pg/mL, standard range: 62.5 – 4000 pg/mL. **p<0.001, *p<0.01 (ANOVA with Tukey post-hoc) relative to untreated control.C3G, cyanidin-3-glucoside; PCA, protocatechuic acid, PGA, phloroglucinaldehyde; FA, ferulic acid; VA, vanillic acid; IVA, isovanillic acid; PCA-4-Gluc, PCA-4-glucuronide; PCA-3-Gluc, PCA-3-glucuronide; PCA-4-Sulf, PCA-4-sulfate; PCA-3-Sulf, PCA-3-sulfate; VA-4-Sulf, VA-4-sulfate; IVA-3-Sulf, IVA-3-sulfate.

eNOS mRNA levels in HUVECs

Treatment compounds which altered basal eNOS protein concentrations in HUVECs were subsequently screened (at 10 µM) for their effects on eNOS mRNA levels. PGA, VA and PCA-3-Sulf significantly reduced eNOS mRNA levels by >44.4±7% relative to basal (untreated) cells, with the greatest reduction elicited by PGA (69.3±15.2%, p<0.05, **Figure 3.7**).

Figure 3.7 Effect of C3G and selected phenolic metabolites on basal eNOS mRNA levels in HUVECs

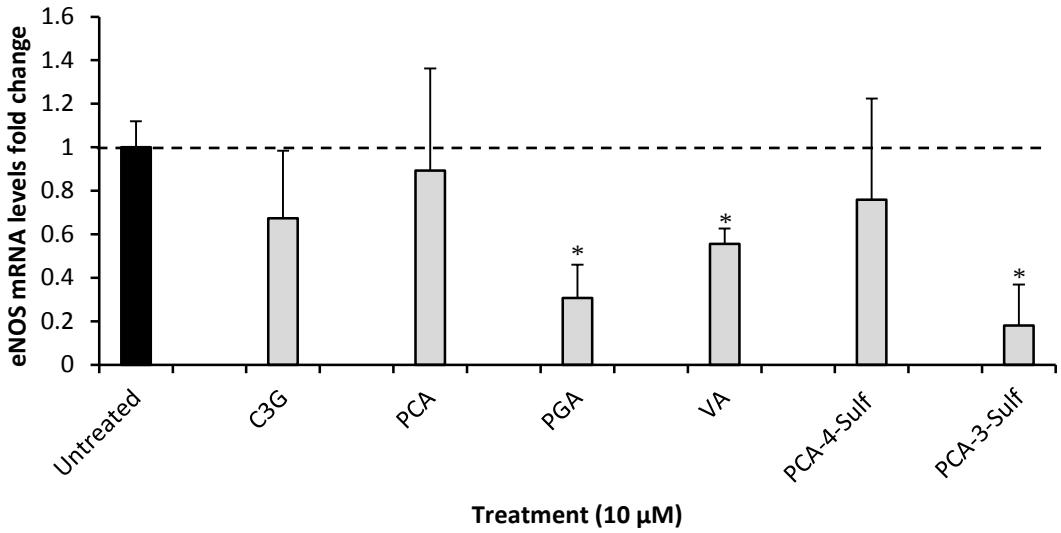

Fold change in untreated (basal) levels of eNOS mRNA in HUVECs incubated with C3G or phenolic metabolites (at 10 µM) for 24 hours. All data expressed graphically as mean fold change (± SD, n=3) relative to basal levels. *p<0.05 (ANOVA with Tukey post-hoc) relative to untreated control. C3G, cyanidin-3-glucoside; PCA, protocatechuic acid; PGA, phloroglucinaldehyde; VA, vanillic acid; PCA-4-Sulf, PCA-4-sulfate; PCA-3-Sulf, PCA-3-sulfate.

ET-1 expression in HUVECs

ET-1 protein production in cultured HUVEC was not modulated following incubation with treatment compounds at 0.1, 1 or 10 µM (**Table 3.2**); however, simvastatin (10 µM) significantly reduced ET-1 protein levels relative to untreated HUVECs (49.1±6.8%, p<0.05), confirming the relevance of the assay.

3.4 Discussion

Increased consumption of dietary anthocyanins has been associated with reduced risk of cardiovascular disease (CVD) (Cassidy, O'Reilly et al. 2010, Cassidy, Mukamal et al. 2013); however the mechanisms of bioactivity of anthocyanins remain relatively elusive. The majority of previous *in vitro* studies have explored the mechanisms of action of parent/un-metabolised forms of anthocyanins, which hold limited physiological relevance, as they are

not found in the circulation at any appreciable concentration and have extremely short half-lives.

Table 3.2: Endothelin-1 protein production in presence of treatment compounds

Compound	Concentration	ET-1
		Mean±SD
Vehicle Control		101±7.1
C3G	0.1 µM	102.4±4.0
	1 µM	121.3±1.5
	10 µM	106.5±13.2
PCA	0.1 µM	124.0±7.8
	1 µM	99.0±4.5
	10 µM	125.3±8.6
PGA	0.1 µM	120.8±1.8
	1 µM	130.5±4.3
	10 µM	113.4±10.9
VA	0.1 µM	109.1±3.4
	1 µM	119.6±4.8
	10 µM	117.9±3.2
IVA	0.1 µM	108.0±9.9
	1 µM	128.0±3.9
	10 µM	119.9±10.0
PCA-4-gluc	0.1 µM	111.3±11.4
	1 µM	120.1±1.8
	10 µM	107.5±2.1
PCA-3-gluc	0.1 µM	131.6±11.6
	1 µM	131.6±8.1
	10 µM	115.5±5.4
PCA-4-sulfate	0.1 µM	107.5±3.5
	1 µM	115.9±22.0
	10 µM	122.7±11.5
PCA-3-sulfate	0.1 µM	115.1±6.5
	1 µM	115.7±14.5
	10 µM	115.6±5.6
VA-4-Sulf	0.1 µM	130.4±11.1
	1 µM	131.7±3.2
	10 µM	127.1±5.3
IVA-3-Sulf	0.1 µM	136.4±2.6
	1 µM	127.4±4.8
	10 µM	127.6±5.4
FA	0.1 µM	129.1±9.0
	1 µM	109.7±2.2
	10 µM	115.9±5.7

HUVECs incubated with C3G or phenolic metabolites for 24 hours at 0.1, 1, 10 µM. All data expressed as mean percentage (± SD, n=3) of untreated Absolute ET-1 protein value in untreated HUVECs – 13.1pg/mL, standard range: 0.33 – 250pg/mL. *$p<0.05$ (ANOVA with Tukey post-hoc) relative to vehicle control.C3G, cyanidin-3-glucoside; PCA, protocatechuic acid, PGA, phloroglucinaldehyde; FA, ferulic acid; VA, vanillic acid; IVA, isovanillic acid; PCA-4-Gluc, PCA-4-glucuronide; PCA-3-Gluc, PCA-3-glucuronide; PCA-4-Sulf, PCA-4-sulfate; PCA-3-Sulf, PCA-3-sulfate; VA-4-Sulf, VA-4-sulfate; IVA-3-Sulf, IVA-3-sulfate.

Therefore the current study investigated the relative vascular bioactivity of newly identified anthocyanin metabolites, utilising novel pure synthetic sulfate and glucuronic acid phenolic conjugates (Zhang, Botting et al. 2011), with the aim of elucidating anthocyanins true *in vivo* biological activity.

The major finding of the present study is that degradation and subsequent metabolism of C3G alters the bioactivity of the anthocyanin. The eNOS screen indicated differential activity of phenolic metabolites relative to the parent compound. Comparative to unstimulated (basal) HUVECs, three of the 12 compounds tested increased eNOS levels and three compounds decreased eNOS (Figure 3.6), with the largest increase in eNOS protein elicited by the methylated form of PCA, VA. Cyanidin-3-glucoside also increased eNOS expression which is in accordance with previously published studies (Xu, Ikeda et al. 2004a, Xu, Ikeda et al. 2004b). Interestingly, the A-ring degradant of C3G, PGA, increased eNOS levels compared to untreated HUVECs, whereas the B-ring degradant PCA decreased eNOS expression; suggesting degradation of C3G resulting in a smaller phenolic acid with a catechol group has inhibitory effects on expression of eNOS. Metabolism of PCA via 3'-methylation of the catechol group, generating VA, resulted in a significant elevation in HUVEC eNOS expression, although 4'-methylation, producing IVA had no effect; suggesting activity is conjugation site specific (3' vs 4'). Moreover, not all conjugates of the phenolic acid catechol resulted in increased bioactivity, as both forms of sulfated PCA decreased eNOS protein below basal levels and appeared to result in a biologically unfavourable transformation.

In order to investigate the mechanisms by which bioactive metabolites of C3G potentially modulated eNOS expression, their effects on eNOS mRNA levels were examined. Interestingly, none of the compounds tested increased HUVEC eNOS mRNA levels following 24 hour incubation; in fact, PGA, VA and PCA-4-Sulf decreased mRNA levels relative to basal (Figure 3.7). The observed discrepancy between mRNA levels and protein concentrations may be due to a single time point measurement of mRNA levels, and the use of multiple and/or shorter time points may provide more insight to the correlation between mRNA and protein levels of eNOS.

The present study also investigated the effects of C3G and its metabolites on Ang II-stimulated $O_2^{\cdot-}$ production in HUVECs. The Ang II stimulation of HUVECs did not appear to

result in detectable $O_2^{\cdot-}$ production as measured by reduction of cytochrome c. In order to confirm if they assay system is responsive, the HUVECs were pre-incubated with VAS2870 which attenuated $O_2^{\cdot-}$ below basal levels confirming the involvement of NOX enzymes in reduction of cytochrome c reduction via $O_2^{\cdot-}$ production. Though, reduction of cytochrome c has previously been used to quantify Ang II-stimulated $O_2^{\cdot-}$ production in HUVECs (Steffen, Schewe et al. 2007b), and therefore, in order to confirm the stimulatory effect of Ang II on HUVECs to produce $O_2^{\cdot-}$, an EPR method was employed which is considered a gold standard in analysing extremely unstable radicals including $O_2^{\cdot-}$(Dikalov, Kirilyuk et al. 2011). The results from EPR experiment clearly suggest that there was no induction in $O_2^{\cdot-}$ production achieved due to Ang II-stimulation and confirms the findings from cytochrome c assay in the present study that Ang II-stimulation does not yield $O_2^{\cdot-}$ in present assay system. Ang II stimulates $O_2^{\cdot-}$ production via AT1 receptor, however if Ang II interacts with AT2 receptor it functionally antagonises AT1 and it produces H_2O_2(Sohn, Raff et al. 2000). HUVECs express AT2 receptor and it can be hypothesised that the observed lack of effect of Ang II stimulation on HUVECs may be due to Ang II acting via AT2 receptor and therefore producing H_2O_2 instead of $O_2^{\cdot-}$. However, further research is required to confirm this hypothesis, perhaps by blocking of AT1 and/or AT2 receptors (Candesartan and PD123319 - AT1 and AT2 blockers respectively)(Sohn, Raff et al. 2000).

A limitation of the present investigation was the use of HUVECs, which are a well characterised cell type for endothelial research; however a different cell type such as human aortic endothelial cells could provide greater insight to the bioactivity of screened compounds. Another limitation of the present study was that the 1 and 10 µM doses of C3G utilised were relatively high compared to the plasma levels of C3G previously reported (often less than 0.1 µM) (Manach, Williamson et al. 2005, McGhie and Walton 2007). Czank et al(2013) recently reported a maximal serum level of C3G around 0.14 µM following consumption of 500 mg of pure ^{13}C-labelled C3G (Czank, Cassidy et al. 2013), thus bioactivity of C3G observed in the present study may not be biologically relevant. The levels of the phenolic acids used in the present study are more physiologically relevant as Czank et al described maximal serum concentrations of phenolic metabolites up to 2.5 µM (Czank, Cassidy et al. 2013), and therefore the findings from this study for metabolites are physiologically more relevant. Moreover, lack of correlations between protein and mRNA levels of eNOS may be a result of single time point examination of eNOS mRNA levels and time course may beprovide better correlation between eNOS mRNA and protein.

The bioactivity of phenolic metabolites of C3G reported in the current investigation appears to be specific for eNOS, as no effects were observed on endothelial production of the vasoconstrictor ET-1 at basal levels (Table 2.2), which is in contrast to existing data of C3G activity on basal ET-1 as Lazze et alreported that C3G decreased basal ET-1 levels however, the activity of C3G was noticed at supraphysiological concentration (50 and 100 µM) whereas in the present study lower concentrations of C3G were investigated. Although, ET-1 production in stimulated conditions, such as use of insulin (Yang and Li 2008), may provide better insights to the activity of selected compounds on ET-1. In addition, there was no effect of the treatments on stimulated endothelial superoxide production, however the modulation of basal superoxide production by Ang II was not indicated using two different methodologies [reduction of cytochrome c and reduction of EPR sensitive CPH probe (Figure 3.4 and Figure 3.5] suggesting using a different, more potent and physiologically relevant stimuli such as oxLDL should be considered (Heinloth, Heermeier et al. 2000). In addition, if using HUVECs the use of AT2 receptor blocker should be considered to minimize H_2O_2 production and therefore increasing selectivity of Ang II towards AT1 receptor and therefore superoxide production. Also use of arterial cell line such as human coronary artery endothelial cells (HCAECs) which may have better expression of NOX family of enzymes (Bonomini, Tengattini et al. 2008) could be considered. In addition, a combine use of better stimuli (oxLDL) and cell type (HCAECs) may provide improved method for $O_2^{\cdot-}$ stimulation in current model. It should also be considered that *in vivo* modulation of eNOS up-regulation and production of $O_2^{\cdot-}$are influenced by shear stress (Boo and Jo 2003, Hwang, Ing et al. 2003, Hsiai, Hwang et al. 2007)and presence of many different types of cells such as smooth muscle cells, arterial cells, neutrophils. Therefore, future research of vascular activity should focus on using co-culture models where two or more types of cells under laminar flow and/or shear stress to produce *in vivo* like conditions.

In conclusion, the intact/un-metabolised anthocyanin (C3G), and its phenolic degradants and metabolites, have differential bioactivity towards eNOS expression and the activity of the metabolites appears to be regulated by conjugation of the B-ring catechol moiety; however, not all modifications elicited apparent biologically favourable vascular effects. As some metabolites had stimulatory effects on eNOS expression while others inhibitory effects, the positive impact of anthocyanin consumption on vascular homeostasis as reported in the literature (human epidemiological and RCT studies) is likely the effects of

multiple metabolites acting on several enzyme systems. Further studies are needed to explore these activities.

Chapter 4. Effects of cyanidin-3-glucoside and its metabolites on VCAM-1 expression in HUVECs

4.1 Introduction

Vascular cell adhesion molecule-1 (VCAM-1) is a transmembrane protein that is expressed by vascular endothelial cells following exposure to inflammatory stimuli (Fotis, Giannakopoulos et al. 2012), including oxidised low density lipoprotein (oxLDL) (Basyouni, Ahmed et al. 2012, Huang, Lin et al. 2013) and cluster of differentiation 40 ligand (CD40L)(Kotowicz, Dixon et al. 2000, Xia, Ling et al. 2009). VCAM-1 plays a vital role in the pathogenesis of atherosclerosis, particularly during early stages, by facilitating the adhesion of monocytes and leucocytes to the endothelium (Cybulsky, Iiyama et al. 2001, Fotis, Giannakopoulos et al. 2012). After rolling of the leucocytes, VCAM-1 ensures their firm attachment to the endothelial layer which leads to endothelial transmigration of leucocytes. This transmigration activates numerous downstream chronic inflammatory responses and therefore progression of atherosclerosis (Zheng, Qian et al. 2005, Preiss and Sattar 2007). The role of VCAM-1 in the progression of atherosclerosis has been demonstrated by Iiyama et al., where elevated levels of VCAM-1 were observed at atherosclerotic plaques and lesions prone to rupture in rabbit and mice models (Iiyama, Hajra et al. 1999). In addition, the down-regulation of VCAM-1 mRNA levels in LDL receptor$^{-/-}$ and apolipoprotien E $^{-/-}$ (Apo E$^{-/-}$) mice impaired the adhesion of monocytes to the endothelial layer, leading to a reduction in the development of atherosclerosis, thereby indicating the vital role of VCAM-1 in the progression of this disease (Cybulsky, Iiyama et al. 2001, Dansky, Barlow et al. 2001).

The anti-inflammatory activities of anthocyanins, in an extract or a purified form, on VCAM-1 production have previously been reported where consumption of 320 mg/day anthocyanins for 24 weeks (Zhu, Ling et al. 2013) resulted in significantly lower plasma levels of VCAM-1. Similarly, mice fed with purple potato also resulted in decreased plasma level of VCAM-1 compared to control group (Miyazaki, Makino et al. 2008). In addition, various *in vitro*studies also showed effect on VCAM-1 levels, for example, anthocyanins from black soy beans reduced VCAM-1 production in tumor necrosis factor – α (TNF-α) stimulated human

umbilical vein endothelial cells (HUVECs) and bovine aortic endothelial cells (BAECs) (Kim, Tsoy et al. 2006, Nizamutdinova, Kim et al. 2009). A pure anthocyanin, cyanidin-3-glucoside (C3G) at 1, 10 and 100μM, reduced VCAM-1 production in CD40L-stimulated HUVECs in a dose-dependent manner (Xia, Ling et al. 2009). Given that anthocyanins degrade during passage through the gastro intestinal tract (GIT), such that very limited amounts of parent anthocyanins (if any) are seen in the blood (Czank, Cassidy et al. 2013), it is possible that the observed anti-inflammatory effects of anthocyanins may result from the action of their degradation products and subsequent metabolites of these degradation products rather than the parent compound alone. Therefore the effects of anthocyanin metabolites on VCAM-1 expression need to be investigated and is the focus of the current chapter; where C3G and 11 of its recently identified metabolites (Figure 3.1) including 6 novel synthetic metabolites, were investigated for their effects on VCAM-1 production. Protocatechuic acid (PCA), the B-ring degradant of C3G, has been demonstrated to reduce VCAM-1 production in TNF-α-induced mouse aortic endothelial cells at 20 and 40μM (Wang, Wei et al. 2010). These initial *in vitro* studies indicate that C3G and its metabolites may elicit anti-inflammatory activity, at least in part, by attenuating VCAM-1 production in endothelial cells.

The present study investigated C3G, the most abundant dietary anthocyanins in the UK, and its 11 recently identified metabolites for their anti-inflammatory activity against VCAM-1 production in oxLDL- and CD40L-stimulated endothelial cells (HUVECs). The final concentrations of compounds screened in the current study were 0.1, 1 and 10μM. The soluble form of VCAM-1 is considered a representative marker to examine the expression of VCAM-1 production (Videm and Albrigtsen 2008), therefore soluble VCAM-1 production in oxLDL- and CD40L-stimulated HUVECs was quantified using commercially available enzyme-linked immunosorbent assay (ELISA) and real time reverse transcription-quantitative polymerase chain reaction (RT-qPCR) was utilised to quantify VCAM-1 mRNA levels.

4.2 Methods and materials

Standards and Materials.

RPMI 1640 media, foetal bovine serum (FBS), glutamine and penicillin/streptomycin were from PAA (Kent, UK). D1.1 cells (a sub-clone of Jurkat cell line constitutively expressing CD40L (Lederman, Yellin et al. 1992)) were generously provided by Dr. Maria O'Connell, Department of Pharmacy, University of East Anglia (Norwich, UK). Agarose and Cu_2SO_4 were purchased from Sigma-Aldrich (Dorset, UK). Monoclonal antibody against CD40 was purchased from Enzo Bioscience (Cambridge, UK). LDL was purchased from Millipore (UK). DuoSet ELISA kits VCAM-1 (DY809)], flat bottom clear polystyrene 96-well ELISA plates (DY990) and reagent diluent (DY995) were purchased from R&D systems (Europe, UK). ELISA protein quantification was established using an Omega BMG plate reader (BMG Labtech, Aylesbury, UK).

Cell culture – D1.1 Jurkat cells. D1.1 cells were routinely cultured in 75cm^2 flask in RPMI1640 media supplemented with 10% FBS, L-Glutamine (200mM) and antibiotics (penicillin/streptomycin, 100x concentrate). The cell density throughout the culture was maintained between 6 x 10^5 and 1 x 10^6 cells/mL.

OxLDL-induced VCAM-1 production in HUVECs. HUVECs were cultured as described above. Human LDL (1 mg/mL) was oxidised by incubation with Cu_2SO_4 (18 mM) solution prepared in 1% phosphate buffer saline (PBS) at 37°C for at least 30 hrs. The oxidation of LDL was confirmed by agarose gel electrophoresis as described previously (refer to appendix 4). All treatment compounds were prepared in HUVEC supplemented media (500 µL/well) at final concentrations of 0.1, 1 and 10µM. Sub-confluent HUVECs (90 – 95%) were co-incubated with oxLDL (5 µg/mL) and treatment compounds for 24 hrs. Each experiment contained un-stimulated, LDL only and oxLDL only treated HUVECs as controls. Supernatant was collected post 24 hrs incubation with treatment compounds in pre-labelled eppendorf tubes and stored at -80°C until utilised for ELISA.

CD40L-induced VCAM-1 production in HUVECs. CD40L expressing Jurkat D1.1 cells were utilised to stimulate HUVECs. D1.1 and HUVECs were cultured as described above. Sub-confluent HUVECs (90 – 95%) were co-incubated with D1.1 cells (1 x 10^6 cells/well) and

treatment compounds for 24 hrs. All treatment compounds were prepared as described above in HUVEC supplemented media (500 µL/well) at 0.1, 1 and 10µM. Each experiment contained un-stimulated and CD40L-stimulated HUVECs as controls. Anti-CD40L antibody (5 µg/mL) was used to confirm the specificity of CD40L stimulation. D1.1 cells were pre-incubated with anti-CD40L antibody for 1hr before HUVEC stimulation. Supernatant was collected after 24 hrs co-incubation of HUVECs with D1.1 cells and treatment compounds; and stored in pre-labelled eppendorf tubes at -80°C until required for ELISA. D1.1 cells were detached from HUVECs by washing 24-well plates with 1% warm PBS three times; and plates with HUVECs stored at -80°C until required for RT-qPCR.

VCAM-1 ELISA. Soluble form of VCAM-1 protein was quantified using ELISA as described in manufacturer's protocol. Once samples were thawed and shaken vigorously, 100 µL from each sample (in duplicate) was used to perform the ELISA. All the samples from CD40L-stimulated experiments were centrifuged for 10 mins at 4°C and 13000 rpm to pellet the D1.1 cells before supernatant was used to quantify VCAM-1 protein concentrations. Briefly, a flat bottomed 96-well ELISA plate was coated with monoclonal capture mouse anti-human VCAM-1 antibody (100 µL/well, 1/180 dilution with 1% PBS), for at least 16 hrs at room temperature. Excess and unbound primary antibody was removed by washing the 96-well plate with PBS washing buffer containing 0.05% Tween® 20 (PBST) at least three times (300 µL/well each wash). Unspecific binding of capture antibody was blocked by incubating the plate with reagent diluent (300 µL/well, 1/10 dilution with milli-Q water) for 1 hr at room temperature. Once the plate was washed and dried, sample or standard (100 µL) was added to each well of micro plate and incubated at room temperature for 2 hrs with continuous rocking at 500 rpm followed by washing and incubation with sheep anti-human detection antibody (100 µL/well, 1/180 dilution with reagent diluent) for 2 hrs with continuous rocking (500 rpm). After washing, the detection antibody was then conjugated by incubating the plate with horseradish-peroxidase (HRP) streptavidin (100 µL/well, 1/200 dilution with reagent diluent) for 30 mins at room temperature in dark, after which the plate was washed and then incubated with substrate reagent A and B (100 µL/well, 1/1 dilution of reagent A and B) for 30 mins in the dark. Stop solution, 2N H_2SO_4 (50 µL/well), was then used to stop the reaction between streptavidin HRP and substrate reagent which resulted in the development of a bright yellow colour and was quantified at 450 nm and 570 nm (as reference wavelength) using a BMG plate reader. Each ELISA plate contained recombinant

VCAM-1 standards (in duplicate) serial diluted in reagent diluent ranging from 1000 pg/mL – 15.625 pg/mL and reagent diluent (in duplicate) as blank. The intra- and inter-assay coefficient of variance (CV) for VCAM-1 ELISA was 7.6 ± 2.2% (mean ± SD, n=33) and 0.69% (n=4) respectively (refer to appendix 5 for standard curve).

CD40L-induced VCAM-1 mRNA levels. RNA extraction and real-time PCR were carried out as described in general methods chapter. Real time qPCR was performed using ABIS7500 (version 2.0.5), where the enzyme was activated at 95°C for 10 mins followed by 50 cycles of denaturation for 15 sec/cycle at 95°C and data collection for 1 min/cycle at 60°C. The target gene (VCAM-1) was normalised against two geNorm reference genes, UBE2D2 and PRDM4, validated based on their expression stability following exposure to the treatment compounds used for screening. The specificity of amplification was confirmed by melt curves and the expression of the target gene was quantified by ΔΔCt, where ΔCt = $Ct_{\text{target gene}} / Ct_{\text{meanCtofreference genes}}$. The forward and reverse primer sequences for VCAM-1 were CAG GCT AAG TTA CAT ATT GAT GAC AT and GAG GAA GGG CTG ACC AAG AC respectively.

4.3 Results

Effect of oxLDL on VCAM-1 protein production in HUVECs.

No increase in VCAM-1 protein production, as quantified by ELISA, was observed in HUVECs stimulated with oxLDL compared to un-stimulated HUVECs ($p>0.05$, n=3, **Figure 4.1**). The production of VCAM-1 in un-stimulated HUVECs was normalised to the production of VCAM-1 in oxLDL-stimulated HUVECs and was 105.7±18.1% (Figure 4.1).

CD40L-induced VCAM-1 protein production in HUVECs.

CD40L expressing D1.1 Jurkat cells and HUVECs were incubated with or without treatment compounds at 0.1, 1 and 10µM for 24 hrs. Co-incubation of D1.1 cells with HUVECs resulted in a 13.5±1.3 fold increase in VCAM-1 protein production compared to un-stimulated HUVECs ($p<0.001$, **Figure 4.2**). However, there was no significant effect observed in VCAM-1 production when HUVECs were treated with vehicle control (0.05% DMSO, 100±1.7% of untreated, $p>0.05$ – data not shown). The stimulation of VCAM-1was significantly reduced by 11.8±0.4 fold when D1.1 cells were pre-incubated with anti-CD40L

antibody. Of the 12 compounds tested, 7 compounds reduced CD40L-induced VCAM-1 protein production by >26.1±8.8% ($p<0.05$) relative to cells treated with CD40L alone (CD40L control), whereas 3 compounds significantly increased VCAM-1 protein production up to 203.5±4.5% ($p< 0.05$).

Figure 4.1 VCAM-1 protein production in oxLDL treated HUVECs

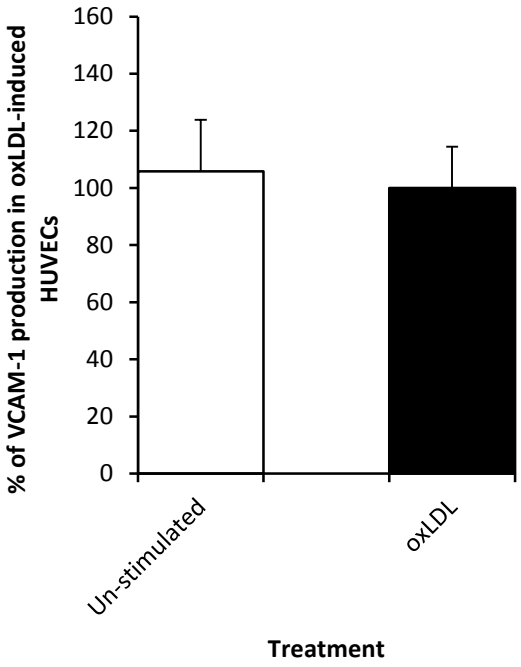

VCAM-1 protein production relative to incubation with oxLDL alone. HUVECs were incubated with OxLDL (5 µg/mL) for 24hrs. Supernatants were used to quantify VCAM-1 protein production using ELISA.All data expressed relative to oxLDL-induced VCAM-1 protein concentrations as mean % ± SD (n=3) . Absolute VCAM-1 protein value in untreated HUVECs – 16.2 pg/mL, standard range 15.625 – 1000 pg/mL. No significance relative to oxLDL control.

C3G, PCA, and PGA significantly reduced CD40L-induced VCAM-1 by >26.1± 8.8% ($p<0.05$) of the CD40L control (Figure 4.2B), while the metabolites of PCA, VA, IVA, PCA-4-sulfate and ferulic acid, reduced CD40L-induced VCAM-1 production by >30.3±4.5% ($p<0.04$), at one or more of the concentrations tested (**Figure 4.3, Figure 4.4A** and **Figure 4.5**). The maximum reduction was observed for ferulic acid (65.9±8.1%; $p<0.001$, Figure 4.5). PCA-4-glucuronide, PCA-3-glucuronide and IVA-3-sulfate showed no activity against CD40L induced VCAM-1 production (Figure 4.3B and Figure 4.4B). Trends were however observed for PCA-3-sulfate at 10 µM, ($p= 0.07$) and VA-4-sulfate at 1 µM ($p=0.09$, Figure 4.4A and B).

Figure 4.2 Effect of C3G, PCA and PGA on VCAM-1 production in CD40L-stimulated HUVECs.

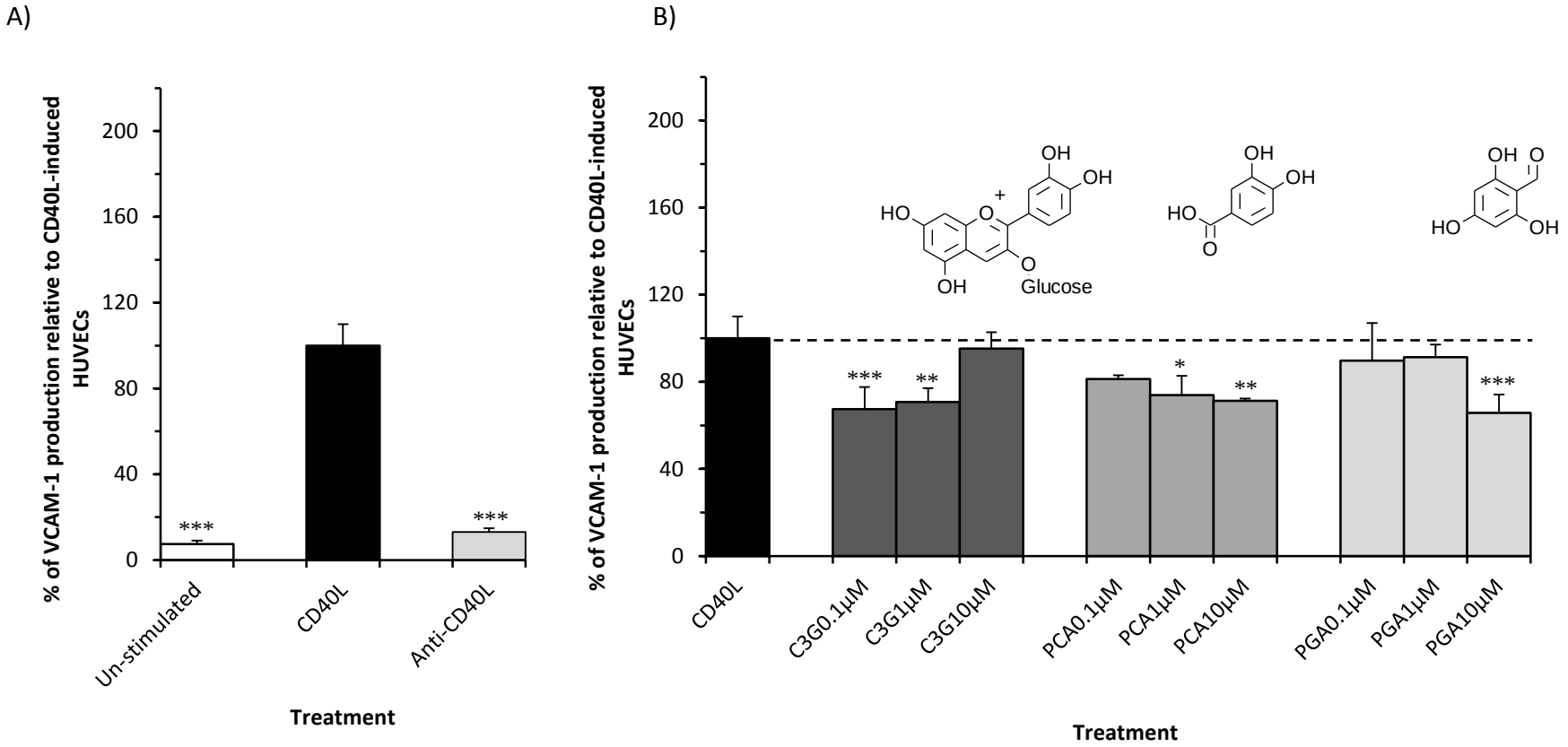

CD40L-stimulated VCAM-1 protein production in HUVECs co-incubated with C3G, phenolic metabolites or CD40L controls for 24 hours. A, cells incubated with or without D1.1 cells (1 x 10^6 cells/well); B, cells incubated with C3G, PCA or PGA at 0.1, 1, 10 μM and D1.1 cells (1 x 10^6 cells/well). All data expressed as mean percentage (± SD, n=3) of CD40L-induced controls. Absolute VCAM-1 protein value in unstimulated HUVECs - 15.7 pg/mL, standard range 15.625 – 1000 pg/mL. ***p<0.001, **p<0.01, *p<0.05 (ANOVA with Tukey post-hoc) relative to CD40L-stimulated control. C3G, cyanidin-3-glucoside; PCA, protocatechuic acid; PGA, phloroglucinaldehyde.

Figure 4.3 Effect of methylated and glucuronidated PCA on VCAM-1 production in CD40L-stimulated HUVECs.

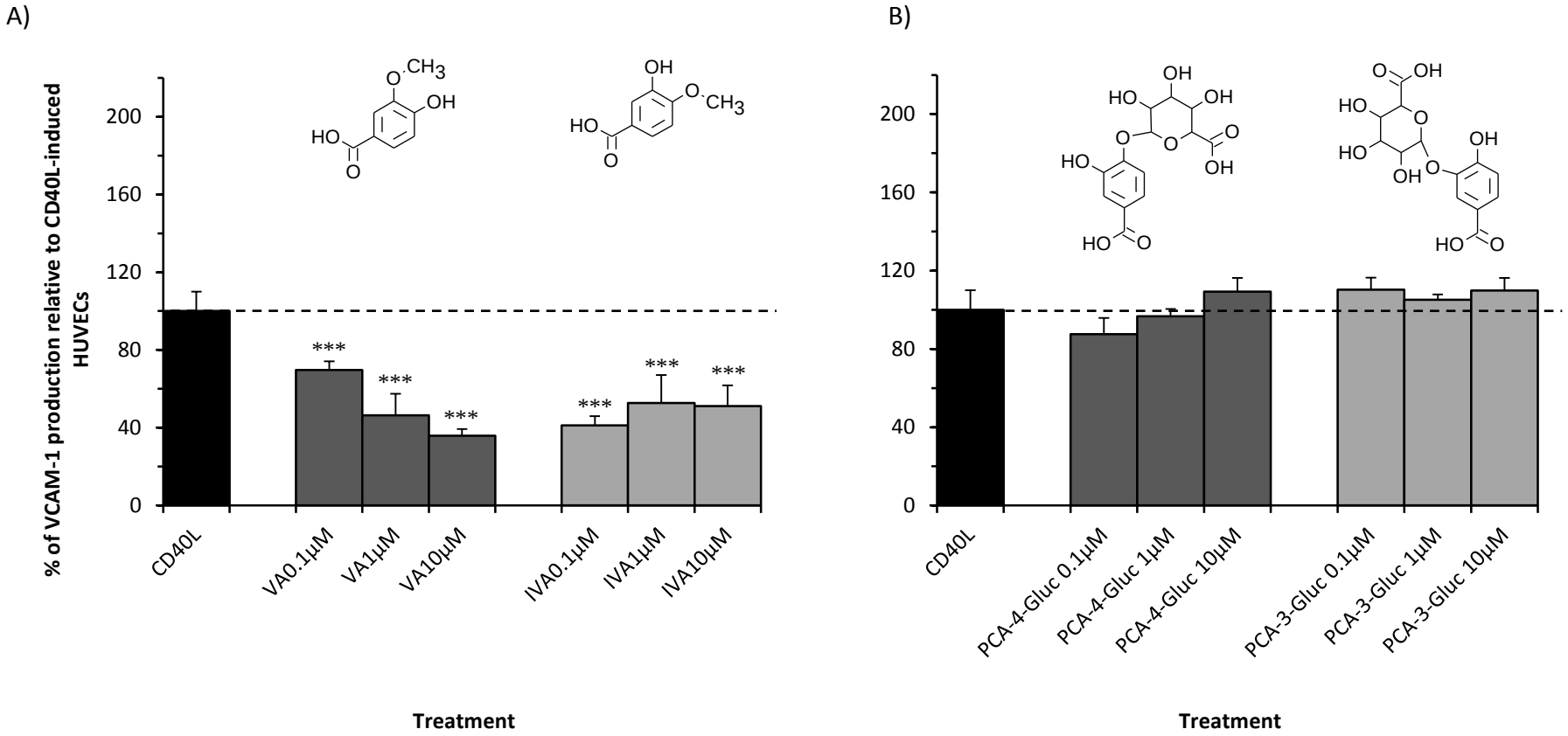

CD40L-stimulated VCAM-1 protein production in HUVECs co-incubated with phenolic metabolites for 24 hours. A, cells incubated with VA or IVA at 0.1, 1, 10 μM and D1.1 cells (1 x 10^6 cells/well); B, cells incubated with PCA-4-Gluc or PCA-3-Gluc at 0.1, 1, 10 μM and D1.1 cells (1 x 10^6 cells/well). All data expressed as mean percentage (± SD, n=3) of CD40L-induced controls. Absolute VCAM-1 protein value in unstimulated HUVECs - 15.7 pg/mL, standard range 15.625 – 1000 pg/mL***p<0.001 (ANOVA with Tukey post-hoc) relative to CD40L-stimulated control. VA, vanillic acid; IVA, isovanillic acid; PCA-4-Gluc, PCA-4-glucuronide; PCA-3-Gluc, PCA-3-glucuronide.

Figure 4.4 Effect of sulfated and multiple-conjugated PCA on VCAM-1 production in CD40L-stimulated HUVECs.

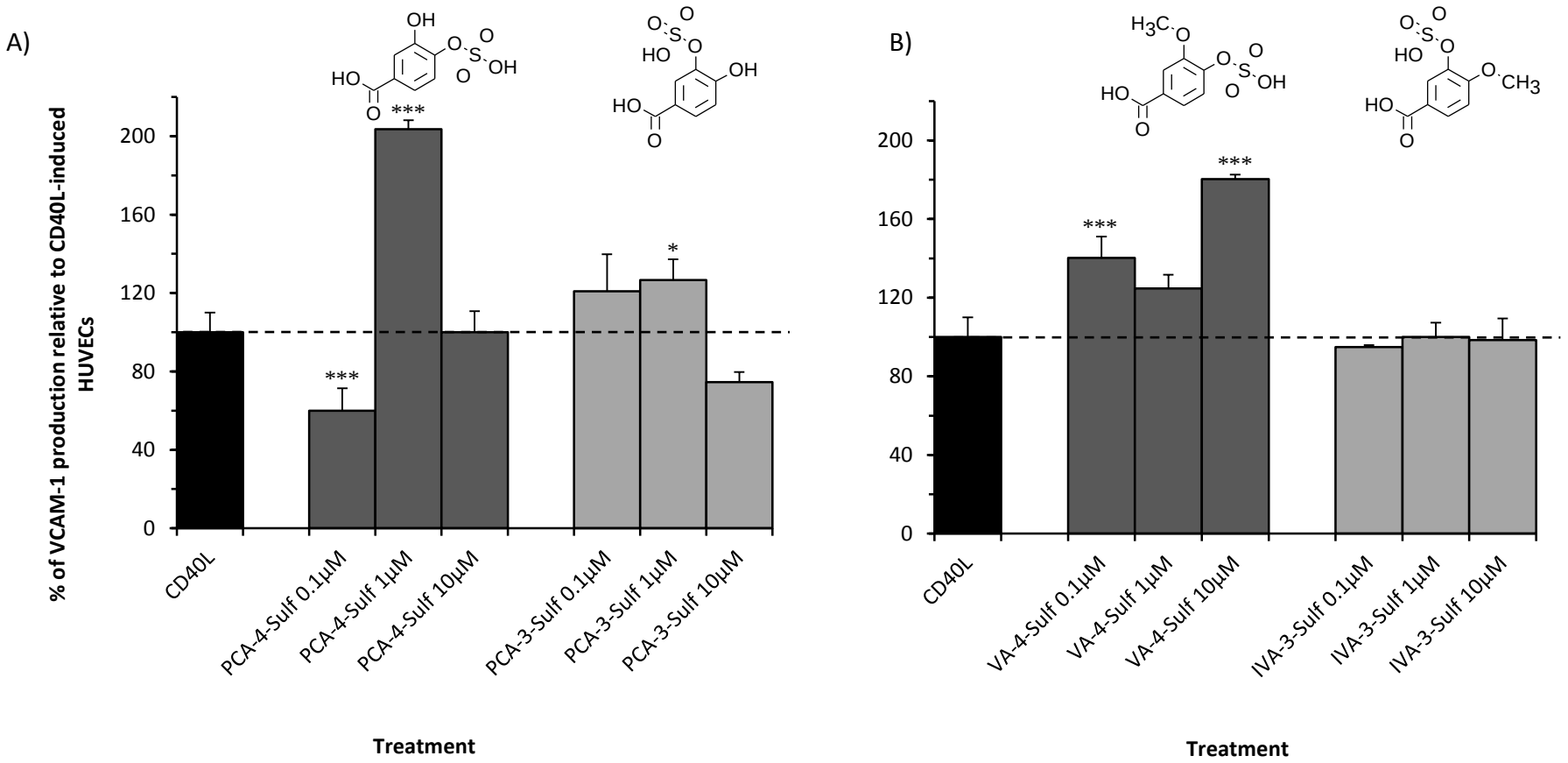

CD40L-stimulated VCAM-1 protein production in HUVECs co-incubated with phenolic metabolites for 24 hours. A, cells incubated with PCA-4-Sulf or PCA-3-Sulf at 0.1, 1, 10 µM and D1.1 cells (1 x 10^6 cells/well); B, cells incubated with VA-4-Sulf or IVA-3-Sulf at 0.1, 1, 10 µM and D1.1 cells (1 x 10^6 cells/well). All data expressed as mean percentage (± SD, n=3) of CD40L-induced controls. Absolute VCAM-1 protein value in unstimulated HUVECs - 15.7 pg/mL, standard range 15.625 – 1000 pg/mL. ***p<0.001, *p<0.05 (ANOVA with Tukey post-hoc) relative to CD40L-stimulated control. PCA-4-Sulf, protocatechuic acid-4-sulfate; PCA-3-Sulf, protocatechuic acid-3-sulfate; VA-4-Sulf, vanillic acid-4-sulfate; IVA-3-Sulf, isovanillic acid-3-sulfate.

Figure 4.5 Effect of ferulic acid on VCAM-1 production in CD40L-stimulated HUVECs.

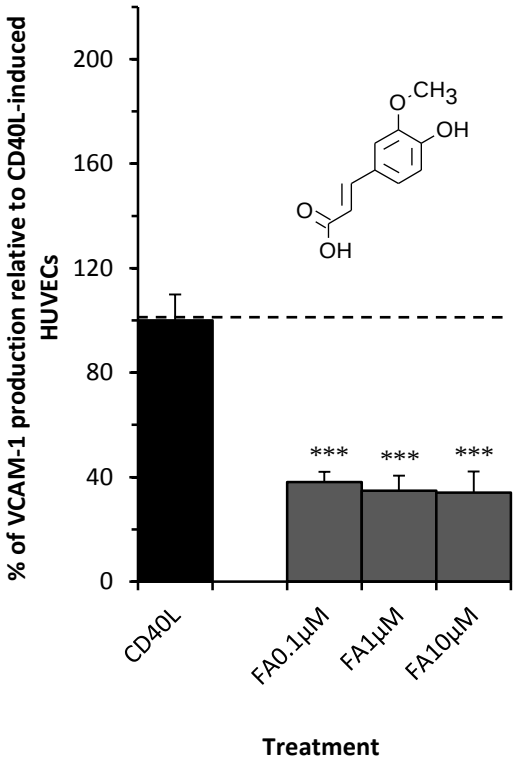

CD40L-stimulated VCAM-1 protein production in HUVECs co-incubated with FA at 0.1, 1, 10 µM and D1.1 cells (1 x 10^6 cells/well) for 24 hours.. All data expressed as mean percentage (± SD, n=3) of CD40L-induced controls. Absolute VCAM-1 protein value in unstimulated HUVECs - 15.7 pg/mL, standard range 15.625 – 1000 pg/mL. ***p<0.001 (ANOVA with Tukey post-hoc) relative to CD40L-stimulated control.FA, ferulic acid.

An increase in VCAM-1 protein production was observed when CD40L-induced HUVECs were co-incubated with PCA-4-sulfate (203.5±4.5% at 1 µM, p<0.001), PCA-3-sulfate (126.5±10.6% at 1 µM, p<0.04) and VA-4-sulfate (140.1± 10.8% at 0.1 µM and 180.3±2.2% at 10 µM, p<0.001) relative to CD40L-induced control (Figure 4.4A and B).

Effects on CD40L-induced VCAM-1 mRNA levels.

The seven compounds that displayed an ability to reduce CD40L-induced VCAM-1 protein concentrations (reported above) were investigated for their effects on CD40L-induced VCAM-1 mRNA levels. Here, CD40L induction increased VCAM-1 mRNA levels by 130.2±46.1 fold relative to untreated HUVECs (p<0.05, n=3, **Figure 4.6**) and this was reduced to 33.8±1.2 fold by pre-incubating D1.1 cells with anti-CD40L antibody prior to their use to stimulate HUVECs (p<0.05, Figure 4.6). Of the 7 compounds tested, 4 reduced VCAM-1 mRNA levels in CD40L-induced HUVECs by >75.8±7.2% (p<0.05, Figure 4.6). The greatest reduction of VCAM-1 mRNA levels was observed for VA which reduced CD40L-induced VCAM-1 by >99.9 ±0.01% of the CD40L control (p<0.04, Figure 4.6).

Figure 4.6 Effect of bioactive compounds at protein level on VCAM-1 mRNA levels in CD40L-stimulated HUVECs.

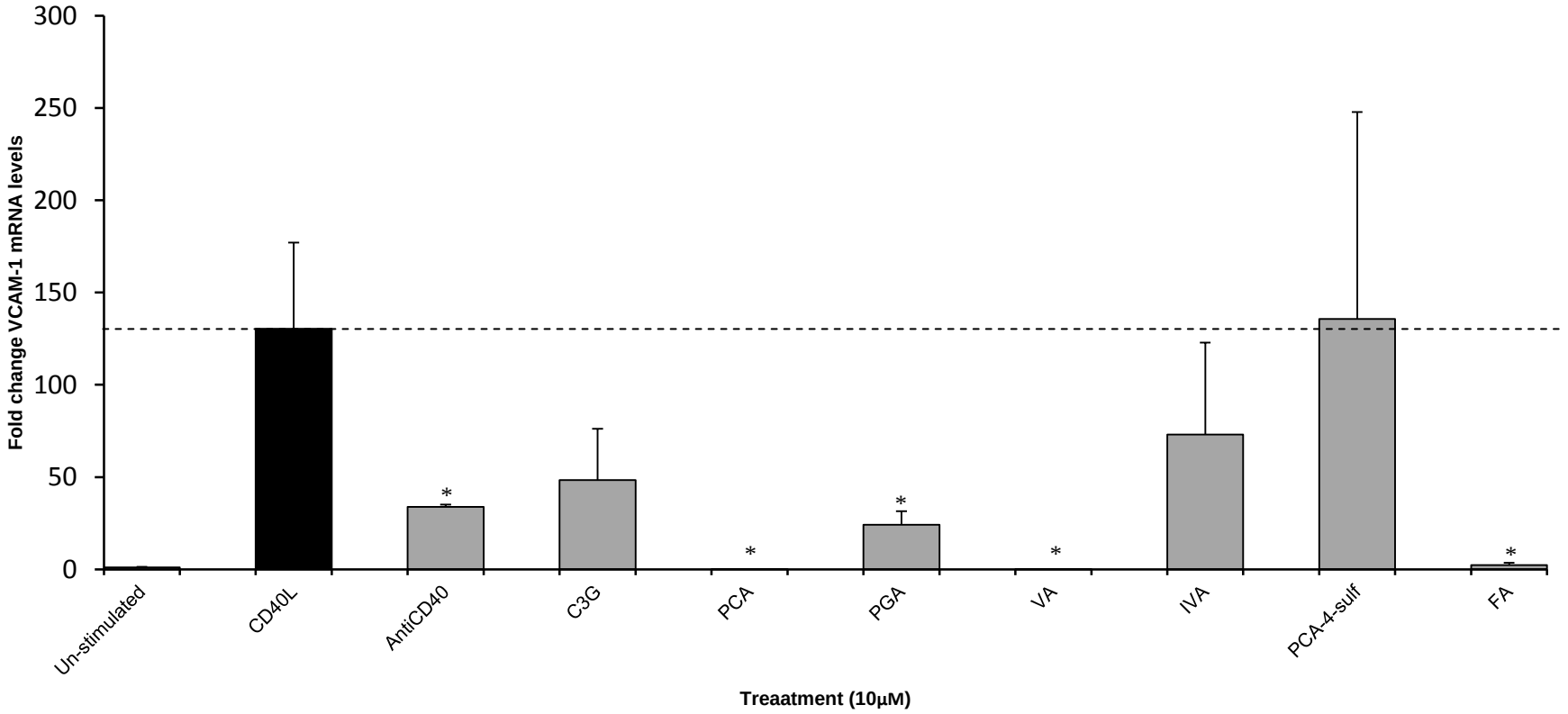

Change in CD40L-stimulated VCAM-1 mRNA in HUVECs co-incubated with C3G and phenolic metabolites or CD40L controls for 24 hrs. VCAM-1 mRNA fold change in cells co-incubated with C3G or phenolic metabolites (10 μM) with or without D1.1 cells (1 x 10^6 cells/well). All data graphically expressed as mean fold change (± SD, n=3) relative to un-stimulated (basal) VCAM-1 mRNA levels. *p<0.05 (ANOVA with Tukey post-hoc) relative to CD40L-stimulated control. C3G, cyanidin-3-glucoside; PCA, protocatechuic acid; PGA, phloroglucinaldehyde; VA, vanillic acid; IVA, isovanillic acid; PCA-4-Sulf, PCA-4-sulfate; FA, ferulic acid.

.

4.4 Discussion

High consumption of dietary anthocyanins is associated with reduced CVD risk (Cassidy, O'Reilly et al. 2010, Cassidy, Mukamal et al. 2013), however the mechanisms involved remain elusive, and the majority of previous animal and *in vitro* studies have explored the activity of parent/un-metabolised forms of anthocyanins. The current study explored the anti-inflammatory activity of newly identified anthocyanin metabolites where, for the first time, novel pure synthetic sulfate and glucuronic acid phenolic conjugates were utilised. As anthocyanins have been shown to reduce oxLDL-induced apoptosis (Yi, Chen et al. 2010) and attenuate downstream effects of CD40L-CD40 interaction (Xia, Ling et al. 2007, Xia, Ling et al. 2009). The major finding of the present study is that degradation and subsequent metabolism of C3G does not reduce its bioactivity and it may in fact increase it. Therefore, C3G may exhibit anti-inflammatory activity via the ability of its metabolites to alter the protein and gene expression of VCAM-1, a key mediator of chronic inflammation, in endothelial cells. VCAM-1 plays a pivotal role in the initiation of chronic inflammation by acting as a bridge between leukocytes and endothelium, and aids the internalisation of leukocytes in endothelial cells which triggers the release of other inflammatory mediators to propagate the inflammatory response(Fotis, Giannakopoulos et al. 2012).

CD40L has been identified as a cardiovascular disease risk factor (Dominguez-Rodriguez, Abreu-Gonzalez et al. 2009, Hassan, Merhi et al. 2012) and has been associated with the progression of atherosclerosis. The CD40 ligation via CD40L is associated with increased production of VCAM-1 (Xia, Ling et al. 2009, Pamukcu, Lip et al. 2011). However, previously very little was known of the effects of anthocyanin metabolites on CD40L-induced VCAM-1 expression. The current study confirmed the involvement of CD40L in inducing VCAM-1 production in endothelial cells, as a significant increase in VCAM-1 production was observed upon CD40L-stimulation of HUVECs, which was attenuated by blocking CD40L using human anti-CD40L antibody. No increase in VCAM-1 protein production was observed when HUVECs were stimulated with oxLDL (5 µg/mL) for 24 hrs, although oxLDL has previously been shown to induce VCAM-1 protein production in endothelial cells (Huang, Lin et al. 2013), where a concentration as high as 40 µg/mL of oxLDL was required to achieve a significant increase of VCAM-1 production in HUVECs. This may explain why no significant increase in VCAM-1 protein production was observed following stimulation of HUVECs with 5 µg/mL oxLDL in the present study.

In the present study, C3G and its metabolites significantly reduced CD40L-induced VCAM-1 production by as much as 65% of the CD40L control (Figure 4.5). Earlier studies investigating structure-function activity have indicated that there is a positive correlation between the number of hydroxyl groups present on the B-ring of flavonoids and their anti-inflammatory (Theoharides, Alexandrakis et al. 2001) and radical scavenging (Yi, Chen et al. 2010) activity and their ability to reduce oxLDL-mediated cell apoptosis (Chang, Huang et al. 2006). Moreover, flavonoids containing an ortho-dihydroxy (catechol) group on the B-ring have been previously shown to reduce the production of inflammatory mediators including interleukin-6 (IL-6) and cyclooxygenase-2 (COX-2) (Theoharides, Alexandrakis et al. 2001, Hou, Yanagita et al. 2005). In the present study, the investigated groups of metabolites were identified as B-ring metabolites of C3G and have either intact or conjugated/modified (methylated, glucuronidated and sulfated) catechol moieties, allowing for basic examination of structure-function relationships.

In CD40L-stimulated HUVECs, 7 of 12 compounds tested, including C3G and both its degradation products, PCA and PGA (Figure 4.2B), significantly reduced VCAM-1 production (Figure 4.2 to Figure 4.5). Following CD40L stimulation, the largest reduction in VCAM-1 was observed for metabolites containing a methylated catechol group, with ferulic acid eliciting the greatest effect, followed by VA and IVA (Figure 4.3A and Figure 4.5). The effects of glucuronic acid and sulfate conjugation were less apparent (Figure 4.3B and Figure 4.4A). The findings from the present study suggest that anthocyanin metabolites possess anti-inflammatory activity and the conjugation of the catechol group on the phenolic metabolites often leads to increased bioactivity, which has also been reported for conjugated forms of other flavonoids, such as methylated (-)-epicatechin and sulfated and glucuronidated quercetin (Steffen, Gruber et al. 2008, Lodi, Jimenez et al. 2009, Al-Shalmani, Suri et al. 2011).Unexpectedly, sulfated PCA, VA and IVA increased CD40L-induced VCAM-1 production (Figure 4.3B and Figure 4.4) at several concentrations in HUVECs implying the sulfation may be unfavourable transformation of these metabolites for CD40L-induced VCAM-1 production in HUVECs. This increased production of soluble VCAM-1 may be due to the effect of metabolites on proteolytic cleavage of VCAM-1 at cell membrane which leads to increased sVCAM-1 (Videm and Albrigtsen 2008, Fotis, Giannakopoulos et al. 2012).

The potential mechanism by which C3G and its metabolites alter VCAM-1 protein production in CD40L-stimulated HUVECs was also investigated by examining their effects on

CD40L-induced VCAM-1 mRNA levels. In most cases, compounds which reduced protein levels of CD40L-induced VCAM-1 also reduced VCAM-1 mRNA levels in the same model. Of the 7 compounds that displayed bioactivity on VCAM-1 protein production, CD40L-induced VCAM-1 mRNA levels were reduced by PCA, PGA, VA and ferulic acid, indicating their bioactivity at the transcriptional level. While this evidence may explain the link between a significant alteration in gene expression and protein levels, several instances were noted where a reduction in protein concentrations (Figure 4.2 to Figure 4.5) was not correlated with a reduction in mRNA levels (Figure 4.6). Such divergence may be the result of post-translational modification as proteolytic cleavage is required to release membrane bound VCAM-1 to produce soluble VCAM-1 (Videm and Albrigtsen 2008).

To the best of my knowledge, this is the first *in vitro* study to examine the effects of metabolites of C3G on VCAM-1 in CD40L-stimulated endothelial cells. Though, the activity of C3G on CD40L-induced VCAM-1 protein production has previously been reported, where C3G significantly reduced CD40L-induced VCAM-1 in endothelial cells (Xia, Ling et al. 2009), the findings from the current study for C3G was in accordance with this previous work and provides additional evidence for C3G activity. Nevertheless, not all studies have supported the activity of C3G on VCAM-1 expression as Hidalgo et al reported no effect of C3G on LPS-INF-γ induced VCAM-1 in endothelial cells (Hidalgo, Martin-Santamaria et al. 2011). This discrepancy could possibly be explained by the exposure time of the endothelial cells to C3G and the stimulant, as the stimulation time was only 6 hrs in the study conducted by Hidalgo et al., as opposed to 24 hrs in the current study. The present study is the first *in vitro* study which investigated activity of PCA in CD40L-stimulated HVUECs however; previous studies using different *in vitro* models have reported the activity of PCA on VCAM-1. For example, significant reductions in VCAM-1 protein production have been reported (Kim, Tsoy et al. 2006, Min, Ryu et al. 2010) in LPS–induced RAW264.7 and TNF-α-induced bovine aortic endothelial cells co-incubated with PCA; which is in accordance with the present study where PCA reduced CD40L-induced VCAM-1 by greater than 26% of controls. However, Kim *et al* (Kim, Tsoy et al. 2006) reported the bioactivity of PCA at ≥20 µM as opposed to the present study where observed effects of PCA on VCAM-1 protein production at concentrations as low as 1 µM [a physiologically relevant concentration (Czank, Cassidy et al. 2013)].

In the current study, the methylated forms of PCA, namely VA and IVA, reduced CD40L-induced VCAM-1 production in HUVECs. In contrast to VA, diminished VCAM-1 protein production caused by IVA was independent of its effect on VCAM-1 mRNA levels suggesting possible interference during post-translational modification of VCAM-1. To the best of my knowledge, this is the first study that reports the potential inhibitory effects of VA and IVA on VCAM-1. It is also apparent from the present study that methylation of PCA at either hydroxyl group on the B-ring increases the inhibitory effect of PCA towards VCAM-1 protein production as VA (at 1 and 10μM) and IVA (at all concentrations) elicited greater reductions of VCAM-1 protein production ($p<0.05$) compared to any concentration of PCA. In addition to VA and IVA, FA – a propenoic acid derivative of VA - also reduced VCAM-1 protein and gene expression at all concentrations tested, suggesting the mono-*O*-methylated catechol group may confer bioactivity towards VCAM-1 production. This finding is in agreement with the study conducted by Hong et al using a different stimulus than utilised in the present study, where FA reduced γ-radiation-induced VCAM-1 production in HUVECs at concentrations of 5, 10 and 20μM (Ma, Hong et al. 2010).

The investigation of glucuronide (PCA-3-Gluc and PCA-4-Gluc) and sulfate (PCA-4-Sulf and PCA-3-Sulf) derivatives of PCA revealed that both types of conjugations at either 3' or 4' –OH of PCA reduce their inhibitory effects towards VCAM-1 protein and mRNA levels. With regards to the multiple-conjugated products (methylation and sulfation) of PCA, VA-4-Sulf increased VCAM-1 protein production by ≈2 fold at 0.1 and 10μM which was not associated with modification at mRNA levels, suggesting a potential interference with proteolytic cleavage of VCAM-1 to increase the production of soluble VCAM-1. However, IVA-3-Sulf had no apparent effect on VCAM-1 protein production and mRNA levels, indicating that multiple-conjugations of PCA also decrease the bioactivity potential of PCA towards VCAM-1 production in endothelial cells.

The observed effects of C3G and its metabolites at the translational level may be due to their ability to inhibit activation of key inflammatory proteins and transcription factors as anthocyanins can reduce the activation of CD40L induced c-Jun N-terminal kinases (JNK) (Xia, Ling et al. 2009) and NF-κB(Kim, Tsoy et al. 2006). C3G has also been reported to diminish CD40L signalling by restricting TNF receptor associated factor-2 (TRAF-2) translocation to the membrane bound CD40 receptor in endothelial cells (Xia, Ling et al. 2007).

Overall, the results from this study indicate that the B-ring degradant of C3G, PCA, has greater bioactivity potential than the parent compound or the A-ring degradant of C3G, PGA. These data also highlight the impact of conjugation upon bioactivity of PCA, with methyl conjugates of PCA eliciting a greater reduction in VCAM-1 protein production than glucuronide, sulfate or multiple-conjugates of PCA. The inhibitory effect of anthocyanin metabolites upon VCAM-1 protein production presented in this study, together with previous reports examining activity of phenolic acids and structurally similar compounds on VCAM-1 production in *in vitro* models; provide strong evidence that these compounds possess an inhibitory effect on VCAM-1 production. Altogether, data from this study indicate that the reported anti-inflammatory effect of C3G may partially be attributed to its metabolites, and that degradation and subsequent metabolism of degradants does not inhibit its bioactivity; in fact in some cases it may increase it. In light of these data, further investigation is warranted to establish specific mechanisms of action by which metabolites of C3G may exhibit anti-inflammatory activity. This may include investigating effect of bioactive compounds on correlation between membrane bound VCAM-1 versus sVCAM-1 in HUVECs, modulation of enzymes facilitating proteolytic cleavage of VCAM-1, interaction of VCAM-1/α4β1, CD40L/TRAF-2 and ultimately on transcription factor such as NF-κB.

Chapter 5. Effects of cyanidin-3-glucoside and its metabolites on endothelial IL-6 expression

5.1 Introduction

Increased dietary consumption of anthocyanins may reduce the risk of cardiovascular disease (CVD) and related pathologies, including high blood pressure, atherosclerosis, myocardial infarction and coronary heart disease (Mink, Scrafford et al. 2007, Cassidy, Mukamal et al. 2013). Cardiovascular disease is a direct result of a combination of vascular endothelial dysfunction and chronic inflammation, where the key cytokine interleukin-6 (IL-6) and its signalling pathways play an important role in the latter process (Schuett, Luchtefeld et al. 2009). Moreover, IL-6 signalling contributes to the development of atherosclerotic plaques and their instability, which leads to critical clinical endpoints such as myocardial infarction and stroke (Schuett, Luchtefeld et al. 2009). High levels of IL-6 causes over-production of other pro-inflammatory cytokines, matrix metalloproteinase and oxidation of lipoprotein to propagate the inflammation further (Yudkin, Kumari et al. 2000, Song and Schindler 2004, Saremi, Anderson et al. 2009).

Anthocyanins have been studied for their anti-inflammatory activity and shown to reduce the production of IL-6 both *in vivo* and *in vitro*(Albrecht, Yang et al. 2007, Karlsen, Paur et al. 2010, Edirisinghe, Banaszewski et al. 2011, Xie, Kang et al. 2011). Plasma levels of IL-6 were significantly reduced following chronic (Karlsen, Paur et al. 2010, Kolehmainen, Mykkänen et al. 2012) and acute (Edirisinghe, Banaszewski et al. 2011) consumption of anthocyanin-containing juice in human participants at elevated risk of CVD. Moreover, animal studies support the notion that anthocyanins possess anti-inflammatory activity, as IL-6 expression was significantly lower in mice fed bilberry extract for 5 weeks compared to a controlled diet (Xie, Kang et al. 2011). *In vitro* data have also demonstrated that cyanidin-3-glucoside (C3G) significantly reduced cluster of differentiation ligand (CD40L)-induced IL-6 production in endothelial cells (Xia, Ling et al. 2007).

Despite promising evidence suggesting anti-inflammatory activity of anthocyanins, very limited information is available concerning the effects of their recently identified metabolites (Czank, Cassidy et al. 2013). In the present study, C3G and 11 of its recently identified (of which 6 were synthesised) metabolites (Figure 3.1) were examined for their effect on IL-6 production under CD40L and oxidised low density lipoprotein (oxLDL) challenged conditions

5.2 Methods and materials

Standards and reagents. DuoSet enzyme-linked immunosorbent assay (ELISA) kits IL-6 (DY206), flat bottom clear polystyrene 96-well ELISA plates (DY990) and reagent diluent (DY995) were purchased from R&D Systems (Abingdon, UK).

oxLDL-induced IL-6 production in HUVECs. Human LDL (1 mg/mL) was oxidised by incubation with Cu_2SO_4 (18 mM) solution prepared in 1% phosphate-buffered saline (PBS) at 37°C for at least 30 hrs. The oxidation of LDL was confirmed by protein agarose electrophoresis as described previously (refer to appendix 4) (Autio, Jaakkola et al. 1990). HUVECs were cultured as described in general methods section. All treatment compounds were prepared in HUVEC supplemented media (500 µL/well) at 0.1, 1 and 10 µM final concentrations. Sub-confluent HUVECs (90-95%) were co-incubated with oxLDL (5 µg/mL) and treatment compounds for 24 hrs. As controls, each experiment contained LDL and oxLDL-stimulated HUVECs as well as un-stimulated HUVECs. The supernatants were collected 24 hrs post incubation with treatment compounds, and stored in eppendorf tubes at -80°C until utilised for ELISA. Plates were then stored at -80°C until required for RT-qPCR.

CD40L-induced IL-6 production in HUVECs. Sub-confluent HUVECs (90-95%) were co-incubated with D1.1 cells (1 x 10^6 cells/well, cultured as described in general methods section) and treatment compounds for 24 hrs. All treatment compounds were prepared in HUVEC supplemented media (500 µL/well) at 0.1, 1 and 10 µM final concentrations. Each experiment contained unstimulated and CD40L-stimulated HUVECs as controls. Anti-CD40L antibody (5 µg/mL) was used to confirm the specificity of the assay, where D1.1 cells were pre-incubated with anti-CD40L antibody for 1 hr prior to stimulation of HUVECs.

Supernatants were collected after 24 hrs co-incubation of HUVECs with D1.1 cells with treatment compounds; and stored in pre-labelled eppendorf tubes at -80°C until required for ELISA. D1.1 cells were removed by washing 24-well plates with 1% warm PBS three times, and plates were then stored at -80°C until required for RT-qPCR.

IL-6 ELISA. Production ofIL-6 protein was quantified using ELISA according to the manufacturer's protocol, and as detailed previously for VCAM-1 (Chapter 3). Briefly, 100 µL of each sample (in duplicate) was dispensed into separate wells of flat bottom plates coated with monoclonal mouse anti-human IL-6 primary antibody (100 µL/well, 1/180 dilution with 1% PBS). After two hrs incubation with samples, ELISA plates were incubated with sheep anti-human detection antibody (100 µL/well, 1/180 dilution with reagent diluent) for a further two hrs. Thereafter, plates were incubated with horseradish-peroxidase (HRP) streptavidin (100 µL/well, 1/200 dilution with reagent diluent) for 30 mins at room temperature in the dark, followed by incubation with substrate reagents A & B (100 µL/well, 1/1 dilution of reagent A and B) for 30 mins in the dark at room temperature. The reaction was then terminated using a stop solution (50 µL/well, 2N H_2SO_4) to develop a bright yellow colour and absorbance measured at 450 nm (reference wavelength 570 nm) using a BMG plate reader. The IL-6 ELISA intra- and inter-assay coefficients of variation (CV) were 4.3±1.3% and 1.49% respectively (mean±SD, n=4, refer to appendix 6 for standard curve).

Real-time PCR. Real-timePCR was performed as described previously (Chapter 2). The target gene (IL-6) was normalised against two geNorm reference genes, UBE2D2 and PRDM4, validated based on stability of expression following incubation with the treatment compounds used for screening (chapter 2). Gene expression was quantified using comparative C_t method (Schmittgen and Livak 2008) incorporating the geometric mean of reference genes as the normalisation factor. The forward and reverse primer sequences for IL-6 were CAG GCT AAG TTA CAT ATT GAT GAC AT and GAG GAA GGG CTG ACC AAG AC respectively.

5.3 Results

OxLDL-induced IL-6 protein production in HUVECs

OxLDL-stimulation of HUVECs resulted in a 6.9±0.4 fold increase in IL-6 protein production relative to the un-stimulated control ($p<0.001$, **Figure 5.1A**), whereas only a 2.9 fold increase in IL-6 protein production ($p<0.05$, Figure 5.1A) was observed in HUVECs treated with LDL alone. In addition, no significant effect on IL-6 production was observed when HUVECs were treated with vehicle control (0.05% DMSO, 110±8.9% of untreated, $p>0.05$ – data not shown) IL-6 production was not altered when HUVECs were incubated with a vehicle control (VC) consisting of Cu_2SO_4 (5 µM) and 0.05% DMSO ($p>0.05$, Figure 5.1A). Of the 12 compounds tested, 9 reduced oxLDL-induced IL-6 production by >32% ($p<0.05$, **Figure 5.1** to **Figure 5.4**) relative to the cells treated with oxLDL alone (oxLDL control), at one or more of the tested treatment concentrations (0.1, 1, 10 µM). Cyanidin-3-glucoside had no effect on oxLDL-induced IL-6 production, however its B-ring degradation product, PCA, reduced IL-6 production by >53.6±7.6% relative to the oxLDL control ($p<0.001$, Figure 5.1); whereas PGA had no effect. Among the methyl, glucuronide and sulphate conjugated metabolites of PCA, PCA glucuronides and PCA sulfates elicited the greatest reductions in oxLDL-induced IL-6 production (for all concentrations tested), with sulfate conjugates of PCA eliciting maximal decreases (99.1±0.1%, $p<0.001$, Figure 5.2 to Figure 5.3A). In addition, VA-4-sulfate, IVA-3-sulfate and FA also displayed bioactivity against oxLDL-induced IL-6 production, (between 54.1±4.4 and 98.2±0.2% reduction, $p<0.05$) relative to the oxLDL control (Figure 5.3B and Figure 5.4). The isomer of VA, IVA, showed no significant activity, though a trend was observed at 0.1 µM ($p<0.09$, Figure 5.3A).

OxLDL-stimulated IL-6 mRNA expression

The 9 compounds which elicited reductions in IL-6 protein production (reported above) were further investigated for their effects on IL-6 mRNA levels following incubation of HUVEC with 10 µM of treatment compounds for 24 hours. IL-6 mRNA expression was increased by 3.5±0.9 fold ($p<0.05$, **Figure 5.5**) in cells treated with oxLDL alone (oxLDL control) compared to unstimulated cells. All compounds except FA reduced oxLDL-induced IL-6 mRNA expression by >55.2±7.3% of the oxLDL control ($p<0.006$, Figure 5.5). VA elicited

Figure 5.1 Effect of various controls, C3G and its degradants on oxLDL-induced IL-6 protein production

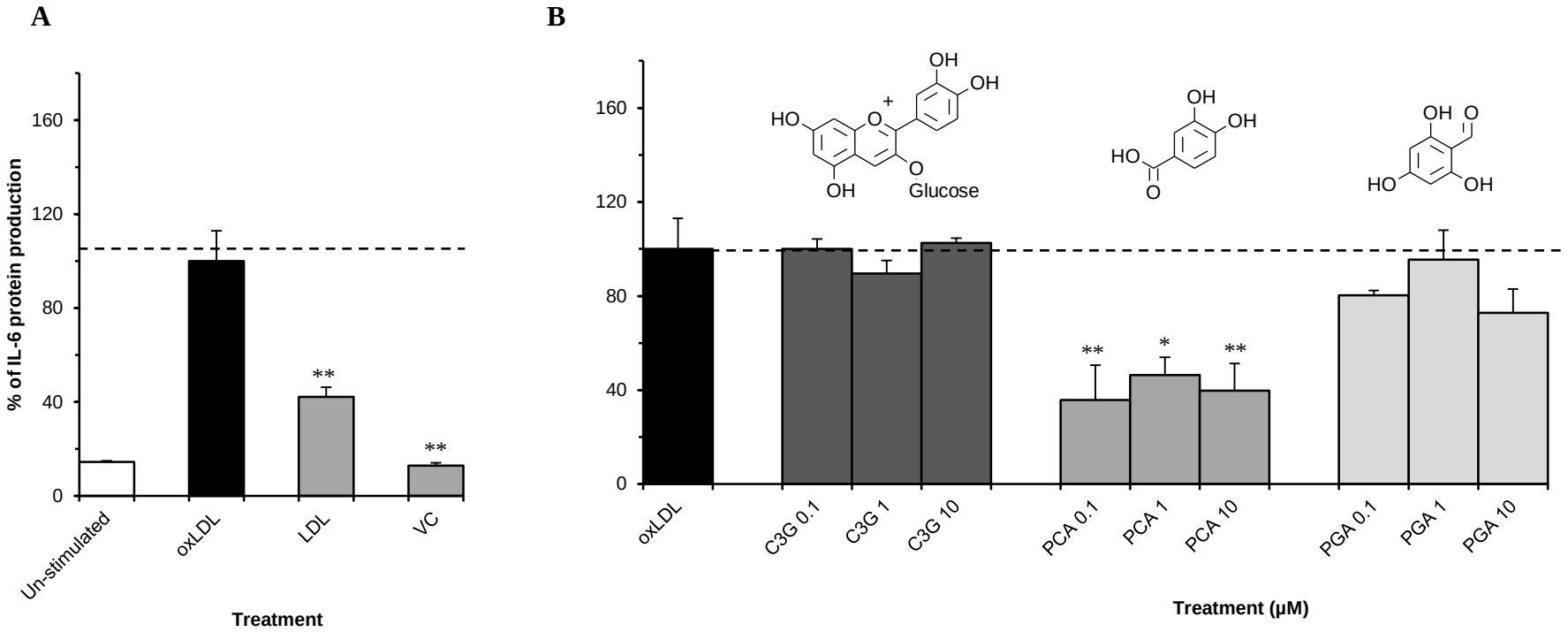

HUVECs co-incubated with C3G, PCA, PGA, or controls for 24 hours. A, cells incubated with or without LDL (5 µg/mL) or VC; B, cells incubated with C3G, PCA or PGA at 0.1, 1 and 10 µM and oxLDL. All data expressed as mean percentage (± SD, n=3) of oxLDL-induced controls (expressed as 100%). Absolute IL-6 protein value in unstimulated HUVECs - 37.2pg/mL, standard range 9.375 – 600pg/mL **p<0.001, *p<0.01 (ANOVA with Tukey post-hoc) relative to oxLDL-stimulated control cells. C3G, cyanidin-3-glucoside; PCA, protocatechuic acid; PGA, phloroglucinaldehyde; VC, vehicle control [Cu_2SO_4 (5 µM) + 0.05% DMSO].

Figure 5.2 Effect of methylated and glucuronidated phenolic metabolites of PCA on oxLDL-induced IL-6 protein production

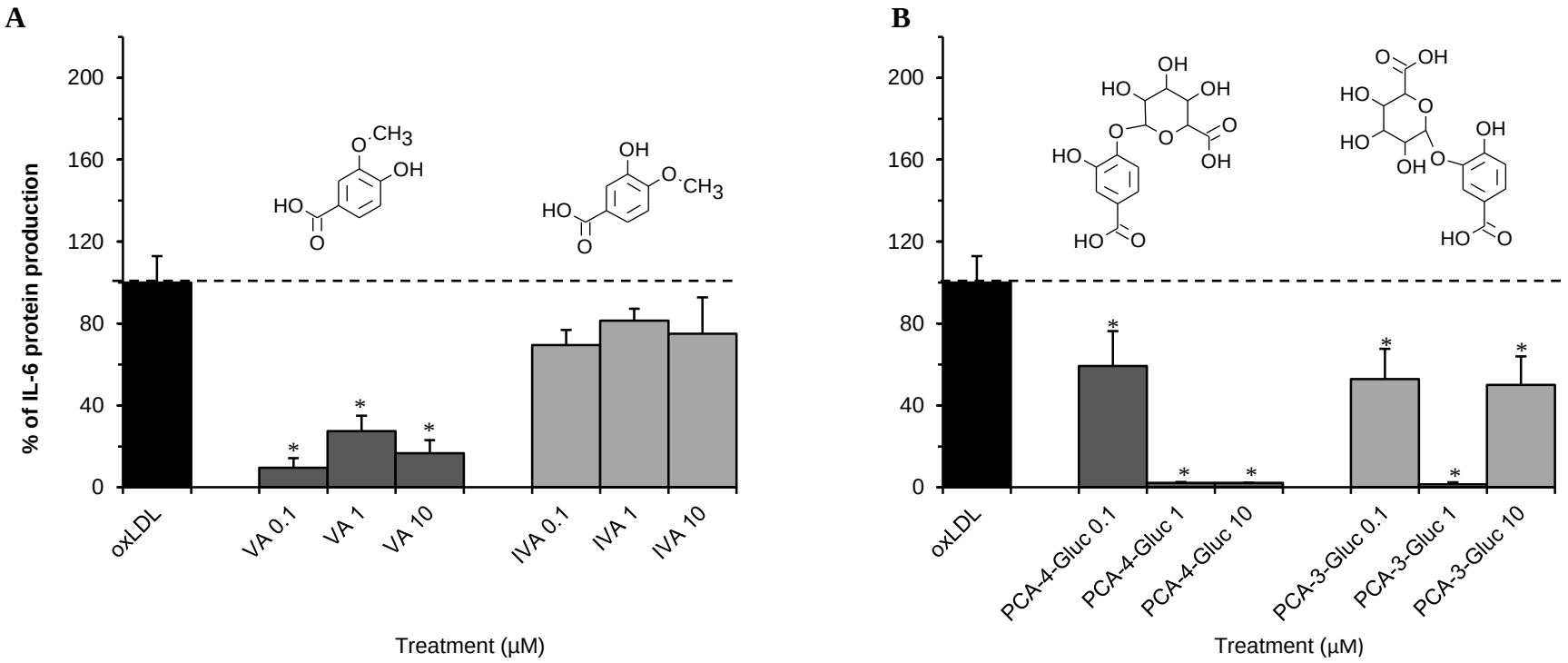

HUVECs co-incubated with VA, IVA, PCA-4-Gluc or PCA-3-Gluc for 24 hours. A, cells incubated with VA or IVA at 0.1, 1 and 10 µM and oxLDL (5 µg/mL); B, cells incubated with PCA-4-Gluc or PCA-3-Gluc at 0.1, 1 and 10 µM and oxLDL (5 µg/mL). All data expressed as mean percentage (± SD, n=3) of oxLDL-induced controls (expressed as 100%).Absolute IL-6 protein value in unstimulated HUVECs - 37.2 pg/mL, standard range 9.375 – 600 pg/mL. *p<0.001 (ANOVA with Tukey post-hoc) relative to oxLDL-stimulated control cells. %).VA, vanillic acid; IVA, isovanillic acid; PCA-4-Gluc, protocatechuic acid-4-glucuronide; PCA-3-Gluc, protocatechuic acid-3-glucuronide.

Figure 5.3 Effect of sulfated and/or methylated phenolic metabolites of PCA on oxLDL-induced IL-6 protein production

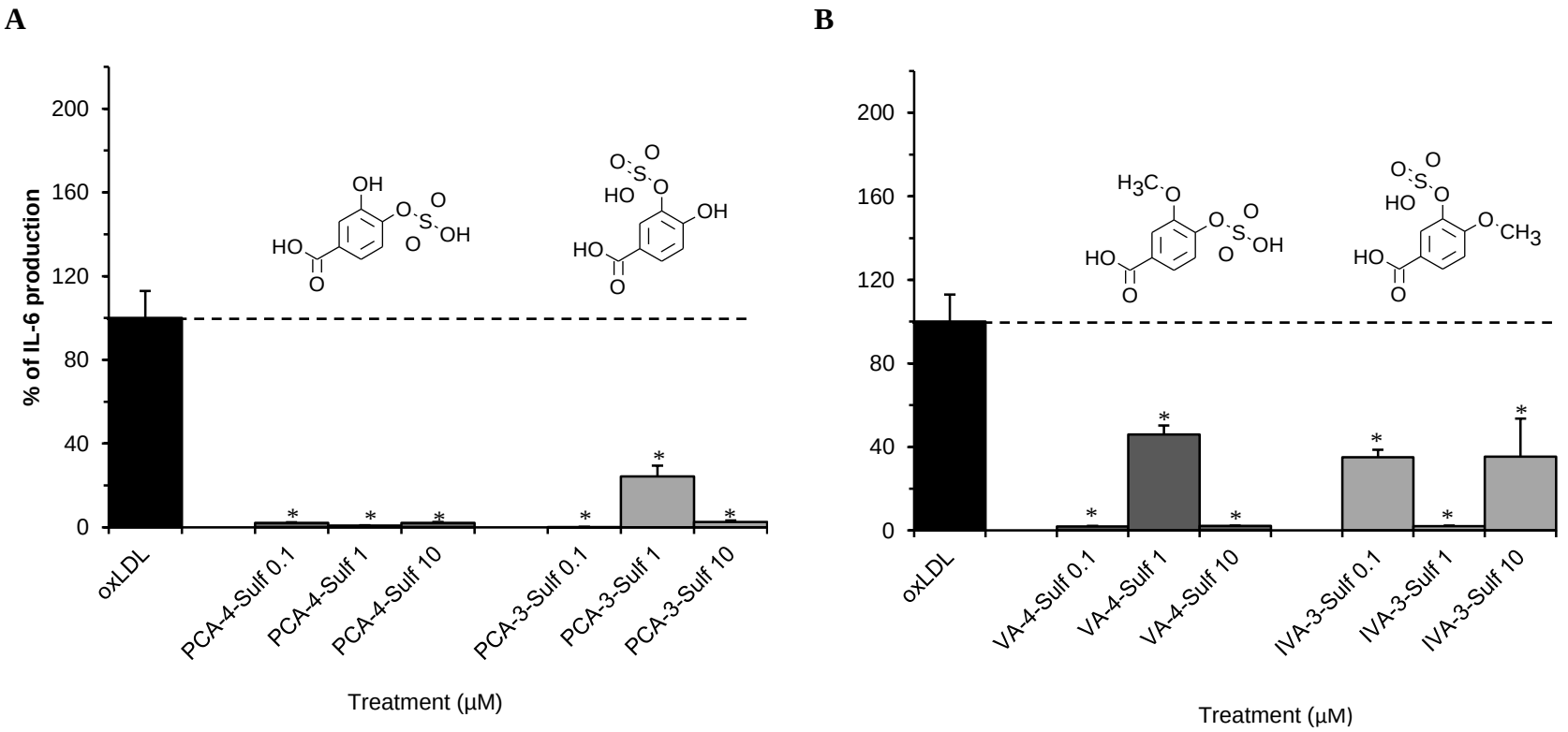

OxLDL-stimulated IL-6 protein production in HUVECs co-incubated with PCA-4-Sulf, PCA-3-Sulf, VA-4-Sulf or IVA-3-Sulf for 24 hours. A, cells incubated with PCA-4-Sulf or PCA-3-Sulf at 0.1, 1 and 10 μM and oxLDL (5 μg/mL); B, cells incubated with VA-4-Sulf or IVA-3-Sulf at 0.1, 1 and 10 μM and oxLDL (5 μg/mL). All data expressed as mean percentage (± SD, n=3) of oxLDL-induced controls (expressed as 100%). Absolute IL-6 protein value in unstimulated HUVECs - 37.2 pg/mL, standard range 9.375 – 600 pg/mL. *p<0.001 (ANOVA with Tukey post-hoc) relative to oxLDL-stimulated control cells. PCA-4-Sulf, protocatechuic acid-4-sulfate; PCA-3-Sulf, protocatechuic acid-3-sulfate; VA-4-Sulf, vanillic acid-4-sulfate; IVA-3-Sulf, isovanillic acid-3-sulfate.

Figure 5.4 Effect of ferulic acid metabolite on oxLDL-induced IL-6 protein production

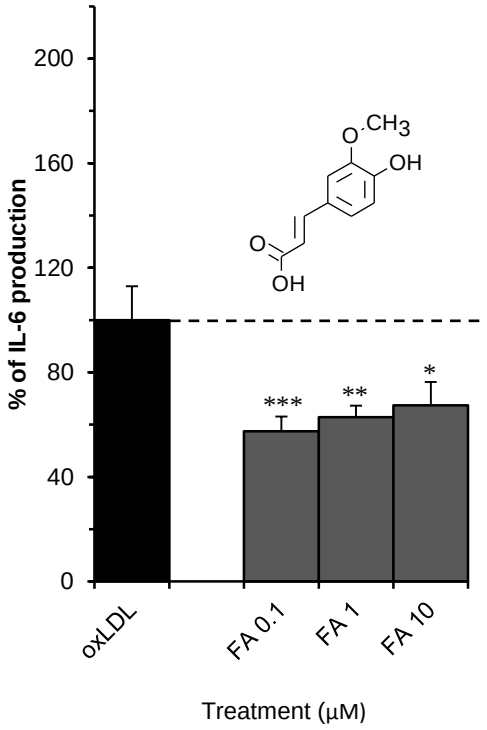

HUVECs co-incubated with FA at 0.1, 1, 10 μM and oxLDL (5 μg/mL) for 24 hours. All data expressed as mean percentage (± SD, n=3) of oxLDL-induced controls. Absolute IL-6 protein value in unstimulated HUVECs - 37.2 pg/mL, standard range 9.375 – 600 pg/mL. ***p<0.001, **p<0.01, *p<0.05 (ANOVA with Tukey post-hoc) relative to CD40L-stimulated control. FA, ferulic acid.

Figure 5.5 Modulation of oxLDL induced IL-6 mRNA levels in HUVECs co-incubated with bioactive metabolites of C3G.

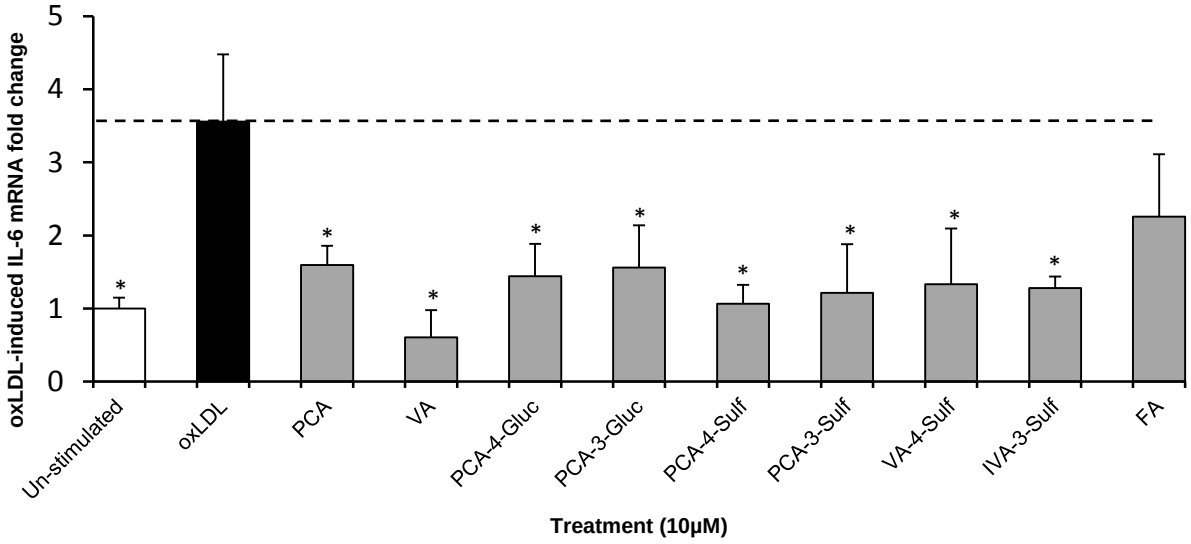

HUVECs were co-incubated with phenolic metabolites of C3G at 10 μM or oxLDL controls for 24 hours. All graphical data expressed as mean fold change (± SD, n=3) of un-stimulated (basal) IL-6 mRNA levels. *p<0.05 (ANOVA with Tukey post-hoc) relative to oxLDL-stimulated control. PCA, protocatechuic acid; VA, vanillic acid; PCA-4-Gluc, PCA-4-glucuronide; PCA-3-Gluc, PCA-3-glucuronide; PCA-3-Sulf, PCA-3-sulfate; PCA-4-Sulf, PCA-4-sulfate; VA-4-Sulf, VA-4-sulfate, IVA-3-Sulf, IVA-3-sulfate, FA, ferulic acid.

the greatest reduction in oxLDL-induced IL-6 mRNA expression of 82.9±10.4% relative to the oxLDL control ($p<0.001$).

CD40L-stimulated IL-6 protein production

The effect of C3G and its metabolites on CD40L-induced IL-6 protein production was explored by co-incubation of CD40L-expressing D1.1 cells with HUVECs. Here, IL-6 protein expression was significantly increased (3.2±1.5 fold) in CD40L-treated HUVECs, but reduced (by 44.4±1.7%) when D1.1 cells were pre-incubated with anti-CD40L antibody, confirming the role of CD40L in the production of IL-6 in the present model (**Figure 5.6A**). Of the 12 compounds tested, 8 reduced CD40L-induced IL-6 protein production by >41.7±3.5%, relative to cells treated with CD40L alone (CD40L control) ($p<0.03$, **Figure 5.6B to Figure 5.9**).

C3G and PCA both reduced CD40L-induced IL-6 protein production by >44.6±23.0% relative to the CD40L control ($p<0.05$, Figure 5.6B), whilst PGA was without effect. Six conjugated metabolites of PCA, namely VA, IVA, PCA-3-glucuronide, PCA-3-sulfate, PCA-4-sulfate, and IVA-3-sulfate, reduced CD40L-induced IL-6 production by >41.7±3.5%($p<0.03$) at one or more of the concentrations tested (Figure 5.7 and Figure 5.8), with a maximal reduction of 95.8±1.3% ($p<0.001$) observed for the sulfate conjugate of PCA, PCA-4-sulfate (Figure 5.8A). PCA-4-glucuronide, VA-4-sulfate and ferulic acid showed no significant activity against CD40L induced IL-6 production (Figure 5.7B, Figure 5.8B and Figure 5.9). Trends were observed for C3G at 10 µM ($p< 0.13$, Figure 5.6B) and VA-4-sulfate at 0.1 µM ($p<0.06$, Figure 5.8B).

The 8 compounds which reduced CD40L-induced IL-6 production, as reported above, were further investigated for their effects on IL-6 mRNA levels following incubation of HUVEC with the treatment compounds at 10 µM for 24 hours. Co-incubation of HUVECs with CD40L increased IL-6 mRNA expression by 2.3±0.3 fold ($p<0.05$, **Figure 5.10**), while anti-CD40L reduced IL-6 mRNA levels to below that observed in untreated HUVECs (0.2±0.1 fold, $p<0.05$). With the exception of IVA, all compounds reduced CD40L-induced IL-6 mRNA expression by >85.3 ±2.5% ($p <0.01$, Figure 5.10) relative to the CD40L-treated control. PCA elicited the greatest reduction in CD40L-induced IL-6 mRNA expression, where mRNA levels were reduced by 94.9±8.3% of the CD40L-induced control ($p<0.001$).

Figure 5.6 Effect of CD40L controls, C3G and its degradants on CD40L-induced IL-6 protein production

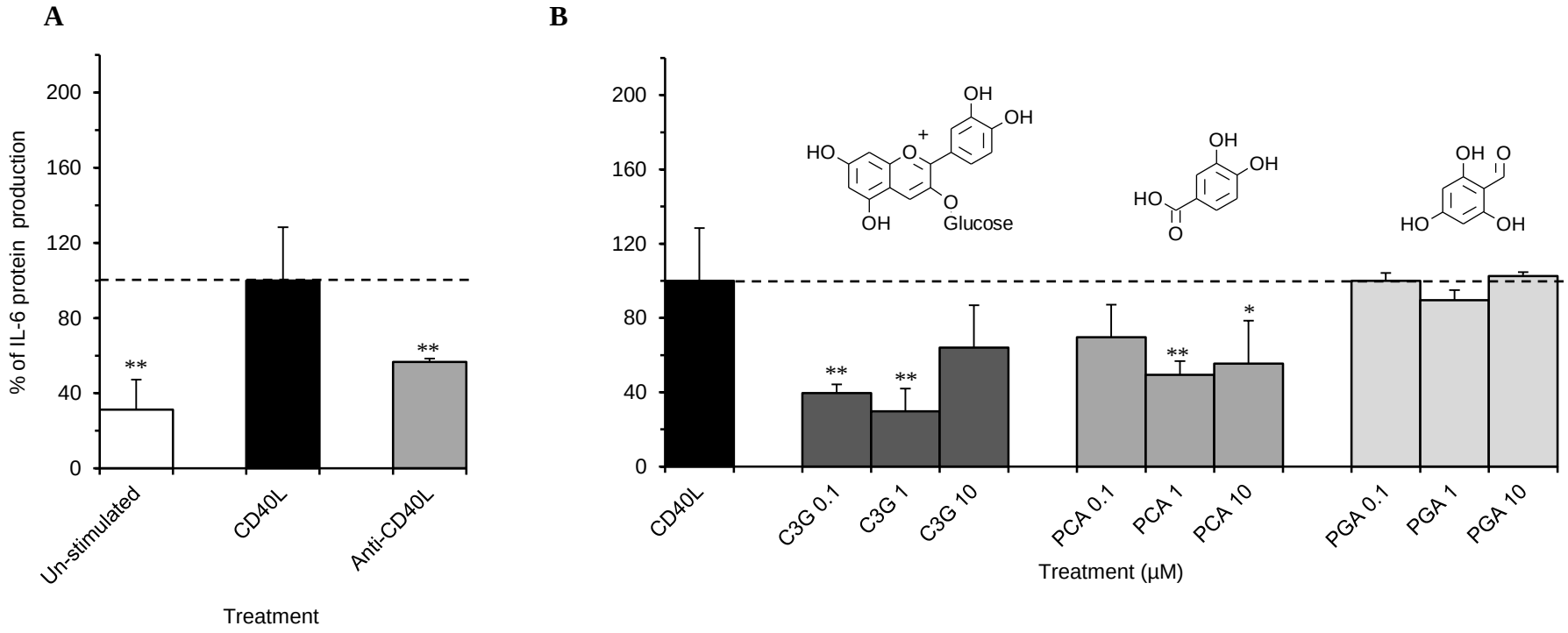

HUVECs co-incubated with C3G, PCA, PGA or CD40L controls for 24 hours. A, cells incubated with or without D1.1 cells (1 x 10^6 cells/well); B, cells incubated with C3G, PCA or PGA at 0.1, 1, 10 µM and D1.1 cells (1 x 10^6 cells/well). All data expressed as mean percentage (± SD, n=3) of CD40L-induced controls. Absolute IL-6 protein value in unstimulated HUVECs - 30.3 pg/mL, standard range 9.375 – 600 pg/mL. **p<0.001, *p<0.01 (ANOVA with Tukey post-hoc) relative to CD40L-stimulated control. C3G, cyanidin-3-glucoside; PCA, protocatechuic acid; PGA, phloroglucinaldehyde.

Figure 5.7 Effect of methylated and glucuronidated phenolic metabolites on CD40L-induced IL-6 protein production

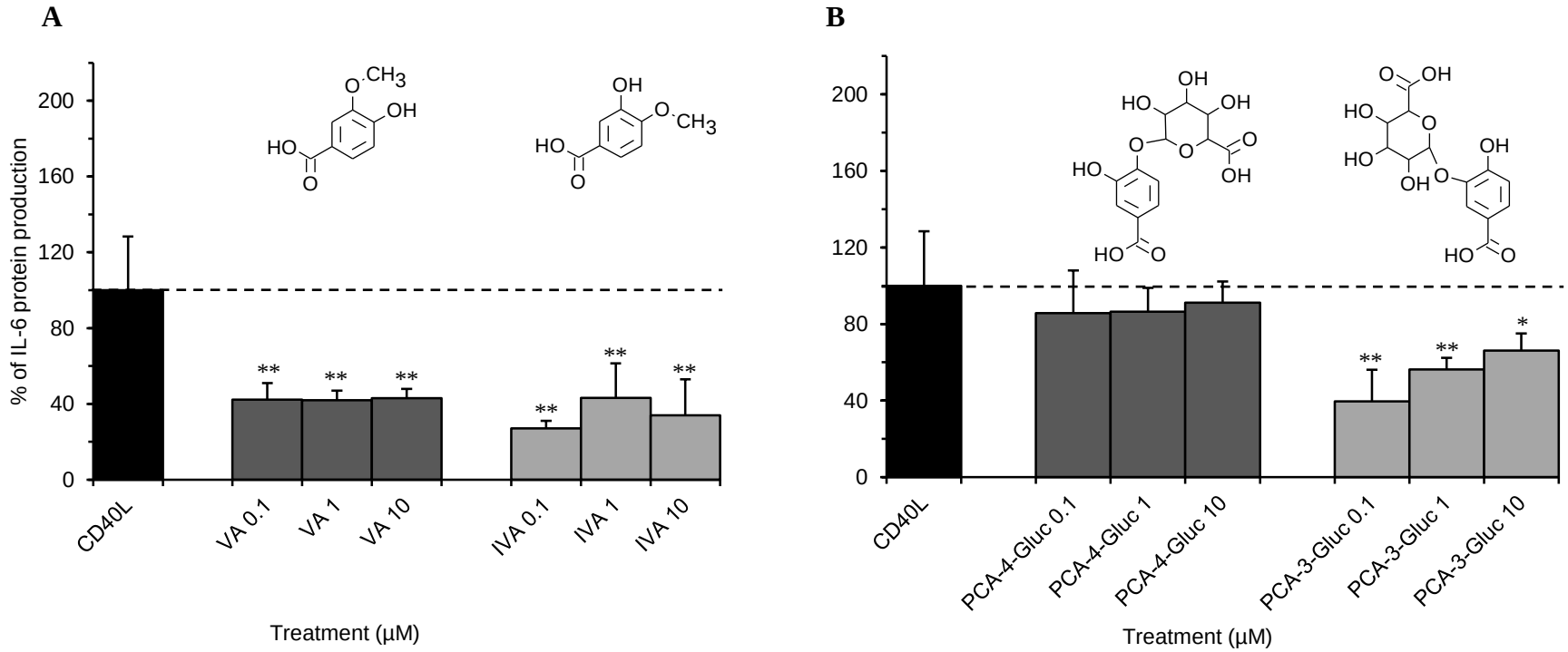

HUVECs co-incubated with VA, IVA, PCA-4-Gluc or PCA-3-Gluc for 24 hours. A, B, cells incubated with VA, IVA, PCA-4-Gluc or PCA-3-Gluc at 0.1, 1, 10 μM and D1.1 cells (1 x 10^6 cells/well). All data expressed as mean percentage (± SD, n=3) of CD40L-induced controls. Absolute IL-6 protein value in unstimulated HUVECs - 30.3 pg/mL, standard range 9.375 – 600 pg/mL. **p<0.001, *p<0.01 (ANOVA with Tukey post-hoc) relative to CD40L-stimulated control. ; VA, vanillic acid; IVA, isovanillic acid; PCA-4-Gluc, protocatechuic acid-4-glucuronide; PCA-3-Gluc, protocatechuic acid-3-glucuronide.

Figure 5.8 Effect of sulfated and multiple conjugated phenolic metabolites on CD40L-induced IL-6 protein production

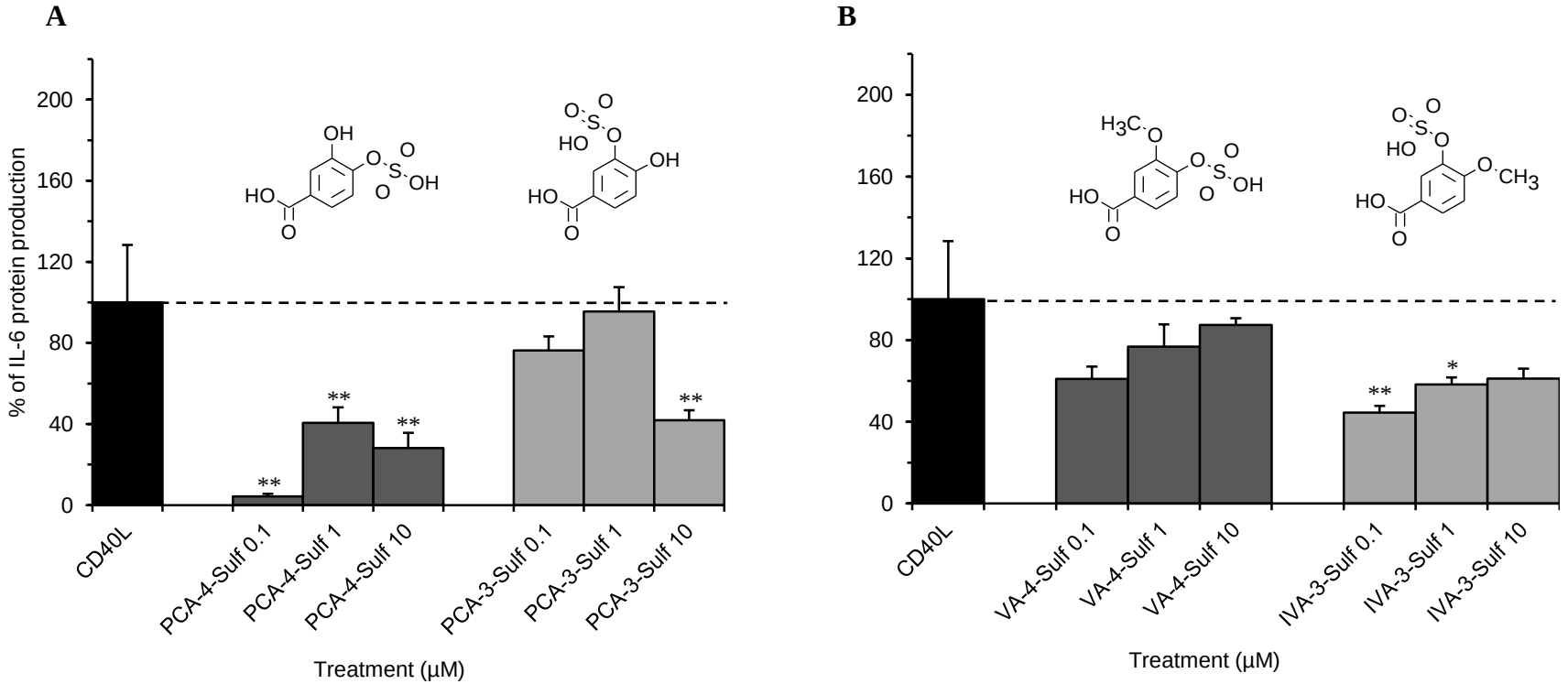

HUVECs co-incubated with PCA-4-Sulf, PCA-3-Sulf, VA-4-Sulf or IVA-3-Sulf or for 24 hours. A, B, cells incubated with PCA-4-Sulf, PCA-3-Sulf, VA-4-Sulf or IVA-3-Sulf at 0.1, 1, 10 µM and D1.1 cells (1 x 10^6 cells/well). All data expressed as mean percentage (± SD, n=3) of CD40L-induced controls. Absolute IL-6 protein value in unstimulated HUVECs - 30.3 pg/mL, standard range 9.375 – 600 pg/mL. **p<0.001, *p<0.01 (ANOVA with Tukey post-hoc) relative to CD40L-stimulated control. PCA-4-Sulf, protocatechuic acid-4-sulfate; PCA-3-Sulf, protocatechuic acid-3-sulfate; VA-4-Sulf, vanillic acid-4-sulfate; IVA-3-Sulf, isovanillic acid-3-sulfate.

Figure 5.9 Effect of ferulic acid metabolite on CD40L-induced IL-6 protein production

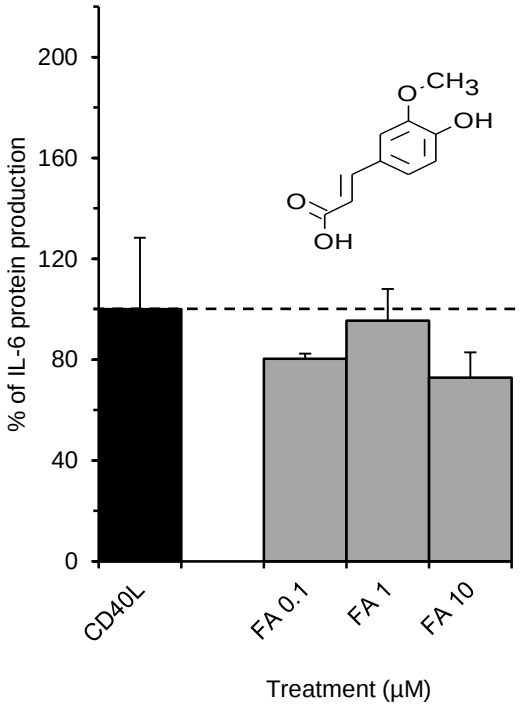

HUVECs co-incubated with FA at 0.1, 1, 10 µM and D1.1 cells (1 x 10^6 cells/well) for 24 hours. All data expressed as mean percentage (± SD, n=3) of oxLDL-induced controls. Absolute IL-6 protein value in unstimulated HUVECs - 30.3 pg/mL, standard range 9.375 – 600 pg/mL. ***p<0.001 (ANOVA with Tukey post-hoc) relative to CD40L-stimulated control. FA, ferulic acid.

Figure 5.10 Effect of C3G and bioactive phenolic metabolites on CD40L-induced IL-6 mRNA expression.

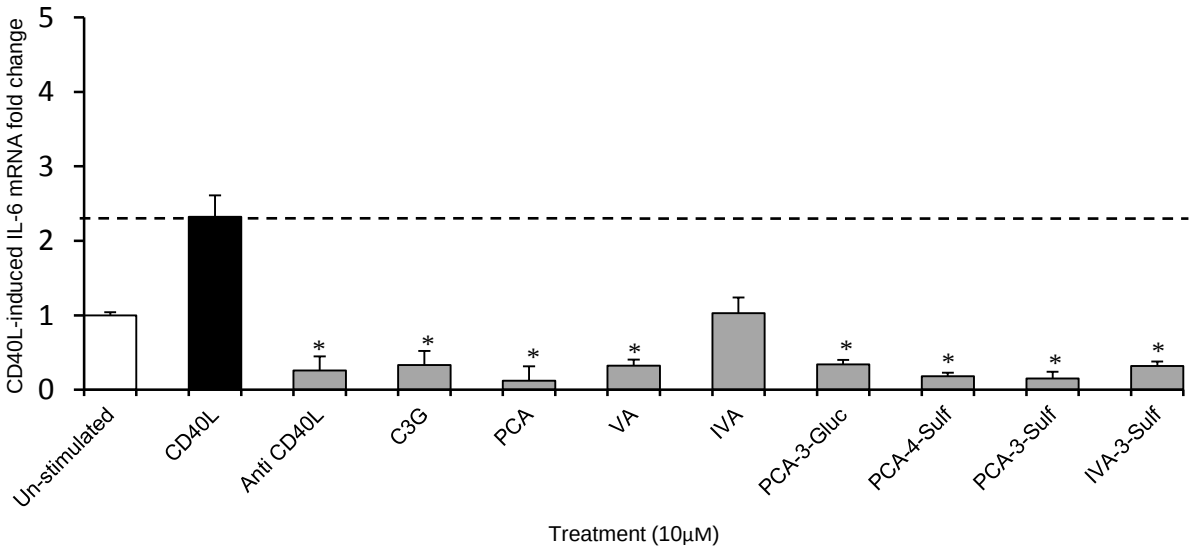

HUVECs co-incubated with C3G and phenolic metabolites at 10 µM or CD40L controls for 24 hours. All graphical data expressed as mean fold change (± SD, n=3) of un-stimulated (basal) IL-6 mRNA levels. *p<0.05 (ANOVA with Tukey post-hoc) relative to CD40L-stimulated control. C3G, cyanidin-3-glucoside; PCA, protocatechuic acid; VA, vanillic acid; IVA, isovanillic acid; PCA-3-Gluc, PCA-3-glucuronide; PCA-4-Sulf, PCA-4-sulfate; PCA-3-Sulf, PCA-3-sulfate; IVA-3-Sulf, IVA-3-sulfate.

5.4 Discussion

Anthocyanin consumption is inversely associated with CVD risk (Cassidy, Mukamal et al. 2013), and most previous animal and *in vitro* studies have examined the activity of parent (un-metabolized) anthocyanins in models of inflammation, where they have been reported to have anti-inflammatory activity (Karlsen, Retterstøl et al. 2007, Xia, Ling et al. 2007, Edirisinghe, Banaszewski et al. 2011, Kolehmainen, Mykkänen et al. 2012). In the present study 11 *in vivo* metabolites of C3G (Czank, Cassidy et al. 2013) were explored for their activity on oxLDL- and CD40L-induced IL-6 expression in HUVECs.As discussed previously (Chapter 3), anthocyanins have been shown to reduce the effect of oxLDL (Yi, Chen et al. 2010) and CD40L signaling (Xia, Ling et al. 2007) in endothelial cells. The major finding of the present study is that anthocyanin degradation and subsequent metabolism of the degradation product PCA does not reduce the bioactivity of the derived metabolites but perhaps increases it.

Oxidised LDL is a potent chronic inflammatory activator and established risk factor for CVD (Holvoet, Mertens et al. 2001), and has also been shown to increase levels of IL-6 in vascular endothelial cells (Lee, Ou et al. 2010). However, very little is known of the effects of physiologically relevant anthocyanin metabolites on oxLDL-mediated inflammation. Oxidised LDL is known to be pro-apoptotic at high concentrations (such as 100 µg/mL) in vascular endothelial cells (Galle, Schneider et al. 1999), thus the present study has utilized considerably lower concentrations (5 µg/mL) than previous *in vitro* investigations (Wahyudi and Sargowo 2007, Lee, Ou et al. 2010) in an attempt to create a more physiologically relevant model of vascular dysfunction. The levels of oxLDL utilized in the present investigation are comparable to those identified in the blood of patients with coronary artery disease (Holvoet, Mertens et al. 2001). Moreover, the present study is the first to investigate the effects of C3G metabolites on oxLDL-induced IL-6 production *in vitro*, and our findings suggests that anti-inflammatory effects of anthocyanins are not limited to the parent compounds themselves; as their lower molecular weight phenolic metabolites also displayed significant bioactivity, as observed by reductions in oxLDL-induced IL-6 protein production by as much as 99% relative to control cells (Figure 5.3). This suggests anthocyanin degradation and conjugation of phenolic metabolites does not reduce biological activity, and may in fact result in greater efficacy of the metabolites relative to the parent structure.

As discussed previously (Chapter 3), the activation of CD40 via its ligand, CD40L, is also associated with promotion of chronic inflammation and the expression of pro-inflammatory mediators, including IL-6 (Xia, Ling et al. 2007) and therefore plays a pivotal role in the development of CVD. Thus it is crucial to investigate the effect of C3G metabolites on CD40L-mediated inflammation. The current study again revealed increased bioactivity of lower molecular weight phenolic metabolites relative to the parent anthocyanin, as demonstrated by the reductions in CD40L-induced IL-6 protein production, by as much as 95% (Figure 5.8A). The effects of C3G on CD40L-induced IL-6 expression have previously been reported by Xia et al. (Xia, Ling et al. 2007), where they observed a significant reduction in CD40L-induced IL-6 protein production following incubation of endothelial cells with C3G. The present findings are in accordance with this previous work and provide additional evidence for the activity of C3G.

Previous structure-function studies have indicated that there is a positive correlation between the number of hydroxyl groups present on the B-ring of flavonoids and their anti-inflammatory (Theoharides, Alexandrakis et al. 2001) and radical scavenging activity (Yi, Chen et al. 2010), and their ability to reduce oxLDL-mediated cell apoptosis (Chang, Huang et al. 2006). Moreover, compounds containing an ortho-dihydroxy (catechol) group on the B-ring have been previously been shown to reduce the production of inflammatory mediators including IL-6 and cyclo-oxygenase (COX)-2 (Theoharides, Alexandrakis et al. 2001, Hou, Yanagita et al. 2005). The present study investigated groups of metabolites which have either intact or conjugated/modified (methylated, glucuronidated and sulfated) catechol moieties, allowing for examination of structure-function relationships. In oxLDL-stimulated HUVECs, IL-6 protein production was significantly decreased by 9 of 12 compounds tested (Figure 5.1 to Figure 5.4). Amongst these, one of the degradation products of C3G, PCA, reduced oxLDL-induced IL-6 production significantly, whereas C3G and PGA had no effect (Figure 5.1B); suggesting that the degradation of C3G to PCA may increase the bioactivity of the anthocyanin derivative. However, as both C3G and PCA have a catechol moiety, this group is unlikely to be the only structural requirement for biological activity under the culture conditions used in the present study. All PCA conjugates tested, except IVA, reduced oxLDL-induced IL-6 production significantly (32-99% reduction, Figure 5.2 to Figure 5.4) regardless of conjugation position; suggesting further metabolism does not result in decreased bioactivity. Sulfate conjugation at either hydroxyl (3' or 4') reduced oxLDL-induced IL-6 production to the greatest extent (by as much as 99% of control levels), compared to

other conjugation reactions (methylation or glucuronidation), suggesting sulfation of PCA has the greatest impact on bioactivity in the present model. PCA-3-glucuronide and PCA-3-sulfate elicited similar biological activities as their respective counterparts, suggesting there was no hierarchical activity for 3' vs. 4' conjugation of the catechol moiety of PCA with sulfate and glucuronic acid. However, this was not the case for methylation, as methylation at the 3' position (VA) resulted in increased bioactivity while the 4'-methyl conjugate (IVA) was inactive. The bioactivity of VA (the 3'-methyl derivative of PCA) has previously been reported in *in vitro* models by Kim et al, 2011 (Kim, Kim et al. 2011), where VA reduced IL-6 production in lipopolysaccharide (LPS)-induced mouse peritoneal macrophages. Furthermore, in the present study, VA reduced IL-6 production under both stimulation conditions (oxLDL and CD40L), suggesting significant anti-inflammatory activity. With regard to the other phase II conjugated derivatives of PCA tested (PCA-3-glucuronide, PCA-4-glucuronide, PCA-3-sulfate, PCA-4-sulfate, VA-4-sulfate and IVA-3-sulfate) this is the first *in vitro* study to report their anti-inflammatory activity.

In CD40L-stimulated HUVECs, eight of 12 compounds examined reduced IL-6 protein production at one or more concentrations (between 41-96% of CD40L control). Cyanidin-3-glucoside and its B-ring degradation product, PCA, significantly reduced IL-6 production (Figure 5.6B), whilst PGA did not; again suggesting the catechol group imparts some anti-inflammatory activity under CD40L-stimulated conditions. However, further metabolic conjugation of the catechol group does not appear to significantly reduce this activity. Of the conjugated metabolites of PCA tested, all compounds except PCA-4-glucuronide, VA-4-sulfate and FA, reduced CD40L-induced IL-6 production, with a maximum reduction observed for PCA-4-sulfate (95.8% reduction relative to CD40L control), again indicating sulfate conjugation has the greatest impact on bioactivity. The structure-activity relationship of PCA conjugation relative to inhibition of CD40L-induced IL-6 production is less apparent than for oxLDL-stimulated conditions, as PCA-3-glucuronide, PCA-3-sulfate, PCA-4-sulfate and IVA-3-sulfate all significantly reduced CD40L-stimulated IL-6 protein production (Figure 5.7andFigure 5.8).

It must be noted that some of the metabolites elicited differential effects on IL-6 production according to the stimulus applied to endothelial cells. For example, IVA reduced IL-6 protein production significantly in CD40L-stimulated HUVECs (by 56-73% of CD40L control, Figure 5.7A) but had no effect on oxLDL-challenged HUVECs (Figure 5.2A). Similarly,

FA significantly reduced oxLDL-induced IL-6 production (by 32-42% of oxLDL control, Figure 5.4) but did not alter CD40L-stimulated IL-6 production (Figure 5.9). Considering the above, the anti-inflammatory activity of these metabolites appears to differ depending on the inflammatory stimulus present, suggesting that these compounds may act by targeting unique signalling pathways (i.e. unique to either CD40L or oxLDL signalling); potentially by acting on tumour necrosis factor alpha receptor associated factor-2 (TRAF-2) (Xia, Ling et al. 2007) during CD40L signalling, and LOX-1 (oxLDL receptor) during oxLDL signalling(Morawietz 2007). Further research is necessary to establish the direct pathways affected.

In most cases, metabolites which reduced protein levels of IL-6 also reduced IL-6 mRNA levels. In oxLDL-stimulated HUVECs, all bioactive compounds, except FA, reduced IL-6 mRNA levels by between 55-83% compared to the oxLDL control. Similarly, in CD40L-stimulated HUVECs, all compounds, except IVA, reduced IL-6 mRNA levels (between 85-95% of the CD40L control), indicating that the effect of these metabolites on CD40L-induced IL-6 mRNA levels may play a key role in reducing IL-6 protein production. Whilst this evidence may explain the association between a significant alteration in gene expression and protein levels, several instances were noted where a reduction in protein levels (Figure 5.4 and Figure 5.7A) was not correlated with a reduction in mRNA levels (Figure 5.5 and Figure 5.10). Such divergence may be the result of post-translational modification of IL-6, as it is subject to phosphorylation and glycosylation (Santhanam, Ghrayeb et al. 1989, Van Snick 1990, May and Sehgal 1992).

A possible mechanism by which metabolites may alter IL-6 mRNA levels is by modulating the activation of NF-κB, which affects IL-6 production (Xia, Ling et al. 2007, Terasaka, Miyazaki et al. 2010). Anthocyanin-enriched extracts have been demonstrated to inhibit the activation of NF-κB in *in vitro* studies using blueberries (Xie, Kang et al. 2011) and black rice extract (Min, Ryu et al. 2010). Furthermore, PCA, VA, and FA have been demonstrated to inhibit NF-κB activation in various *in vitro* models (Ma, Hong et al. 2010, Wang, Wei et al. 2010, Kim, Kim et al. 2011). Cyanidin-3-glucoside has also been reported to attenuate NF-κB activity through impairing the translocation of TRAF-2 to lipid rafts (Xia, Ling et al. 2007). The present study examined the effect of anthocyanin metabolites at three concentrations (0.1, 1 and 10 μM), and a non-linear dose responses were observed; which has previously been reported for other flavonoids such as quercetin and genistein, and may

have important biological implications (Kato, Horie et al. 2008, Chirumbolo, Marzotto et al. 2010).

While the present study provides novel insight into the anti-inflammatory activity of recently identified anthocyanin metabolites, there are certain limitations of this experimental approach. First, the measurement of IL-6 protein production under stimulated conditions was carried out at a single time point (after 24 hours stimulation), and the effects may differ following shorter periods of incubation. Further time course studies are required to establish peak effects. The present study also utilized a co-incubation model of activity, and effects of anthocyanin metabolites may differ according to their presence pre- or post-stimulation (CD40L or oxLDL). In addition, even though HUVECs are a well-established model for endothelial cell research (Baudin, Bruneel et al. 2007), these results should be confirmed in a different cell type such as human coronary artery endothelial cells. Furthermore, the present study used D1.1 cells as a source of CD40L and the results should be confirmed using recombinant CD40L (soluble CD40L). This aside, the present study is a preliminary screen for the biological activity of anthocyanin metabolites, and provides future directions for anthocyanin research.

It is apparent from the present study that C3G metabolites are bioactive at physiologically relevant concentrations, and are able to alter the production of IL-6 protein. Moreover, there is a relationship between anti-inflammatory activities of these metabolites and their structures.Further research is required to establish not only the underlying mechanisms involved, but also the physiological relevance of these findings in humans. The future studies to explore underlying mechanism may include effects of bioactive compounds on post-translation modification of IL-6, modulation of oxLDL/LOX-1 interaction in HUVECs, CD40/TRAF-2 interaction in HUVECs and on transcription factors such as NF-κB. In order to establish human relevance, the bioactive compounds may be explore in atherosclerotic mice model as described before by Wang et al (Wang, Wei et al. 2010).The current study provides the first evidence that anthocyanin metabolites possess anti-inflammatory effects, which are likely to contribute to the reduced risk of CVD associated with the chronic consumption of anthocyanins, as reported by epidemiological studies (Mink, Scrafford et al. 2007, Cassidy, O'Reilly et al. 2010, Cassidy, Mukamal et al. 2013).

Chapter 6. Effects of phenolic metabolites of anthocyanins on activation of NF-κB

6.1 Introduction

Chronic consumption of anthocyanins has been associated with reduced risk of cardiovascular disease (CVD) (Mink, Scrafford et al. 2007, Wallace 2011, McCullough, Peterson et al. 2012), and potential cardioprotective effects of anthocyanins are also supported by data from randomised controlled trials (Karlsen, Paur et al. 2010, Zhu, Xia et al. 2011), animal studies (Elks, Reed et al. 2011) and *in vitro* investigations (Lazze, Pizzala et al. 2006, Xia, Ling et al. 2007, Xie, Kang et al. 2011). These effects of anthocyanins may be attributable to their activity as anti-inflammatory agents, as described previously (Chapters 3 and 4), where cyanidin-3-glucoside (C3G) and its lower molecular weight degradants and metabolites demonstrated anti-inflammatory activity in an endothelial cell model. Moreover, the majority of the phenolic metabolites tested significantly attenuated expression of vascular cell adhesion molecule-1 (VCAM-1) and interleukin-6 (IL-6) in stimulated human umbilical vein endothelial cells (HUVEC). However, the mechanisms of action underlying the observed activity of phenolic metabolites remain largely unknown. Since VCAM-1 and IL-6 expression are up-regulated through the activity of the transcription factor NF-κB, and C3G has been shown to attenuate activation of NF-κB *in vitro* (Karlsen, Retterstøl et al. 2007, Xia, Ling et al. 2007, Karlsen, Paur et al. 2010, Xie, Kang et al. 2011), the present study explored NF-κB activation as a potential mechanism by which C3G and its phenolic metabolites might exert anti-inflammatory activity. Amongst the compounds previously screened for such activity (Chapters 3 and 4), protocatechuic acid (PCA) and vanillic acid (VA) (**Figure 6.1**) exhibited significant bioactivity across multiple assays and were therefore selected for the current investigation. Both PCA and VA have been previously shown to reduce NF-κB activation by blocking the translocation of the p65 subunit to the nucleus in *ex vivo* mouse models (Kim, Kim et al. 2010, Wang, Wei et al. 2010, Kim, Kim et al. 2011, Wei, Chu et al. 2013) which provides further support to the hypothesis that phenolic metabolites may modulate NF-κB signalling. NF-κB p65 is a key subunit of NF-κB protein that, after translocation to the nucleus, binds to κB enhancer and stimulates gene expression through the transcriptional activation domain of NF-κB p65 (Huang, Yang et al.

2010). However, the effect of PCA and VA at physiologically relevant concentrations upon NF-κB activation is largely unknown, and the present study aimed to address this deficiency in current scientific knowledge. In order to evaluate NF-κB activation, the phosphorylation of the p65 subunit was examined using a flow cytometry-based methodology.

Figure 6.1 Chemical structures of PCA and VA

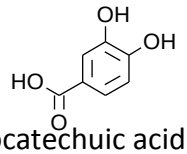

Protocatechuic acid (PCA)

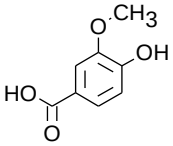

Vanillic Acid (VA)

6.2 Methods and materials

Standards and Materials. Anti-human phospho-NF kappa B p65 (S529) eFluor® 660 and Mouse IgG2a, K Isotype Control eFluor® 660 (Alexa Fluor® 647 replacement) were purchased from eBioscience (Hatfield, UK) IL-1β was generous gift from Dr Rosemary Davidson, Senior Post Doctoral Research Associate, School of Biological Sciences (UEA, Norwich)

Cell fixation, permeabilisation and staining. Cells were fixed and permeabilised using a protocol obtained from Beckman Coulter (High Wycombe, UK) for fixation and permeabilisation (protocol for Alexa Fluor® 488 conjugate, catalogue no: A88886). Briefly, once trypsinised and transferred into 1.5 mL eppendolf tubes, HUVECs were centrifuged at 400 x *g* for 10 minutes at 4°C then re-suspended in ice-cold 4% methanol-free formaldehyde (500 µL/tube) and incubated for 10 minutes at 37°C. Cells were then permeabilised using ice-cold 90% methanol (500 µL/tube) and stored at -20°C until used for staining. Once thawed, HUVECs were washed with incubation buffer, 0.5 g of BSA per 100 mL of 1%phosphate buffered saline (PBS) (1.5 mL/tube, with centrifugation at 600 x *g* at 4°C for 10 minutes;, repeated three times) followed by blocking using incubation buffer (50 µL/tube) for 10 minutes before staining with anti-human phospho-NF kappa B p65 (S529) eFluor® 660 (0.012 µg/tube) and isotype control antibody mouse IgG2a, K Isotype Control eFluor® 660 (Alexa Fluor® 647 Replacement, 0.012 µg/tube) for 1 hour at room temperature. Post-staining, excess antibodies were removed by washing as described above, and HUVECs were re-

suspended in 150 µL of 1% PBS followed by analysis using flow cytometery for phospho-NF-κB p65 intensity measurement using BD Accuri™ C6 instrument (BD Biosciences, Oxford, UK) at 660 nm (excitation at 640 nm). The sample was injected [at 62 µL/min (fast)] to collect a maximum of 5000 events in plot 1 [P1 (X-axis, forward scattered area; Y-axis side scattered area)]. P1 was structured to exclude cells debris, BSA particulates and cell doublets. Data collected in P1 was then analysed using BD Accuri™ C6 software (version 1.0.264.21) to collect median FL4 (excitation 640 nm, emission 675/25) data of eFLuor 660A intensity (Y-axis) against forward scatter (X-axis).

NF-κB p65 phosphorylation Method Optimisation.

Stimulation time optimisation. HUVECs and D1.1 cells were cultured as described in chapter 2. Oxidised LDL (oxLDL, 5 µg/mL), cluster of differentiation 40 ligand (CD40L) expressing D1.1 cells (1 x 10^6 cells/well) and interleukin-1 beta (IL-1β) (5 ng/mL) were utilised to induce phosphorylation of NF-κB p65 in HUVECs. Sub-confluent HUVECs (90 – 95%) were stimulated with oxLDL, D1.1 or IL-1β for 15 minutes, 30 minutes, 1 hour, 2 hours, 3 hours and 4 hours. Supernatants were discarded following cell stimulation, and cells were washed with warm 1% PBS (to remove D1.1 cells) before trypsinisation and collection in 1.5 mL tubes for fixation, permeabilisation and staining as described above.

Preliminary data from optimisation of stimulation time for oxLDL and CD40L showed no significant increase in NF-κB p65 phosphorylation at any time point tested ($p>0.05$, n=1, **Figure 6.2A and B**); while IL-1β significantly increased phosphorylation of NF-κB p65 after 15 minutes stimulation ($p<0.001$, n=1, Figure 6.2**C**), and hence this time point was selected as optimal to stimulate phosphorylation of NF-κB p65 in HUVEC using IL-1β in future experiments.

.

Figure 6.2 Time course for the effect of oxLDL (A), CD40L (B) and IL-1β (C) stimulation on phosphorylation of NF-κB p65

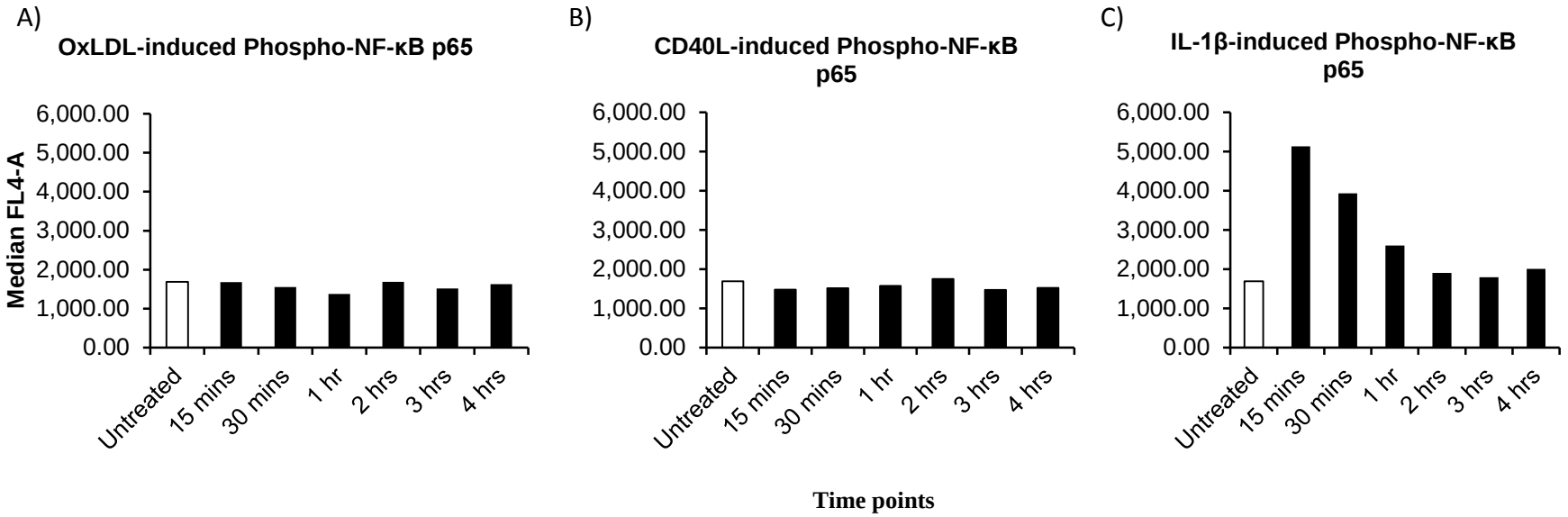

Median fluorescent intensity (FL4-A) data measured by flow cytometry at 660nm for oxLDL (5 µg/mL), CD40L (1 x 10^6 D1.1 cells/treatment) and IL-1β (5 ng/mL) stimulated HUVEC at 15 minutes, 30 minutes, 1 hour, 2 hours, 3 hours and 4 hours post stimulation (n=1). OxLDL, oxidised low density lipoprotein; CD40L, cluster of differentiation 40 ligand, IL-1β, interleukin-1 beta.

Final methodology. HUVECs were incubated with or without treatment compounds (PCA and VA) at 0.1, 1 and 10μM for 24 hours. Treatment media was then removed and cells were washed with warm 1% PBS, before stimulation with IL-1β (5 ng/mL) for 15 minutes. Post-stimulation, supernatants were discarded and cells were harvested with trypsin prior to fixation, permeabilisation and staining as described above. For gating strategy refer to applendix 7.

6.3 Results

Stimulation of HUVECs by IL-1β (5 ng/mL) resulted in a ~2 fold increase in phospho-NF-κB p65 compared to untreated HUVECs ($p<0.001$, **Figure 6.3A**). However, there was no difference observed in phospho-NF-κB p65 in HUVECs treated with 0.05% DMSO (vehicle control, data not shown). The IL-1β-stimulated phosphorylation of NF-κB p65 was attenuated by PCA and VA, between 27.4±2.8% and 40.5±4.5% (respectively) following pre-incubation at one or more concentrations tested, relative to IL-1β control. The greatest reduction in phosphorylation of NF-κB p65 was induced by VA, where 40.5±4.5% of IL-1β-induced NF-κB p65 phosphorylation was inhibited (Figure 6.3A). The effect of PCA and VA on phospho-NF-κB p65 was also evident in intensity plots (Figure 6.3B) where a clear shift in eFluor intensity towards that recorded for untreated HUVECs suggested a decreasein NF-κB p65 phosphorylation following incubation with PCA and VA prior to IL-1β stimulation (Figure 6.3B).

6.4 Discussion

The anti-inflammatory activity of lower molecular weight degradants and metabolites of C3G has been described previously (Chapters 3 and 4), where treatment compounds significantly decreased endothelial mRNA and protein levels of VCAM-1 and IL-6 levels under stimulated conditions; however, the mechanisms of action underlying these observed effects are mostly unknown.

Figure 6.3 Modulation of IL-1β-induced phosphorylation of NF-κB p65 in HUVECs by PCA and VA at 0.1 - 10µM, expressed as % of median intensity for IL1βtreated HUVECs (A) and as eFlour (660A) intensity plots for untreated (black), IL-1β (red), PCA (blue) and VA (green) HUVECs (B)

A)

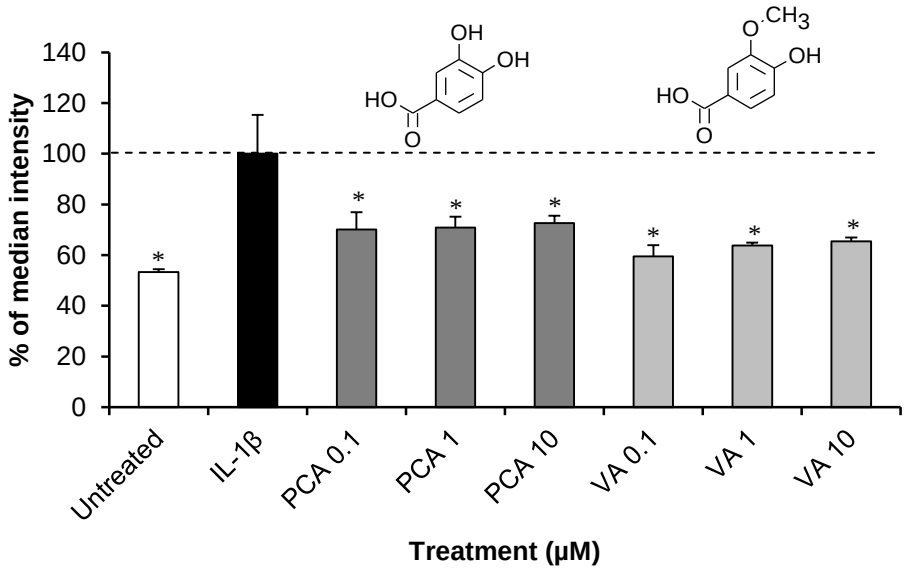

B)

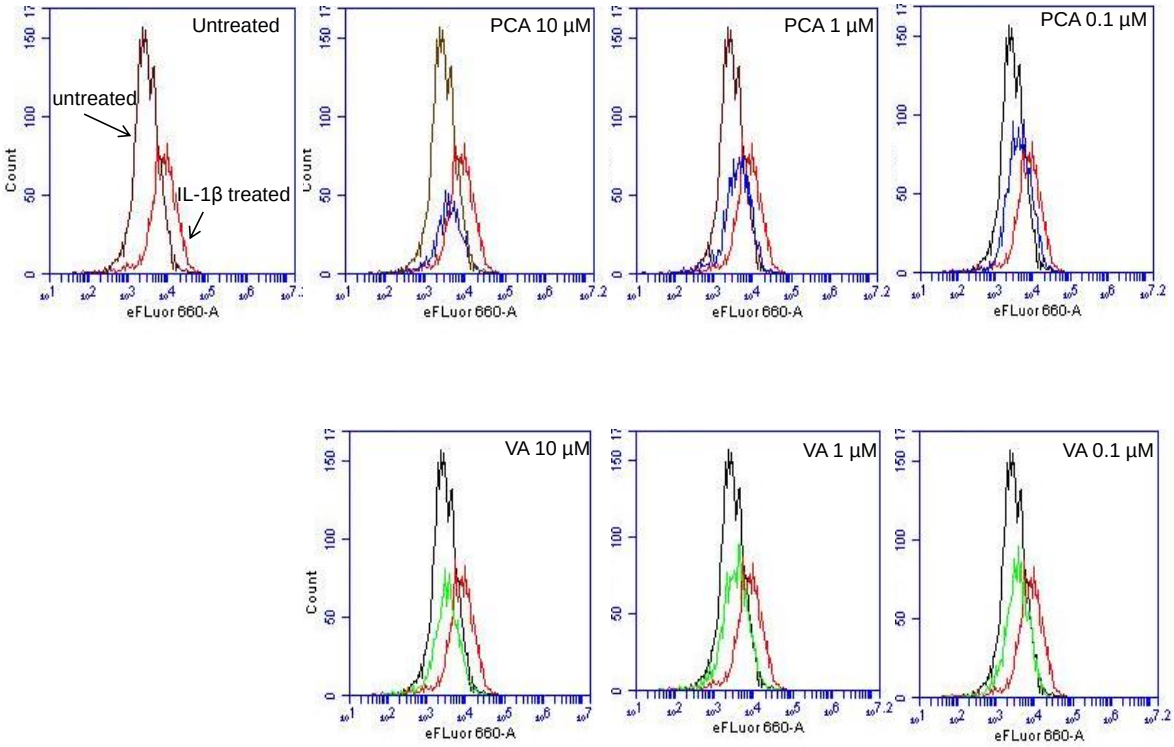

Fluorescence intensity data for HUVECs pre-incubated with or without treatment compounds (PCA and VA) at 0.1, 1 and 10 µM for 24 hours followed by IL-1β-stimulation for 15 minutes. A) All data expressed as mean percentage (± SD, n=3) of median florescent intensity (measured by flow cytometer at 660 nm) relative to IL-1β-induced controls. B) Median florescent intensity plot comparison of untreated, IL-1β stimulation and pre-incubation with treatment compounds. *p<0.001 (ANOVA with Tukey post-hoc) relative to IL-1β-induced controls. IL-1β, interleukin-1 beta; PCA, protocatechuic acid; VA, vanillic acid.

Since IL-6 and VCAM-1 are both regulated by the transcription factor NF-κB (Zheng, Qian et al. 2005, Schuett, Luchtefeld et al. 2009, Karlsen, Paur et al. 2010), the present study aimed to explore modulation of stimulated NF-κB activation by PCA and VA as a mechanism potentially underlying their observed anti-inflammatory activity against oxLDL- and CD40L-stimulated IL-6 and VCAM-1 expression in HUVECs (Chapters 3 and 4). The phosphorylation of NF-κB p65 was examined to investigate modulation of NF-κB activation (Nelson, Paraoan et al. 2002, Huang, Yang et al. 2010). Of the degradants and metabolites of C3G investigated, PCA and VA reduced IL-6 and VCAM-1 expression under both stimulation conditions, and therefore were selected for the present study. Whilst oxLDL and CD40L were used to stimulate phosphorylation of NF-κB p65, no induction was observed for both stimulus and therefore IL-1β, a known inducer of NF-κB p65 phosphorylation (Nelson, Paraoan et al. 2002) was used to stimulate NF-κB in the cultured HUVECs.

The main finding of the current investigation was that both PCA and VA attenuated the phosphorylation of NF-κB p65, and were bioactive at concentration as low as 0.1μM, reflecting their anti-inflammatory activity observed at the protein level (for IL-6 and VCAM-1, Chapters 3 and 4). The maximum reduction in phosphorylation of NF-κB p65 was observed for VA at 0.1μM, where phospho-NF-κB p65 was reduced by 40.5±4.5% relative to IL-1β control (Figure 6.3A). Although comparable reports are scarce, activity of PCA and VA against NF-κB activation has been described previously, and is accordance with the findings of the present study. For example, Wang et al(2010) reported inhibition by PCA of TNF-α induced translocation of the p65 subunit of NF-κB in mice aortic endothelial cells (Wang, Wei et al. 2010). In addition, Wei et al (2013) also observed decreased nuclear translocation of p65 in ovalbumin challenged mouse lung tissues co-incubated with PCA (Wei, Chu et al. 2013). However, this activity was observed at supra-physiological concentration of PCA (≥20 μM), whereas in the present study the phosphorylation of NF-κB p65 was inhibited by PCA at physiologically relevant concentration as low as 0.1 μM. Similarly, VA has also been shown to reduce activation of NF-κB p65 in colon tissue from dextran sulfate sodium-challenged mice (Kim, Kim et al. 2010) and LPS-challenged mouse peritoneal macrophages (Kim, Kim et al. 2011). Again, supra-physiological concentrations of VA (>200 mg/kg) were utilised in these studies, whereas the present study investigated physiologically relevant concentrations (Czank, Cassidy et al. 2013).

Although the present study provides novel insights into potential mechanisms of PCA and VA anti-inflammatory activity at low concentrations, there are several limitations to this investigation. For example, IL-1β is a potent inducer of phosphorylation of NF-κB p65 (Albrecht, Yang et al. 2007), however only an ~2 fold increase in phosphorylation was observed in the current investigation; thus the use of immunoblotting methodology to quantify phospho-p65 protein levels could prove more sensitive. Immunoblotting (Albrecht, Yang et al. 2007) or NF-κB reporter and NF-κB DNA binding activity assays (Xia, Ling et al. 2007)may also be sufficiently sensitive to observe activation of NF-κB following stimulation by oxLDL and CD40L, which both are potent activators of NF-κB (Chen, Huang et al. 2006, Xia, Ling et al. 2007, Mazière and Mazière 2009). A related limitation of the current assay was the use of IL-1β as a stimulus, as opposed to a more atherogenic stimuli such as oxLDL or CD40L, as both oxLDL (Huang, Lin et al. 2013) and CD40L (Xia, Ling et al. 2007) have previously been shown to activate NF-κB, as confirmed by NF-κB reporter assay and NF-κB DNA binding activity and therefore; as mentioned earlier, employing NF-κB reporter and DNA binding activity assays may address this issue and allow the use of oxLDL and CD40L as stimulus. Finally, the methodology employed in the present investigation does not provide insight into the translocation of phospho-NF-κB p65 to the nucleus, thus immunoblotting of nuclear fractions should be used in conjunction with flow cytometry analysis to elucidate molecular mechanisms more fully.

In conclusion, the present study demonstrates that PCA and VA modulated phosphorylation of NF-κB p65 in IL-1β-stimulated HUVECs, suggesting a potential mechanism by which these phenolic acid metabolites could mediate the observed vascular activity of anthocyanins previously reported. Considering the central role of NF-κB activation in chronic inflammation (Kaĭdashev 2012), including pathogenesis of endothelial dysfunction and the production of pro-inflammatory mediators, the findings from the present study indicate that anthocyanins may exert their beneficial effect on the vasculature indirectly by attenuating the activation of NF-κB and therefore improving vascular function, as the role of anthocyanin (namely, malvidin-3-glucoside) in attenuation of peroxinitrite-induced NF-κB activation has previously been reported to improve vascular function (Paixao, Dinis et al. 2012). In addition, these effects were seen at physiologically relevant concentrations, indicating that anthocyanin metabolites possess differential biological activities than those reported for their parent structures as often studied at supraphysiological concentrations *in vitro*. The bioactivity of these and other anthocyanin metabolites requires confirmation in future

animal and human interventions. The activity of PCA and VA on NF-κB should be investigated using reporter assays to confirm the translocation of p65 subunit to the nucleus and also on other transcription factors such as JNK under stimulated conditions. Finally, it is also important to investigate synergic/additive effect of PCA and VA on NF-κB and JNK as these metabolites are likely to be present at the same time *in vivo*.

Chapter 7. Overview and future perspectives

7.1 General Discussion

High dietary consumption of anthocyanins has been associated with reduced risk of cardiovascular disease (CVD) and improved vascular function (Jennings, Welch et al. 2012, McCullough, Peterson et al. 2012, Cassidy, Mukamal et al. 2013). The beneficial effects of anthocyanins have also been supported by randomised controlled trials, for example, in a trial conducted by Zhu et al(Zhu, Xia et al. 2011, Zhu, Ling et al.), hypercholesterolaemic volunteers ingested anthocyanins (320 mg/day) daily in short term (4 hrs) and long term (24 weeks) interventions, which resulted in improved flow-mediated dilatation and lipid profile in peripheral blood serum. In addition, randomised controlled trials investigating anti-inflammatory activities of bilberry anthocyanins reported reduced inflammatory markers [interleukin-6 (IL-6)] in subjects with metabolic syndrome and at elevated risk of CVD (Karlsen, Paur et al. 2010, Kolehmainen, Mykkänen et al. 2012). The bioactivity of anthocyanins has also been studied extensively *in vitro* to understand underlying mechanisms of action, and anthocyanins have been shown to up-regulate endothelial nitric oxide synthase (eNOS) (Xu, Ikeda et al. 2004a, Xu, Ikeda et al. 2004b) and attenuate expression of key inflammatory markers such as IL-6 and vascular cell adhesion molecule-1 (VCAM-1) in HUVECs(Xia, Ling et al. 2007, Xia, Ling et al. 2009). Though anthocyanins have been reported to possess bioactivity, their poor bioavailability and instability at physiological pH suggest that their reported bioactivity may come, at least in part, from their degradants and subsequent metabolites (Del Rio, Borges et al. 2010, Williamson and Clifford 2010). In fact, recently published human bioavailability studies report that degradants and metabolites of anthocyanins are present in much greater concentrations than their parent structures in the circulation (Azzini, Vitaglione et al. 2010, Czank, Cassidy et al. 2013). However, the bioactivity of these phenolic metabolites of anthocyanins remains relatively unknown. The current thesis sought to address this discrepancy in scientific literature by investigating recently identified metabolites of cyanidin-3-glucoside (C3G) for their *in vitro* vascular and anti-inflammatory activity. Moreover, the activity of metabolites was

investigated at physiologically relevant concentrations, namely 0.1, 1 and10 µM(Czank, Cassidy et al. 2013).

A total of 12 compounds were screened for bioactivity **(Figure 7.1)**, specifically the parent anthocyanin – C3G - and 11 of its metabolites. The selection of metabolites was targeted to allow basic structure activity relationship examination. For example, both degradants of C3G, protocatechuic acid (PCA) and phloroglucinaldehyde (PGA), were chosen to examine the effect of degradation on bioactivity. The products of methyl, glucuronide and sulfatate conjugation of PCA were also included to investigate the effect of B-ring catechol modification via phase II metabolism on bioactivity. Finally, ferulic acid (FA) was one of the common metabolites identified in ^{13}C-C3G bioavailability study (Czank, Cassidy et al. 2013) and therefore included in the present investigation.

Nitric oxide (NO) is a key mediator in maintaining endothelial homeostasis and its loss leads to endothelial dysfunction (Bian, Doursout et al. 2008). The loss of NO could result from down regulation of eNOS, or over production of superoxide which reacts with NO to produce the extremely reactive species peroxynitrite. Therefore, the vascular activity of C3G and selected metabolites was examined by investigating effects on basal eNOS up-regulation [Figure 7.1(1)].

In these experiments three of the 12 compounds significantly up-regulated basal levels of eNOS [Chapter 2, $p<0.05$, C3G, PGA and vanillic acid (VA)], three compounds significantly reduced eNOS [$p<0.05$, PCA, PCA-3-sulfate (PCA-3-sulf) and PCA-4-sulfate (PCA-4-sulf), Chapter 2], while 7 had no activity. These experiments showed that degradation and subsequent metabolism of C3G has variable effects on eNOS regulation as some metabolites retained the activity of the parent structure, while other showed reduced activity.

Figure 7.1 Experimental scheme for assessment of vascular and anti-inflammatory activity *in vitro*

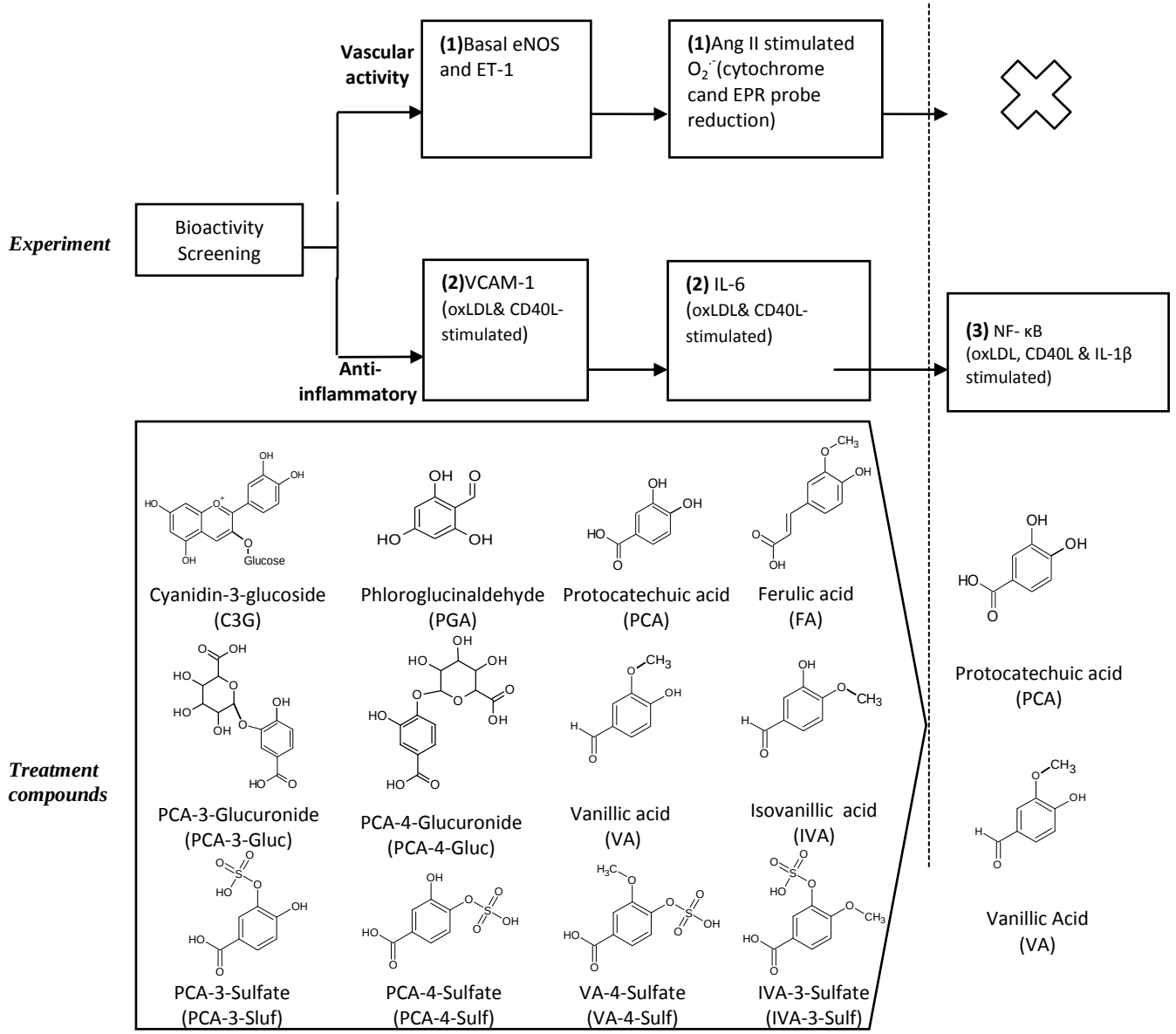

Scheme for investigation of vascular (1) & anti-inflammatory (2) activity *in vitro*, in primary human endothelial cell model, of selected treatment compounds, and exploration of mechanisms potentially underlying observed bioactivity with identified lead compounds (3). 'X' denotes possible bioactivity mechanism not selected for further investigation owing to lack of activity of anthocyanin degradants in previous experiments. CD40L, cluster of differentiation 40 ligand; EPR, electro paramagnetic resonance; ET-1, endothelin–1; eNOS, endothelial nitric oxide synthase; IL-1β, interleukin-1 beta; IL-6, interleukin-6; oxLDL, oxidised low density lipoprotein; $O_2^{\cdot-}$, superoxide; NF-κB, nuclear factor kappa B; VCAM-1, vascular cell adhesion molecule–1.

In addition, there was no effect observed for any of the compounds screened on basal endothelin–1 (ET-1) expression in endothelial cells [Figure 7.1(1)], though perhaps a cell model of stimulated ET-1 expression may provide a better insight into the vasodilatory bioactivity of the selected metabolites. Moreover, no effect was observed for any of the compounds tested on stimulated endothelial superoxide production [Figure 7.1(1)], owing to the lack of effect of the stimulus (angiotensin II) in the cell model utilised (HUVEC) as measured by reduction of cytochrome c (measured by spectrophotometry) and 1-hydroxy-3-carboxy- 2,2,5,5-tetramethylpyrrolidine (CPH) probe [measured by electro paramagnetic resonance (EPR)]. Hence, a more potent stimulus such as oxidised low density lipoprotein (oxLDL) (Heinloth, Heermeier et al. 2000) may be required to stimulate superoxide production in HUVECs, or a different cell type such as human coronary arterial endothelial cells (HCAECs) or monocytes. In addition to the use of a more potent stimulus to stimulate superoxide production, a shear stress effect (laminar vs oscillatory) might also be employed to modulate endothelial superoxide production and eNOS expression (Boo and Jo 2003, Hwang, Ing et al. 2003, Hsiai, Hwang et al. 2007).

Key inflammatory mediators such as VCAM-1 and IL-6 propagate the formation of atherosclerotic plaques which eventually result in significant clinical events (Cybulsky, Iiyama et al. 2001, Schuett, Luchtefeld et al. 2009). Therefore, all 12 compounds were also screened for their anti-inflammatory activity against VCAM-1 and IL-6 expression [Figure 7.1(2)] in response to two physiologically relevant stimuli, namely, oxLDL and cluster of differentiation 40 – ligand (CD40L) (Ishigaki, Oka et al. 2009, Pamukcu, Lip et al. 2011). In this case the majority of the compounds tested reduced expression of VCAM-1 (Chapter 3) and IL-6 (Chapter 4) under both stimulation conditions. Of the 12 compounds tested, seven reduced CD40L-stimulated VCAM-1 production (Chapter 3), eight reduced CD40L-stimulated IL-6 expression (Chapter 4), and nine compounds reduced oxLDL-stimulated IL-6 production in HUVECs (Chapter 4). Alternatively, three compounds, increased CD40L-induced VCAM-1 protein production in HUVECs, namely PCA-4-sulf, PCA-3-sulf and VA-4-sulf. In the present study soluble VCAM-1 was quantified, however proteolytic cleavage is required to produce the soluble form and an assay comparing levels of the soluble form of VCAM-1 and membrane bound VCAM-1 may provide more insight into the mechanistic activity of the phenolic metabolites. The bioactive compounds in the current study showed greater effects onanti-inflammatory activity, as opposed to vascular activity, it is possible that anthocyanin metabolites elicit the majority of the perceived health effects of anthocyanin through anti-

inflammatory activities. Therefore, an understanding of the underlying mechanisms of action is crucial, and as such activation of a key inflammatory transcription factor, nuclear factor kappa-B (NF-κB), which up-regulates VCAM-1 and IL-6 expression, was investigated (Chapter 5). As the aim was to investigate the underlying mechanisms of action for the most bioactive metabolites of C3G tested, PCA and VA were chosen as they attenuated both VCAM-1 and IL-6 expression under both stimulation conditions [Figure 7.1(3)].

NF-κB activation was investigated by measuring phosphorylation of the p65 subunit of NF-κB (using flow cytometry), which results in translocation of NF-κB p65 to the nucleus and up-regulation of pro-inflammatory cytokines (Huang, Yang et al. 2010). However, no increase in phosphorylation of NF-κB p65 was observed following oxLDL and CD40L stimulation of HUVECs. Therefore, to explore the activity of PCA and VA on NF-κB p65 phosphorylation, HUVEC stimulation was performed using a more potent stimulus of p65 physphorylation, namely, IL-1β (Nelson, Paraoan et al. 2002). The results from this investigation indicated that both PCA and VA were capable of reducing the phosphorylation of NF-κB p65, and therefore, it can be postulated that this is one mechanism by which anthocyanin phenolic metabolites, exert their activity. However, these observations should also be confirmed using methodologies such as an NF-κB reporter assay (luciferase assay) or an NF-κB DNA binding activity assay (Xia, Ling et al. 2007).

7.2 Future perspectives

Elucidating the mechanisms of action underlying the *in vitro* activity of anthocyanins is key to understanding the reported health related benefits of anthocyanin consumption. One of the limitations of the present study is the use of HUVEC as an *in vitro* model. Whilst HUVEC represent a well characterised cell type for endothelial research, all bioactivity observed should be confirmed indifferent cell models of endothelial function in the context of atherosclerosis, such as HCAEC, which have better expression of key vascular proteins including NAD(P)H oxidase (NOX)-2, which is main source of superoxide in endothelial cells and over expression of NOX-2 results in endothelial dysfunction (Bonomini, Tengattini et al. 2008). In addition, the effect of phenolic metabolites on eNOS expression and superoxide production in the endothelium should also be investigated under conditions of laminar and oscillatory stress, which modulates eNOS and NOX) expression (Boo and Jo 2003, Hwang, Ing et al. 2003, Hsiai, Hwang et al. 2007) and represents a more physiologically relevant model.

It is also important to investigate the effects of anthocyanin metabolites on stimulated endothelial superoxide production, as superoxide contributes significantly to endothelial dysfunction (Flammer and Luscher 2010). Therefore, the use of stimuli other than angiotensin II, such as oxLDL (Heinloth, Heermeier et al. 2000), in conjunction with HCAECs or co culture with neutrophils [which produce large amounts of superoxide (Segal 2006)], may be employed to address the issue of limited superoxide production observed in the present study. Furthermore, utilisation of the EPR probe CPH, is considered the 'gold standard' for quantifying superoxide levels (Dikalov, Kirilyuk et al. 2011) and should also be utilised in order to investigate the bioactivity of anthocyanins and their metabolites on NOX enzyme function and/or superoxide production. The EPR probe CPH was utilised in the present study; however, as discussed earlier, due to lack of stimulation by angiotensin II no significant effect of selected compounds was observed and therefore, use of oxLDL with EPR probe CPH may be an ultimate method to provide insights to the vascular activity of phenolic metabolites.

The major finding of the present study is that newly identified C3G metabolites possessanti-inflammatory activity *in vitro* under oxLDL- and CD40L-stimulated conditions, at physiologically relevant concentrations (i.e. 0.1 to 10 μM), however, future studies should explore the effect of the combination of all identified metabolites in equamolar concentrations on oxLDL- and CD40L-stimulated VCAM-1 and IL-6 in HUVECs to investigate synergic effects of metabolise. Although preliminary investigations exploring underlying potential mechanism of action for reported anti-inflammatory activity suggest metabolites of C3G (namely PCA and VA) can modulate activation of NF-κB in HUVECs, other targets which may be affected by these metabolites and should be explored. One such example is the phosphorylation of mitogen activated protein kinases (MAPK) p38 and c-jun N-terminal kinase (JNK), as C3G has been shown to modulate these enzymes under CD40L-stimulated conditions in HUVECs (Xia, Ling et al. 2009). In addition, cyclooxygenase-2 (COX-2), which is responsible for CD40L-induced IL-6 production in HUVECs (Dongari-Bagtzoglou, Thienel et al. 2003), could be investigated as another potential mechanism for the modulation of IL-6 production. Furthermore, C3G has also been shown to diminish CD40L-CD40-induced inflammation by limiting tumour necrosis factor receptor associated factor – 2 (TRAF-2) translocation to lipid rafts via modulation of cholesterol distribution (Xia, Ling et al. 2007), hence the effect of bioactive metabolites on TRAF-2 translocation and cholesterol distribution should also be explored. With regard to oxLDL-induced IL-6 expression, and

considering the magnitude of reduction in oxLDL-induced IL-6 production (up to 99% relative to control) elicited by nine of the 12 compounds tested, it can be postulated that the effects of anthocyanin metabolites on oxLDL signalling occur at the receptor level; and therefore the effect of bioactive metabolites on the interaction between oxLDL and its cell surface receptor, lectin-like receptor – 1 (LOX-1), which represents another target for future investigation (Mitra, Goyal et al. 2011)].

The findings from the present study show *in vitro* activity of newly identified metabolites of anthocyanin at physiological concentrations; however, it is vital to confirm their activity in animal disease models before any definitive conclusions are proposed. For example, chronic consumption of PCA by diabetic mice (for 8 weeks) lowered plasma levels of glucose, IL-6 and tumour necrosis factor-alpha (TNF-α) (Lin, Huang et al. 2009) compared to a control group; whereas acute consumption of PCA (1 hour) prior to ovalbumin-stimulation inhibited NF-κB activation in a mouse allergic asthma model (Wei, Chu et al. 2013). Though these animal disease models provide useful data, the activity of PCA and other bioactive metabolites should be tested in further disease models at more physiologically relevant concentrations; as the above studies used doses of up to 30 mg/kg per day PCA, whereas human consumption is approximately 500 mg/day per adult (Czank, Cassidy et al. 2013). Based on the available data from animal models and considering the bioavailability of phenolic metabolites, human studies should be designed to investigate their bioactivity. For example, Edirisinghe et al measured meal-induced postprandial inflammatory and insulin responses in overweight adult subjects given strawberry juice, and discovered significantly lower levels of IL-6 in the strawberry juice group compared to the control group (Edirisinghe, Banaszewski et al. 2011). Similarly, a human study feeding combinations of phenolic metabolites at physiologically relevant concentrations for short term (eg. Between 6-24 hours) and long term (eg. for 24 weeks) can be carried out to measure IL-6 production in meal-induced postprandial inflammation. In addition, level of oxLDL and soluble VCAM-1 are considered as good biomarkers of CVD (Holvoet, Mertens et al. 2001, Videm and Albrigtsen 2008, Ishigaki, Oka et al. 2009) and therefore the effect of phenolic metabolites consumption on circulating oxLDL and soluble VCAM-1 in subjects at risk of CVD can be evaluated. Moreover, in a long term human study, chronic consumption of recently identified metabolites by type-2 diabetes subjects on coronary artery calcium score (a non-invasive method to measure plaque build-up) may be an ultimate study to truly observe the effect of phenolic metabolites on plaque build-up and therefore on

pathogenesis of atherosclerosis in disease set-up. Finally, as reported by Czank et al (2013) that multiple metabolites are present in circulation at the same time, an experimentwith all metabolites(combined in equimolar versusC_{max} concentrations)investigating their synergic/additive effect on vascular proteins, inflammatory markers and NF-κB should be investigated.

In summary, the present thesis provides novel insights into the bioactivity of anthocyanins and potential mechanisms by which they may exert beneficial effects on the cardiovascular system. The majority of reported *in vitro* studies focus on the activity of the parent/precursor unmetabolised anthocyanins, but considering their instability and the presence of relatively high concentrations of degradation products and metabolites in the circulation of humans, it is important to understand the bioactivity of these metabolites and not only the parent anthocyanins. The present study, to the best of the author's knowledge, is the first study that has investigated newly identified metabolites of C3G and provides evidence that these metabolites may possess bioactivity and, at least in part, could contribute to the observed bioactivity of anthocyanins in humans.

References

Al-Shalmani, S., S. Suri, D. A. Hughes, P. A. Kroon, P. W. Needs, M. A. Taylor, S. Tribolo and V. G. Wilson (2011). "Quercetin and its principal metabolites, but not myricetin, oppose lipopolysaccharide-induced hyporesponsiveness of the porcine isolated coronary artery." British Journal of Pharmacology **162**(7): 1485-1497.

Albrecht, U., X. Yang, R. Asselta, V. Keitel, M. L. Tenchini, S. Ludwig, P. C. Heinrich, D. Häussinger, F. Schaper and J. G. Bode (2007). "Activation of NF-κB by IL-1β blocks IL-6-induced sustained STAT3 activation and STAT3-dependent gene expression of the human γ-fibrinogen gene." Cellular Signalling **19**(9): 1866-1878.

Altenhofer, S., P. W. Kleikers, K. A. Radermacher, P. Scheurer, J. J. Rob Hermans, P. Schiffers, H. Ho, K. Wingler and H. H. Schmidt (2012). "The NOX toolbox: validating the role of NADPH oxidases in physiology and disease." Cellular and molecular life sciences : CMLS **69**(14): 2327-2343.

Asenstorfer, R. E., P. G. Iland, M. E. Tate and G. P. Jones (2003). "Charge equilibria and pK(a) of malvidin-3-glucoside by electrophoresis." Anal Biochem **318**(2): 291-299.

Autio, I., O. Jaakkola, T. Solakivi and T. Nikkari (1990). "Oxidized low-density lipoprotein is chemotactic for arterial smooth muscle cells in culture." FEBS Letters **277**(1–2): 247-249.

Azzini, E., P. Vitaglione, F. Intorre, A. Napolitano, A. Durazzo, M. S. Foddai, A. Fumagalli, G. Catasta, L. Rossi, E. Venneria, A. Raguzzini, L. Palomba, V. Fogliano and G. Maiani (2010). "Bioavailability of strawberry antioxidants in human subjects." The British journal of nutrition **104**(8): 1165-1173.

Bailey, D. M., B. Davies, I. S. Young, M. J. Jackson, G. W. Davison, R. Isaacson and R. S. Richardson (2003). EPR spectroscopic detection of free radical outflow from an isolated muscle bed in exercising humans.

Basyouni, M., M. Ahmed, H. Ismail and I. Esmat (2012). "Potential Role of Oxidized LDL (ox-LDL) and Adhesion Molecules (VCAM-1, ICAM-1) in Type 2 Diabetes Mellitus Patients in Qassim region, KSA." J Invest Biochem **1**(1): 48-54.

Baud, V. and M. Karin (2001). "Signal transduction by tumor necrosis factor and its relatives." Trends in cell biology **11**(9): 372-377.

Baudin, B., A. Bruneel, N. Bosselut and M. Vaubourdolle (2007). "A protocol for isolation and culture of human umbilical vein endothelial cells." Nat. Protocols **2**(3): 481-485.

Bedard, K. and K. H. Krause (2007). "The NOX family of ROS-generating NADPH oxidases: physiology and pathophysiology." Physiol Rev **87**(1): 245-313.

Bell, D. R. and K. Gochenaur (2006). "Direct vasoactive and vasoprotective properties of anthocyanin-rich extracts." J Appl Physiol **100**(4): 1164-1170.

Bian, K., M.-F. Doursout and F. Murad (2008). "Vascular System: Role of Nitric Oxide in Cardiovascular Diseases." The Journal of Clinical Hypertension **10**(4): 304-310.

Blankenberg, S., S. Barbaux and L. Tiret (2003). "Adhesion molecules and atherosclerosis." Atherosclerosis **170**(2): 191-203.

Bonomini, F., S. Tengattini, A. Fabiano, R. Bianchi and R. Rezzani (2008). "Atherosclerosis and oxidative stress." Histol Histopathol **23**(3): 381-390.

Boo, Y. C. and H. Jo (2003). "Flow-dependent regulation of endothelial nitric oxide synthase: role of protein kinases." Am J Physiol **285**(3): C499-C508.

Brandes, R. P., N. Weissmann and K. Schroder (2010). "NADPH oxidases in cardiovascular disease." Free Radic Biol Med **49**(5): 687-706.

Brown, D. I. and K. K. Griendling (2009). "Nox proteins in signal transduction." Free Radic Biol Med **47**(9): 1239-1253.

Brunner, H., J. R. Cockcroft, J. Deanfield, A. Donald, E. Ferrannini, J. Halcox, W. Kiowski, T. F. Luscher, G. Mancia, A. Natali, J. J. Oliver, A. C. Pessina, D. Rizzoni, G. P. Rossi, A. Salvetti, L. E. Spieker, S. Taddei and D. J. Webb (2005). "Endothelial function and dysfunction. Part II: Association with cardiovascular risk factors and diseases. A statement by the Working Group on Endothelins and Endothelial Factors of the European Society of Hypertension." J Hypertens **23**(2): 233-246.

Cassidy, A., K. J. Mukamal, L. Liu, M. Franz, A. H. Eliassen and E. B. Rimm (2013). "High Anthocyanin Intake Is Associated With a Reduced Risk of Myocardial Infarction in Young and Middle-Aged Women." Circulation **127**(2): 188-196.

Cassidy, A., E. J. O'Reilly, C. Kay, L. Sampson, M. Franz, J. Forman, G. Curhan and E. B. Rimm (2010). "Habitual intake of flavonoid subclasses and incident hypertension in adults." Am J Clin Nutr **93**: 338-347.

Castañeda-Ovando, A., M. d. L. Pacheco-Hernández, M. E. Páez-Hernández, J. A. Rodríguez and C. A. Galán-Vidal (2009). "Chemical studies of anthocyanins: A review." Food Chemistry **113**(4): 859-871.

Chan, S.-L., A. Tabellion, D. Bagrel, C. Perrin-Sarrado, C. Capdeville-Atkinson and J. Atkinson (2008). "Impact of Chronic Treatment With Red Wine Polyphenols (RWP) on Cerebral Arterioles in the Spontaneous Hypertensive Rat." Journal of Cardiovascular Pharmacology **51**(3): 304-310 310.1097/FJC.1090b1013e318163a318946.

Chang, Y. C., K. X. Huang, A. C. Huang, Y. C. Ho and C. J. Wang (2006). "Hibiscus anthocyanins-rich extract inhibited LDL oxidation and oxLDL-mediated macrophages

apoptosis." Food and chemical toxicology : an international journal published for the British Industrial Biological Research Association **44**(7): 1015-1023.

Chen, K., J. Huang, W. Gong, L. Zhang, P. Yu and J. M. Wang (2006). "CD40/CD40L dyad in the inflammatory and immune responses in the central nervous system." Cellular & molecular immunology **3**(3): 163-169.

Chirumbolo, S., M. Marzotto, A. Conforti, A. Vella, R. Ortolani and P. Bellavite (2010). "Bimodal action of the flavonoid quercetin on basophil function: an investigation of the putative biochemical targets." Clinical and molecular allergy : CMA **8**: 13.

Crozier, A., I. B. Jaganath and M. N. Clifford (2009). "Dietary phenolics: chemistry, bioavailability and effects on health." Nat Prod Rep **26**(8): 1001-1043.

Curtis, P. J., P. A. Kroon, W. J. Hollands, R. Walls, G. Jenkins, C. D. Kay and A. Cassidy (2009). "Cardiovascular disease risk biomarkers and liver and kidney function are not altered in postmenopausal women after ingesting an elderberry extract rich in anthocyanins for 12 weeks." J Nutr **139**(12): 2266-2271.

Cybulsky, M. I., K. Iiyama, H. Li, S. Zhu, M. Chen, M. Iiyama, V. Davis, J.-C. Gutierrez-Ramos, P. W. Connelly and D. S. Milstone (2001). "A major role for VCAM-1, but not ICAM-1, in early atherosclerosis." The Journal of Clinical Investigation **107**(10): 1255-1262.

Czank, C., A. Cassidy, Q. Zhang, D. J. Morrison, T. Preston, P. A. Kroon, N. P. Botting and C. D. Kay (2013). "Human metabolism and elimination of the anthocyanin, cyanidin-3-glucoside: a 13C-tracer study." The American Journal of Clinical Nutrition **97**(5): 995-1003.

Dansky, H. M., C. B. Barlow, C. Lominska, J. L. Sikes, C. Kao, J. Weinsaft, M. I. Cybulsky and J. D. Smith (2001). "Adhesion of Monocytes to Arterial Endothelium and Initiation of Atherosclerosis Are Critically Dependent on Vascular Cell Adhesion Molecule-1 Gene Dosage." Arteriosclerosis, Thrombosis, and Vascular Biology **21**(10): 1662-1667.

de Pascual-Teresa, S., D. A. Moreno and C. Garcia-Viguera (2010). "Flavanols and anthocyanins in cardiovascular health: a review of current evidence." Int J Mol Sci **11**(4): 1679-1703.

Del Rio, D., G. Borges and A. Crozier (2010). "Berry flavonoids and phenolics: bioavailability and evidence of protective effects." Br J Nutr **104 Suppl 3**: S67-90.

Del Rio, D., G. Borges and A. Crozier (2010). "Berry flavonoids and phenolics: bioavailability and evidence of protective effects." The British journal of nutrition **104 Suppl 3**: S67-90.

Del Rio, D., A. Rodriguez-Mateos, J. P. Spencer, M. Tognolini, G. Borges and A. Crozier (2013). "Dietary (poly)phenolics in human health: structures, bioavailability, and evidence of protective effects against chronic diseases." Antioxidants & redox signaling **18**(14): 1818-1892.

Dikalov, S. I., I. A. Kirilyuk, M. Voinov and I. A. Grigor'ev (2011). "EPR detection of cellular and mitochondrial superoxide using cyclic hydroxylamines." Free Radical Research **45**(4): 417-430.

Dominguez-Rodriguez, A., P. Abreu-Gonzalez and J. C. Kaski (2009). "Inflammatory systemic biomarkers in setting acute coronary syndromes--effects of the diurnal variation." Current drug targets **10**(10): 1001-1008.

Dongari-Bagtzoglou, A. I., U. Thienel and M. J. Yellin (2003). "CD40 ligation triggers COX-2 expression in endothelial cells: evidence that CD40-mediated IL-6 synthesis is COX-2-dependent." Inflammation Research **52**(1): 18-25.

Drummond, G. R., S. Selemidis, K. K. Griendling and C. G. Sobey (2011). "Combating oxidative stress in vascular disease: NADPH oxidases as therapeutic targets." Nat Rev Drug Discov **10**(6): 453-471.

Eberhardt, R. T., M. A. Forgione, A. Cap, J. A. Leopold, M. A. Rudd, M. Trolliet, S. Heydrick, R. Stark, E. S. Klings, N. I. Moldovan, M. Yaghoubi, P. J. Goldschmidt-Clermont, H. W. Farber, R. Cohen and J. Loscalzo (2000). "Endothelial dysfunction in a murine model of mild hyperhomocyst(e)inemia." The Journal of Clinical Investigation **106**(4): 483-491.

Edirisinghe, I., K. Banaszewski, J. Cappozzo, D. McCarthy and B. M. Burton-Freeman (2011). "Effect of Black Currant Anthocyanins on the Activation of Endothelial Nitric Oxide Synthase (eNOS) in Vitro in Human Endothelial Cells." Journal of Agricultural and Food Chemistry **59**(16): 8616-8624.

Edirisinghe, I., K. Banaszewski, J. Cappozzo, K. Sandhya, C. L. Ellis, R. Tadapaneni, C. T. Kappagoda and B. M. Burton-Freeman (2011). "Strawberry anthocyanin and its association with postprandial inflammation and insulin." British Journal of Nutrition **106**(06): 913-922.

Elks, C. M., S. D. Reed, N. Mariappan, B. Shukitt-Hale, J. A. Joseph, D. K. Ingram and J. Francis (2011). "A Blueberry-Enriched Diet Attenuates Nephropathy in a Rat Model of Hypertension via Reduction in Oxidative Stress." PLoS ONE **6**(9): e24028.

Erdman, J. W., Jr., D. Balentine, L. Arab, G. Beecher, J. T. Dwyer, J. Folts, J. Harnly, P. Hollman, C. L. Keen, G. Mazza, M. Messina, A. Scalbert, J. Vita, G. Williamson and J. Burrowes (2007). "Flavonoids and heart health: proceedings of the ILSI North America Flavonoids Workshop, May 31-June 1, 2005, Washington, DC." J Nutr **137**(3 Suppl 1): 718S-737S.

Felgines, C., S. Talavera, O. Texier, A. Gil-Izquierdo, J.-L. Lamaison and C. Remesy (2005). "Blackberry Anthocyanins Are Mainly Recovered from Urine as Methylated and Glucuronidated Conjugates in Humans." Journal of Agricultural and Food Chemistry **53**(20): 7721-7727.

Flammer, A. J. and T. F. Luscher (2010). "Human endothelial dysfunction: EDRFs." Pflugers Arch **459**(6): 1005-1013.

Fleming, I. and R. Busse (2003). "Molecular mechanisms involved in the regulation of the endothelial nitric oxide synthase." Am J Physiol Regul Integr Comp Physiol **284**(1): R1-12.

Fleschhut, J., F. Kratzer, G. Rechkemmer and S. Kulling (2006). "Stability and biotransformation of various dietary anthocyanins in vitro." European Journal of Nutrition **45**(1): 7-18.

Fotis, L., D. Giannakopoulos, L. Stamogiannou and M. Xatzipsalti (2012). "Intercellular cell adhesion molecule-1 and vascular cell adhesion molecule-1 in children. Do they play a role in the progression of atherosclerosis?" Hormones **11**(2): 140-146.

Galle, J., R. Schneider, A. Heinloth, C. Wanner, P. R. Galle, E. Conzelmann, S. Dimmeler and K. Heermeier (1999). "Lp(a) and LDL induce apoptosis in human endothelial cells and in rabbit aorta: role of oxidative stress." Kidney international **55**(4): 1450-1461.

Gamkrelidze, M., N. Mamamtavrishvili, N. Bejitashvili, T. Sanikidze and L. Ratiani (2008). "Role of oxidative stress in pathogenesis of atherosclerosis." Georgian Med News(163): 54-57.

García-Lafuente, A., E. Guillamón, A. Villares, M. Rostagno and J. Martínez (2009). "Flavonoids as anti-inflammatory agents: implications in cancer and cardiovascular disease." Inflammation Research **58**(9): 537-552.

Geleijnse, J. M. and P. Hollman (2008). "Flavonoids and cardiovascular health: which compounds, what mechanisms?" Am J Clin Nutr **88**(1): 12-13.

George, S. and J. Johnson (2010). "Atherosclerosis : molecular and cellular mechanisms." Weinheim : Wiley-VCH(1).

Grassi, D., G. Desideri, G. Croce, S. Tiberti, A. Aggio and C. Ferri (2009). "Flavonoids, vascular function and cardiovascular protection." Curr Pharm Des **15**(10): 1072-1084.

Greig, F. H., S. Kennedy and C. M. Spickett (2012). "Physiological effects of oxidized phospholipids and their cellular signaling mechanisms in inflammation." Free Radical Biology and Medicine **52**(2): 266-280.

Griendling, K. K., D. Sorescu and M. Ushio-Fukai (2000). "NAD(P)H oxidase: role in cardiovascular biology and disease." Circ Res **86**(5): 494-501.

Hassan, G. S., Y. Merhi and W. Mourad (2012). "CD40 ligand: a neo-inflammatory molecule in vascular diseases." Immunobiology **217**(5): 521-532.

He, J., T. C. Wallace, K. E. Keatley, M. L. Failla and M. M. Giusti (2009). "Stability of black raspberry anthocyanins in the digestive tract lumen and transport efficiency into gastric and small intestinal tissues in the rat." J Agric Food Chem **57**(8): 3141-3148.

Heinloth, A., K. Heermeier, U. Raff, C. Wanner and J. Galle (2000). "Stimulation of NADPH oxidase by oxidized low-density lipoprotein induces proliferation of human vascular endothelial cells." J Am Soc Nephrol **11**(10): 1819-1825.

Hidalgo, M., S. Martin-Santamaria, I. Recio, C. Sanchez-Moreno, B. de Pascual-Teresa, G. Rimbach and S. de Pascual-Teresa (2011). "Potential anti-inflammatory, anti-adhesive, anti/estrogenic, and angiotensin-converting enzyme inhibitory activities of anthocyanins and their gut metabolites." Genes & Nutrition: 1-12.

Hirooka, Y., M. Gotoh, J. Takagi, K. Otake, Y. Mori, S. Habu and T. Nogimori (2001). "[Implication on thyroid function tests]." Rinsho Byori **49**(11): 1122-1128.

Hobbs, A. J., A. Higgs and S. Moncada (1999). "Inhibition of nitric oxide synthase as a potential therapeutic target." Annu Rev Pharmacol Toxicol **39**: 191-220.

Holvoet, P., A. Mertens, P. Verhamme, K. Bogaerts, G. Beyens, R. Verhaeghe, D. Collen, E. Muls and F. Van de Werf (2001). "Circulating Oxidized LDL Is a Useful Marker for Identifying Patients With Coronary Artery Disease." Arteriosclerosis, Thrombosis, and Vascular Biology **21**(5): 844-848.

Hou, D.-X., T. Yanagita, T. Uto, S. Masuzaki and M. Fujii (2005). "Anthocyanidins inhibit cyclooxygenase-2 expression in LPS-evoked macrophages: Structure–activity relationship and molecular mechanisms involved." Biochemical Pharmacology **70**(3): 417-425.

Hsiai, T. K., J. Hwang, M. L. Barr, A. Correa, R. Hamilton, M. Alavi, M. Rouhanizadeh, E. Cadenas and S. L. Hazen (2007). "Hemodynamics influences vascular peroxynitrite formation: Implication for low-density lipoprotein apo-B-100 nitration." Free radical biology & medicine **42**(4): 519-529.

Huang, B., X. D. Yang, A. Lamb and L. F. Chen (2010). "Posttranslational modifications of NF-kappaB: another layer of regulation for NF-kappaB signaling pathway." Cellular Signalling **22**(9): 1282-1290.

Huang, C.-S., A.-H. Lin, C.-T. Liu, C.-W. Tsai, I.-S. Chang, H.-W. Chen and C.-K. Lii (2013). "Isothiocyanates protect against oxidized LDL-induced endothelial dysfunction by upregulating Nrf2-dependent antioxidation and suppressing NFκB activation." Molecular Nutrition & Food Research **57**(11): 1918-1930.

Hwang, J., M. H. Ing, A. Salazar, B. Lassègue, K. Griendling, M. Navab, A. Sevanian and T. K. Hsiai (2003). "Pulsatile Versus Oscillatory Shear Stress Regulates NADPH Oxidase Subunit Expression: Implication for Native LDL Oxidation." Circulation Research **93**(12): 1225-1232.

Iiyama, K., L. Hajra, M. Iiyama, H. Li, M. DiChiara, B. D. Medoff and M. I. Cybulsky (1999). "Patterns of Vascular Cell Adhesion Molecule-1 and Intercellular Adhesion Molecule-1 Expression in Rabbit and Mouse Atherosclerotic Lesions and at Sites Predisposed to Lesion Formation." Circulation Research **85**(2): 199-207.

Ishigaki, Y., Y. Oka and H. Katagiri (2009). "Circulating oxidized LDL: a biomarker and a pathogenic factor." Current Opinion in Lipidology **20**(5): 363-369.

Jennings, A., A. A. Welch, S. J. Fairweather-Tait, C. Kay, A.-M. Minihane, P. Chowienczyk, B. Jiang, M. Cecelja, T. Spector, A. Macgregor and A. Cassidy (2012). "Higher anthocyanin intake is associated with lower arterial stiffness and central blood pressure in women." The American Journal of Clinical Nutrition **96**(4): 781-788.

Johnson, D. K., K. J. Schillinger, D. M. Kwait, C. V. Hughes, E. J. McNamara, F. Ishmael, R. W. O'Donnell, M. M. Chang, M. G. Hogg, J. S. Dordick, L. Santhanam, L. M. Ziegler and J. A. Holland (2002). "Inhibition of NADPH oxidase activation in endothelial cells by ortho-methoxy-substituted catechols." Endothelium **9**(3): 191-203.

Kahle, K., M. Kraus, W. Scheppach, M. Ackermann, F. Ridder and E. Richling (2006). "Studies on apple and blueberry fruit constituents: do the polyphenols reach the colon after ingestion?" Mol Nutr Food Res **50**(4-5): 418-423.

Kaĭdashev, I. P. (2012). "[NF-kB activation as a molecular basis of pathological process by metabolic syndrome]." Fiziolohichnyi zhurnal (Kiev, Ukraine : 1994) **58**(1): 93-101.

Karlsen, A., I. Paur, S. K. Bohn, A. K. Sakhi, G. I. Borge, M. Serafini, I. Erlund, P. Laake, S. Tonstad and R. Blomhoff (2010). "Bilberry juice modulates plasma concentration of NF-kappaB related inflammatory markers in subjects at increased risk of CVD." European Journal of Nutrition **49**(6): 345-355.

Karlsen, A., L. Retterstøl, P. Laake, I. Paur, S. Kjølsrud-Bøhn, L. Sandvik and R. Blomhoff (2007). "Anthocyanins Inhibit Nuclear Factor-kappaB Activation in Monocytes and Reduce Plasma Concentrations of Pro-Inflammatory Mediators in Healthy Adults." The Journal of Nutrition **137**(8): 1951-1954.

Kato, T., N. Horie, K. Hashimoto, K. Satoh, T. Shimoyama, T. Kaneko, K. Kusama and H. Sakagami (2008). "Bimodal effect of glycyrrhizin on macrophage nitric oxide and prostaglandin E2 production." In vivo **22**(5): 583-586.

Kawashima, S. and M. Yokoyama (2004). "Dysfunction of endothelial nitric oxide synthase and atherosclerosis." Arterioscler Thromb Vasc Biol **24**(6): 998-1005.

Kay, C. D. (2006). "Aspects of anthocyanin absorption, metabolism and pharmacokinetics in humans." Nutr Res Rev **19**(1): 137-146.

Kay, C. D., G. Mazza and B. J. Holub (2005). "Anthocyanins Exist in the Circulation Primarily as Metabolites in Adult Men." The Journal of Nutrition **135**(11): 2582-2588.

Kim, H. J., I. Tsoy, J. M. Park, J. I. Chung, S. C. Shin and K. C. Chang (2006). "Anthocyanins from soybean seed coat inhibit the expression of TNF-α-induced genes associated with ischemia/reperfusion in endothelial cell by NF-κB-dependent pathway and reduce rat

myocardial damages incurred by ischemia and reperfusion in vivo." FEBS Letters **580**(5): 1391-1397.

Kim, M.-C., S.-J. Kim, D.-S. Kim, Y.-D. Jeon, S. J. Park, H. S. Lee, J.-Y. Um and S.-H. Hong (2011). "Vanillic acid inhibits inflammatory mediators by suppressing NF-κB in lipopolysaccharide-stimulated mouse peritoneal macrophages." Immunopharmacology and Immunotoxicology **33**(3): 525-532.

Kim, S. J., M. C. Kim, J. Y. Um and S. H. Hong (2010). "The beneficial effect of vanillic acid on ulcerative colitis." Molecules **15**(10): 7208-7217.

Kolehmainen, M., O. Mykkänen, P. V. Kirjavainen, T. Leppänen, E. Moilanen, M. Adriaens, D. E. Laaksonen, M. Hallikainen, R. Puupponen-Pimiä, L. Pulkkinen, H. Mykkänen, H. Gylling, K. Poutanen and R. Törrönen (2012). "Bilberries reduce low-grade inflammation in individuals with features of metabolic syndrome." Molecular Nutrition & Food Research **56**(10): 1501-1510.

Kotowicz, K., G. L. Dixon, N. J. Klein, M. J. Peters and R. E. Callard (2000). "Biological function of CD40 on human endothelial cells: costimulation with CD40 ligand and interleukin-4 selectively induces expression of vascular cell adhesion molecule-1 and P-selectin resulting in preferential adhesion of lymphocytes." Immunology **100**(4): 441-448.

Kulling, S. E., D. M. Honig and M. Metzler (2001). "Oxidative metabolism of the soy isoflavones daidzein and genistein in humans in vitro and in vivo." J Agric Food Chem **49**(6): 3024-3033.

Kuroda, J. and J. Sadoshima (2010). "NADPH Oxidase and Cardiac Failure." Journal of Cardiovascular Translational Research **3**(4): 314-320.

Lazze, M. C., R. Pizzala, P. Perucca, O. Cazzalini, M. Savio, L. Forti, V. Vannini and L. Bianchi (2006). "Anthocyanidins decrease endothelin-1 production and increase endothelial nitric oxide synthase in human endothelial cells." Mol Nutr Food Res **50**(1): 44-51.

Lederman, S., M. J. Yellin, A. Krichevsky, J. Belko, J. J. Lee and L. Chess (1992). "Identification of a novel surface protein on activated CD4+ T cells that induces contact-dependent B cell differentiation (help)." The Journal of experimental medicine **175**(4): 1091-1101.

Lee, W. J., H. C. Ou, W. C. Hsu, M. M. Chou, J. J. Tseng, S. L. Hsu, K. L. Tsai and W. H. Sheu (2010). "Ellagic acid inhibits oxidized LDL-mediated LOX-1 expression, ROS generation, and inflammation in human endothelial cells." Journal of vascular surgery **52**(5): 1290-1300.

Li, N., F.-X. Yi, E. Rute, D. X. Zhang, G. R. Slocum and A.-P. Zou (2002). "Effects of homocysteine on intracellular nitric oxide and superoxide levels in the renal arterial endothelium." American Journal of Physiology - Heart and Circulatory Physiology **283**(3): H1237-H1243.

Lin, C.-Y., C.-S. Huang, C.-Y. Huang and M.-C. Yin (2009). "Anticoagulatory, Antiinflammatory, and Antioxidative Effects of Protocatechuic Acid in Diabetic Mice." Journal of Agricultural and Food Chemistry **57**(15): 6661-6667.

Lodi, F., R. Jimenez, L. Moreno, P. A. Kroon, P. W. Needs, D. A. Hughes, C. Santos-Buelga, A. Gonzalez-Paramas, A. Cogolludo, R. Lopez-Sepulveda, J. Duarte and F. Perez-Vizcaino (2009). "Glucuronidated and sulfated metabolites of the flavonoid quercetin prevent endothelial dysfunction but lack direct vasorelaxant effects in rat aorta." Atherosclerosis **204**(1): 34-39.

Lyle, A. N. and K. K. Griendling (2006). "Modulation of vascular smooth muscle signaling by reactive oxygen species." Physiology (Bethesda) **21**: 269-280.

Ma, Z.-C., Q. Hong, Y.-G. Wang, H.-L. Tan, C.-R. Xiao, Q.-D. Liang, S.-H. Cai and Y. Gao (2010). "Ferulic Acid Attenuates Adhesion Molecule Expression in Gamma-Radiated Human Umbilical Vascular Endothelial Cells." Biological and Pharmaceutical Bulletin **33**(5): 752-758.

Manach, C., G. Williamson, C. Morand, A. Scalbert and C. Remesy (2005). "Bioavailability and bioefficacy of polyphenols in humans. I. Review of 97 bioavailability studies." Am J Clin Nutr **81**(1 Suppl): 230S-242S.

Matheny, H. E., T. L. Deem and J. M. Cook-Mills (2000). "Lymphocyte migration through monolayers of endothelial cell lines involves VCAM-1 signaling via endothelial cell NADPH oxidase." Journal of immunology **164**(12): 6550-6559.

May, L. T. and P. B. Sehgal (1992). "Phosphorylation of interleukin-6 at serine54: An early event in the secretory pathway in human fibroblasts." Biochemical and Biophysical Research Communications **185**(2): 524-530.

Mazière, C. and J.-C. Mazière (2009). "Activation of transcription factors and gene expression by oxidized low-density lipoprotein." Free Radical Biology and Medicine **46**(2): 127-137.

McCullough, M. L., J. J. Peterson, R. Patel, P. F. Jacques, R. Shah and J. T. Dwyer (2012). "Flavonoid intake and cardiovascular disease mortality in a prospective cohort of US adults." The American Journal of Clinical Nutrition **95**(2): 454-464.

McGhie, T. K. and M. C. Walton (2007). "The bioavailability and absorption of anthocyanins: towards a better understanding." Mol Nutr Food Res **51**(6): 702-713.

Michel, T. and P.M.Vanhoutte (2010). "Cellular signaling and NO production." Pflugers Arch **459**(6): 807-816.

Milbury, P. E., G. Cao, R. L. Prior and J. Blumberg (2002). "Bioavailablility of elderberry anthocyanins." Mechanisms of Ageing and Development **123**(8): 997-1006.

Milbury, P. E., J. A. Vita and J. B. Blumberg (2010). "Anthocyanins are Bioavailable in Humans following an Acute Dose of Cranberry Juice." The Journal of Nutrition **140**(6): 1099-1104.

Min, S.-W., S.-N. Ryu and D.-H. Kim (2010). "Anti-inflammatory effects of black rice, cyanidin-3-O-β-d-glycoside, and its metabolites, cyanidin and protocatechuic acid." International Immunopharmacology **10**(8): 959-966.

Mink, P. J., C. G. Scrafford, L. M. Barraj, L. Harnack, C. P. Hong, J. A. Nettleton and D. R. Jacobs, Jr. (2007). "Flavonoid intake and cardiovascular disease mortality: a prospective study in postmenopausal women." Am J Clin Nutr **85**(3): 895-909.

Mitra, S., T. Goyal and J. L. Mehta (2011). "Oxidized LDL, LOX-1 and atherosclerosis." Cardiovascular drugs and therapy **25**(5): 419-429.

Miyazaki, K., K. Makino, E. Iwadate, Y. Deguchi and F. Ishikawa (2008). "Anthocyanins from purple sweet potato Ipomoea batatas cultivar Ayamurasaki suppress the development of atherosclerotic lesions and both enhancements of oxidative stress and soluble vascular cell adhesion molecule-1 in apolipoprotein E-deficient mice." Journal of Agricultural and Food Chemistry **56**(23): 11485-11492.

Morawietz, H. (2007). "LOX-1 and Atherosclerosis: Proof of Concept in LOX-1–Knockout Mice." Circulation Research **100**(11): 1534-1536.

Mraiche, F., J. Cena, D. Das and B. Vollrath (2005). "Effects of statins on vascular function of endothelin-1." British Journal of Pharmacology **144**(5): 715-726.

Naseem, K. M. (2005). "The role of nitric oxide in cardiovascular diseases." Mol Aspects Med **26**(1-2): 33-65.

Nelson, G., L. Paraoan, D. G. Spiller, G. J. Wilde, M. A. Browne, P. K. Djali, J. F. Unitt, E. Sullivan, E. Floettmann and M. R. White (2002). "Multi-parameter analysis of the kinetics of NF-kappaB signalling and transcription in single living cells." Journal of cell science **115**(Pt 6): 1137-1148.

Nishi, N., S. Nanto, S. Shimai, Y. Matsushima, K. Otake, A. Ando, K. Yamasaki, S. Soga and K. Tatara (2001). "Effects of hostility and lifestyle on coronary heart disease among middle-aged urban Japanese." J Epidemiol **11**(6): 243-248.

Nizamutdinova, I. T., Y. M. Kim, J. I. Chung, S. C. Shin, Y.-K. Jeong, H. G. Seo, J. H. Lee, K. C. Chang and H. J. Kim (2009). "Anthocyanins from Black Soybean Seed Coats Preferentially Inhibit TNF-α-Mediated Induction of VCAM-1 over ICAM-1 through the Regulation of GATAs and IRF-1." Journal of Agricultural and Food Chemistry **57**(16): 7324-7330.

Paixao, J., T. C. Dinis and L. M. Almeida (2012). "Malvidin-3-glucoside protects endothelial cells up-regulating endothelial NO synthase and inhibiting peroxynitrite-induced NF-kB activation." Chemico-biological interactions **199**(3): 192-200.

Pamukcu, B., G. Y. Lip, V. Snezhitskiy and E. Shantsila (2011). "The CD40-CD40L system in cardiovascular disease." Ann Med **43**(5): 331-340.

Preiss, D. J. and N. Sattar (2007). "Vascular cell adhesion molecule-1: a viable therapeutic target for atherosclerosis?" International Journal of Clinical Practice **61**(4): 697-701.

Romero, M., R. Jiménez, M. Sánchez, R. López-Sepúlveda, M. J. Zarzuelo, F. O'Valle, A. Zarzuelo, F. Pérez-Vizcaíno and J. Duarte (2009). "Quercetin inhibits vascular superoxide production induced by endothelin-1: Role of NADPH oxidase, uncoupled eNOS and PKC." Atherosclerosis **202**(1): 58-67.

Ross, R. (1999). "Atherosclerosis--an inflammatory disease." N Engl J Med **340**(2): 115-126.

Russell, W. R., L. Scobbie, A. Labat and G. G. Duthie (2009). "Selective bio-availability of phenolic acids from Scottish strawberries." Mol Nutr Food Res **53 Suppl 1**: S85-91.

Sánchez, M., M. Galisteo, R. Vera, I. C. Villar, A. Zarzuelo, J. Tamargo, F. Pérez-Vizcaíno and J. Duarte (2006). "Quercetin downregulates NADPH oxidase, increases eNOS activity and prevents endothelial dysfunction in spontaneously hypertensive rats." Journal of Hypertension **24**(1): 75-84.

Santhanam, U., J. Ghrayeb, P. B. Sehgal and L. T. May (1989). "Post-translational modifications of human interleukin-6." Archives of Biochemistry and Biophysics **274**(1): 161-170.

Saremi, A., R. J. Anderson, P. Luo, T. E. Moritz, D. C. Schwenke, M. Allison and P. D. Reaven (2009). "Association between IL-6 and the extent of coronary atherosclerosis in the veterans affairs diabetes trial (VADT)." Atherosclerosis **203**(2): 610-614.

Schmittgen, T. D. and K. J. Livak (2008). "Analyzing real-time PCR data by the comparative C(T) method." Nature protocols **3**(6): 1101-1108.

Schuett, H., M. Luchtefeld, C. Grothusen, K. Grote and B. Schieffer (2009). "How much is too much? Interleukin-6 and its signalling in atherosclerosis." Thrombosis and Haemostasis **102**(8): 215-222.

Seeram, N. P., L. D. Bourquin and M. G. Nair (2001). "Degradation products of cyanidin glycosides from tart cherries and their bioactivities." J Agric Food Chem **49**(10): 4924-4929.

Segal, A. W. (2006). "How superoxide production by neutrophil leukocytes kills microbes." Novartis Foundation symposium **279**: 92-98; discussion 98-100, 216-109.

Siomek, A. (2012). "NF-kappaB signaling pathway and free radical impact." Acta biochimica Polonica **59**(3): 323-331.

Sohn, H. Y., U. Raff, A. Hoffmann, T. Gloe, K. Heermeier, J. Galle and U. Pohl (2000). "Differential role of angiotensin II receptor subtypes on endothelial superoxide formation." Br J Pharmacol **131**(4): 667-672.

Song, L. and C. Schindler (2004). "IL-6 and the acute phase response in murine atherosclerosis." Atherosclerosis **177**(1): 43-51.

Steffen, Y., C. Gruber, T. Schewe and H. Sies (2008). "Mono-O-methylated flavanols and other flavonoids as inhibitors of endothelial NADPH oxidase." Arch Biochem Biophys **469**(2): 209-219.

Steffen, Y., T. Schewe and H. Sies (2007b). "(-)-Epicatechin elevates nitric oxide in endothelial cells via inhibition of NADPH oxidase." Biochem Biophys Res Commun **359**(3): 828-833.

Stielow, C., R. A. Catar, G. Muller, K. Wingler, P. Scheurer, H. H. Schmidt and H. Morawietz (2006). "Novel Nox inhibitor of oxLDL-induced reactive oxygen species formation in human endothelial cells." Biochemical and Biophysical Research Communications **344**(1): 200-205.

ten Freyhaus, H., M. Huntgeburth, K. Wingler, J. Schnitker, A. T. Bäumer, M. Vantler, M. M. Bekhite, M. Wartenberg, H. Sauer and S. Rosenkranz (2006). "Novel Nox inhibitor VAS2870 attenuates PDGF-dependent smooth muscle cell chemotaxis, but not proliferation." Cardiovascular Research **71**(2): 331-341.

Terasaka, Y., D. Miyazaki, K. Yakura, T. Haruki and Y. Inoue (2010). "Induction of IL-6 in Transcriptional Networks in Corneal Epithelial Cells after Herpes Simplex Virus Type 1 Infection." Investigative Ophthalmology & Visual Science **51**(5): 2441-2449.

Theoharides, T. C., M. Alexandrakis, D. Kempuraj and M. Lytinas (2001). "Anti-inflammatory actions of flavonoids and structural requirements for new design." International journal of immunopathology and pharmacology **14**(3): 119-127.

Van Snick, J. (1990). "Interleukin-6: an overview." Annual review of immunology **8**: 253-278.

Vandesompele, J., K. De Preter, F. Pattyn, B. Poppe, N. Van Roy, A. De Paepe and F. Speleman (2002). "Accurate normalization of real-time quantitative RT-PCR data by geometric averaging of multiple internal control genes." Genome biology **3**(7): RESEARCH0034.

Versari, D., E. Daghini, A. Virdis, L. Ghiadoni and S. Taddei (2009). "Endothelial dysfunction as a target for prevention of cardiovascular disease." Diabetes Care **32 Suppl 2**: S314-321.

Videm, V. and M. Albrigtsen (2008). "Soluble ICAM-1 and VCAM-1 as Markers of Endothelial Activation." Scandinavian Journal of Immunology **67**(5): 523-531.

Vitaglione, P., G. Donnarumma, A. Napolitano, F. Galvano, A. Gallo, L. Scalfi and V. Fogliano (2007). "Protocatechuic acid is the major human metabolite of cyanidin-glucosides." J Nutr **137**(9): 2043-2048.

Wahyudi, S. and D. Sargowo (2007). "Green tea polyphenols inhibit oxidized LDL-induced NF-KB activation in human umbilical vein endothelial cells." Acta medica Indonesiana **39**(2): 66-70.

Wallace, T. (2011). "Anthocyanins in Cardiovascular Disease." Advances in Nutrition **2**(1): 1-7.

Wang, D., X. Wei, X. Yan, T. Jin and W. Ling (2010). "Protocatechuic acid, a metabolite of anthocyanins, inhibits monocyte adhesion and reduces atherosclerosis in apolipoprotein E-deficient mice." J Agric Food Chem **58**(24): 12722-12728.

Wang, H. (1997). "Oxygen Radical Absorbing Capacity of Anthocyanins." J Agric Food Chem **45**(1): 304-309.

Wang, Y. and C. T. Ho (2009). "Metabolism of flavonoids." Forum Nutr **61**: 64-74.

Wei, M., X. Chu, M. Guan, X. Yang, X. xie, F. Liu, C. Chen and X. Deng (2013). "Protocatechuic acid suppresses ovalbumin-induced airway inflammation in a mouse allergic asthma model." International Immunopharmacology **15**(4): 780-788.

WHO (2011). "WHO Fact sheet."

Williamson, G. and M. N. Clifford (2010). "Colonic metabolites of berry polyphenols: the missing link to biological activity?" Br J Nutr **104 Suppl 3**: S48-66.

Xia, M., W. Ling, H. Zhu, J. Ma, Q. Wang, M. Hou, Z. Tang, H. Guo, C. Liu and Q. Ye (2009). "Anthocyanin attenuates CD40-mediated endothelial cell activation and apoptosis by inhibiting CD40-induced MAPK activation." Atherosclerosis **202**(1): 41-47.

Xia, M., W. Ling, H. Zhu, Q. Wang, J. Ma, M. Hou, Z. Tang, L. Li and Q. Ye (2007). "Anthocyanin Prevents CD40-Activated Proinflammatory Signaling in Endothelial Cells by Regulating Cholesterol Distribution." Arteriosclerosis, Thrombosis, and Vascular Biology **27**(3): 519-524.

Xie, C., J. Kang, M. E. Ferguson, S. Nagarajan, T. M. Badger and X. Wu (2011). "Blueberries reduce pro-inflammatory cytokine TNF-alpha and IL-6 production in mouse macrophages by inhibiting NF-kappaB activation and the MAPK pathway." Molecular Nutrition & Food Research **55**(10): 1587-1591.

Xu, J.-W., K. Ikeda and Y. Yamori (2004b). "Cyanidin-3-glucoside regulates phosphorylation of endothelial nitric oxide synthase." FEBS Letters **574**(1-3): 176-180.

Xu, J. W., K. Ikeda and Y. Yamori (2004a). "Upregulation of endothelial nitric oxide synthase by cyanidin-3-glucoside, a typical anthocyanin pigment." Hypertension **44**(2): 217-222.

Yang, Z. and J. C. Li (2008). "Stimulation of endothelin-1 gene expression by insulin via phosphoinositide-3 kinase-glycogen synthase kinase-3beta signaling in endothelial cells." Life Sciences **82**(9-10): 512-518.

Yi, L., C.-y. Chen, X. Jin, M.-t. Mi, B. Yu, H. Chang, W.-h. Ling and T. Zhang (2010). "Structural requirements of anthocyanins in relation to inhibition of endothelial injury induced by oxidized low-density lipoprotein and correlation with radical scavenging activity." FEBS Letters **584**(3): 583-590.

Yudkin, J. S., M. Kumari, S. E. Humphries and V. Mohamed-Ali (2000). "Inflammation, obesity, stress and coronary heart disease: is interleukin-6 the link?" Atherosclerosis **148**(2): 209-214.

Zamora-Ros, R., C. Andres-Lacueva, R. M. Lamuela-Raventos, T. Berenguer, P. Jakszyn, A. Barricarte, E. Ardanaz, P. Amiano, M. Dorronsoro, N. Larranaga, C. Martinez, M. J. Sanchez, C. Navarro, M. D. Chirlaque, M. J. Tormo, J. R. Quiros and C. A. Gonzalez (2010). "Estimation of dietary sources and flavonoid intake in a Spanish adult population (EPIC-Spain)." J Am Diet Assoc **110**(3): 390-398.

Zamora-Ros, R., V. Knaze, L. Lujan-Barroso, N. Slimani, I. Romieu, M. Touillaud, R. Kaaks, B. Teucher, A. Mattiello, S. Grioni, F. Crowe, H. Boeing, J. Forster, J. R. Quiros, E. Molina, J. M. Huerta, D. Engeset, G. Skeie, A. Trichopoulou, V. Dilis, K. Tsiotas, P. H. Peeters, K. T. Khaw, N. Wareham, B. Bueno-de-Mesquita, M. C. Ocke, A. Olsen, A. Tjonneland, R. Tumino, G. Johansson, I. Johansson, E. Ardanaz, C. Sacerdote, E. Sonestedt, U. Ericson, F. Clavel-Chapelon, M. C. Boutron-Ruault, G. Fagherazzi, S. Salvini, P. Amiano, E. Riboli and C. A. Gonzalez (2011). "Estimation of the intake of anthocyanidins and their food sources in the European Prospective Investigation into Cancer and Nutrition (EPIC) study." Br J Nutr **106**(7): 1090-1099.

Zhang, Q., N. P. Botting and C. Kay (2011). "A gram scale synthesis of a multi-13C-labelled anthocyanin, [6,8,10,3',5'-13C5]cyanidin-3-glucoside, for use in oral tracer studies in humans." Chem Commun (Camb) **47**(38): 10596-10598.

Zhang, Q., K. S. Raheem, N. P. Botting, A. M. Z. Slawin, C. D. Kay and D. O'Hagan (2012). "Flavonoid metabolism: the synthesis of phenolic glucuronides and sulfates as candidate metabolites for bioactivity studies of dietary flavonoids." Tetrahedron **68**(22): 4194-4201.

Zheng, S., Z. Qian, F. Tang and L. Sheng (2005). "Suppression of vascular cell adhesion molecule-1 expression by crocetin contributes to attenuation of atherosclerosis in hypercholesterolemic rabbits." Biochemical Pharmacology **70**(8): 1192-1199.

Zheng, W. and S. Y. Wang (2003). "Oxygen radical absorbing capacity of phenolics in blueberries, cranberries, chokeberries, and lingonberries." J Agric Food Chem **51**(2): 502-509.

Zhu, Y., W. Ling, H. Guo, F. Song, Q. Ye, T. Zou, D. Li, Y. Zhang, G. Li, Y. Xiao, F. Liu, Z. Li, Z. Shi and Y. Yang (2013). "Anti-inflammatory effect of purified dietary anthocyanin in adults with hypercholesterolemia: A randomized controlled trial." Nutrition, Metabolism and Cardiovascular Diseases **23**(9): 843-849.

Zhu, Y., M. Xia, Y. Yang, F. Liu, Z. Li, Y. Hao, M. Mi, T. Jin and W. Ling (2011). "Purified Anthocyanin Supplementation Improves Endothelial Function via NO-cGMP Activation in Hypercholesterolemic Individuals." Clin Chem: clinchem.2011.167361.

Ziberna, L., M. Lunder, F. Tramer, G. Drevenšek and S. Passamonti (2010). "The endothelial plasma membrane transporter bilitranslocase mediates rat aortic vasodilation induced by anthocyanins." Nutrition, Metabolism and Cardiovascular Diseases **23**(1): 68-74.

Appendix

1. Cell viability of HUVECs in presence of C3G and 11 of its metabolites (cytotoxicity data)

Compound	Concentration	% of absorbance Mean±SD
Vehicle Control	0.05% DMSO	100.0±2.7
Negative control	1% PBS	2.6±7.2
C3G	0.05 µM	101.6±3.7
	1 µM	100.3±2.3
	10 µM	100.9±3.5
	100 µM	99.8±3.9
PCA	0.05 µM	100.6±5.6
	1 µM	97.2±2.0
	10 µM	100.0±4.8
	100 µM	96.2±4.8
PGA	0.05 µM	102.2±3.1
	1 µM	100.6±4.5
	10 µM	98.7±1.2
	100 µM	100.6±4.1
VA	0.05 µM	101.5±3.7
	1 µM	101.2±2.6
	10 µM	101.2±1.0
	100 µM	105.0±2.5
IVA	0.05 µM	102.8±2.9
	1 µM	104.1±2.4
	10 µM	102.2±0.5
	100 µM	100.7±0.9
PCA-4-gluc	0.05 µM	101.8±2.9
	1 µM	99.5±3.7
	10 µM	104.8±6.5
	100 µM	105.1±1.1
PCA-3-gluc	0.05 µM	100.4±5.3
	1 µM	103.7±4.2
	10 µM	97.4±0.7
	100 µM	99.1±2.4
PCA-4-sulfate	0.05 µM	105.8±5.3
	1 µM	95.3±4.1
	10 µM	103.9±4.7
	100 µM	100.0±5.5
PCA-3-sulfate	0.05 µM	101.7±1.7
	1 µM	98.8±3.2
	10 µM	101.5±2.4
	100 µM	100.1±0.8
VA-4-Sulf	0.05 µM	94.5±6.2
	1 µM	98.8±2.1
	10 µM	100.0±2.2
	100 µM	100.2±2.7
IVA-3-Sulf	0.05 µM	101.4±3.9
	1 µM	100.9±4.3
	10 µM	105.9±2.1
	100 µM	102.2±1.1
FA	0.05 µM	100.7±4.4
	1 µM	104.3±5.7
	10 µM	102.7±3.3
	100 µM	100.7±0.9

HUVECs incubated with C3G or phenolic metabolites for 24 hours at 0.1, 1, 10 and 100 µM followed by incubation with WST reagent for 2 hrs. Viable cells convert WST reagent in to yellow dye which was measured at 440 nm. All data expressed as mean percentage (± SD, n=3) absorbance (440 nm) of vehicle control (0.05% DMSO treated HUVECs) *p≤0.05 (ANOVA with Tukey post-hoc) relative to vehicle control. C3G, cyanidin-3-glucoside; PCA, protocatechuic acid, PGA, phloroglucinaldehyde; FA, ferulic acid; VA, vanillic acid; IVA, isovanillic acid; PCA-4-Gluc, PCA-4-glucuronide; PCA-3-Gluc, PCA-3-glucuronide; PCA-4-Sulf, PCA-4-sulfate; PCA-3-Sulf, PCA-3-sulfate; VA-4-Sulf, VA-4-sulfate; IVA-3-Sulf, IVA-3-sulfate

2. Representative Standard Curve for eNOS ELISA

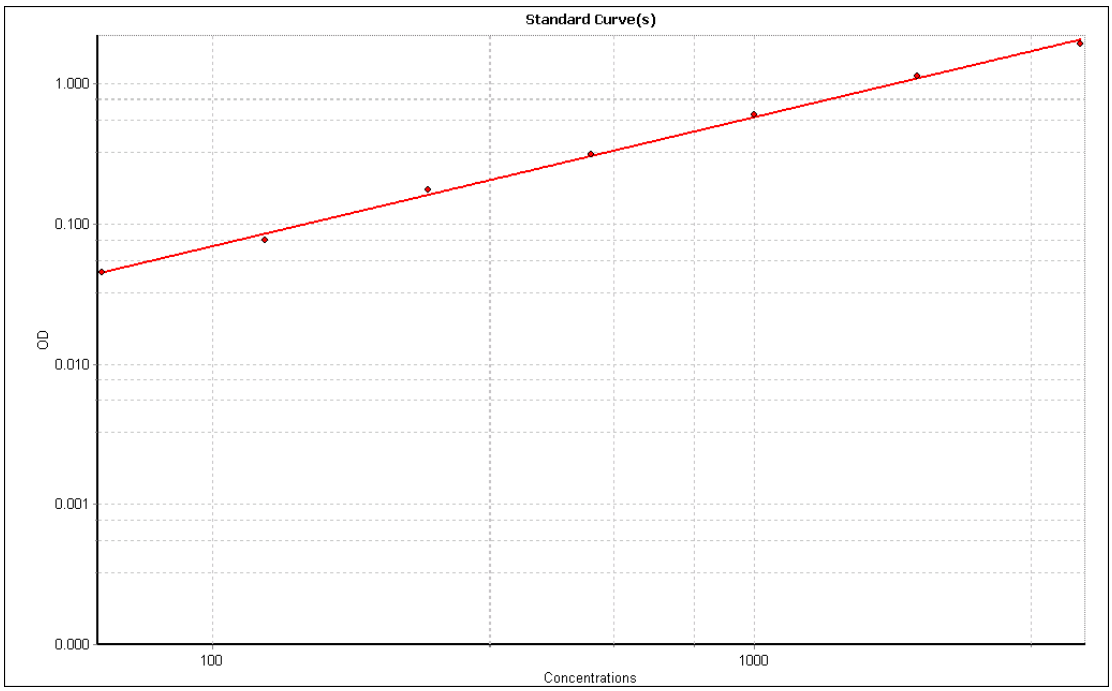

ELISA plate contained recombinant eNOS standards (in duplicate) serial diluted in reagent diluent ranging from 4000pg/mL – 62.5pg/mL and reagent diluent (in duplicate) as blank

3. Representative Standard Curve for ET-1 ELISA

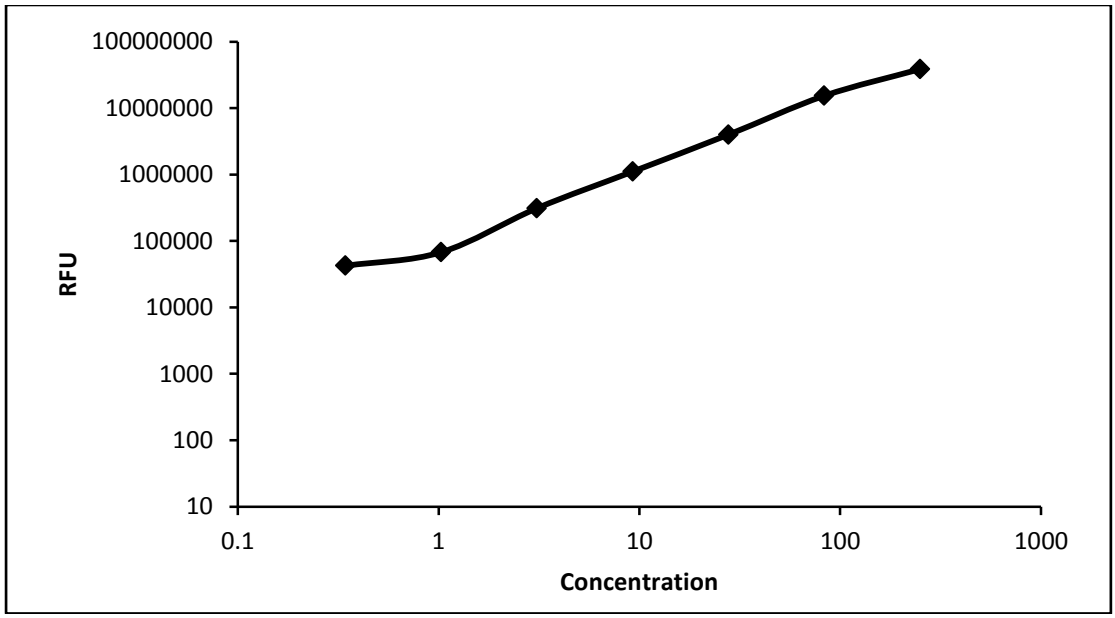

ELISA plate contained recombinant ET-1 standards (in duplicate) serial diluted in reagent diluent ranging from 250pg/mL – 0.33pg/mL and reagent diluent (in duplicate) as blank

4. Confirmation of LDL oxidation using agarose gel

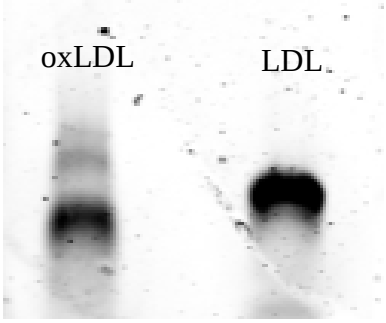

LDL was oxidised using Cu_2SO_4at least 30 hrs. Agarose gel was then ran to confirm the oxidation of LDL.The shift in oxLDL band below the native LDL confirms the oxidation of LDL. The gel was imaged using Odyssey at 700 nm, with a ratio of $R_{oxLD}L:R_{LDL}$ of>1.1.

5. Representative Standard Curves of VCAM-1 ELISA

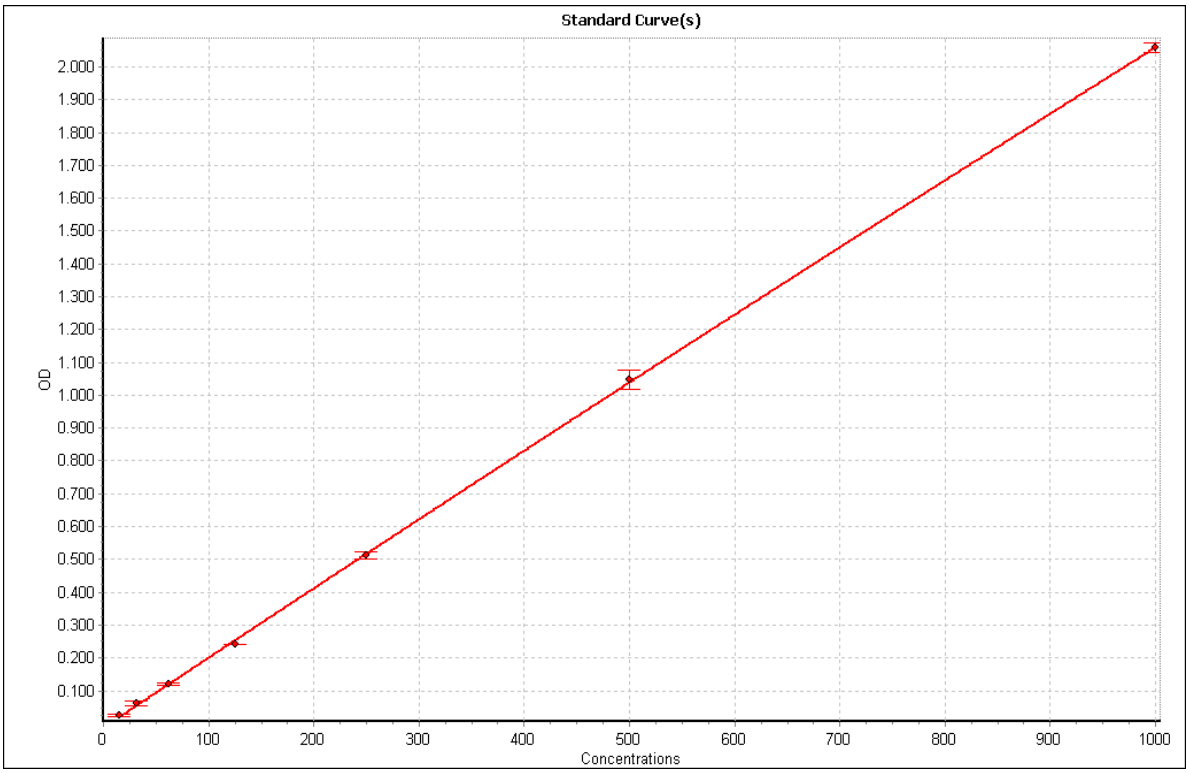

ELISA plate contained recombinant VCAM-1 standards (in duplicate) serial diluted in reagent diluent ranging from 1000 pg/mL – 15.625 pg/mL and reagent diluent (in duplicate) as blank

6. Representative Standard Curves of IL-6 ELISA

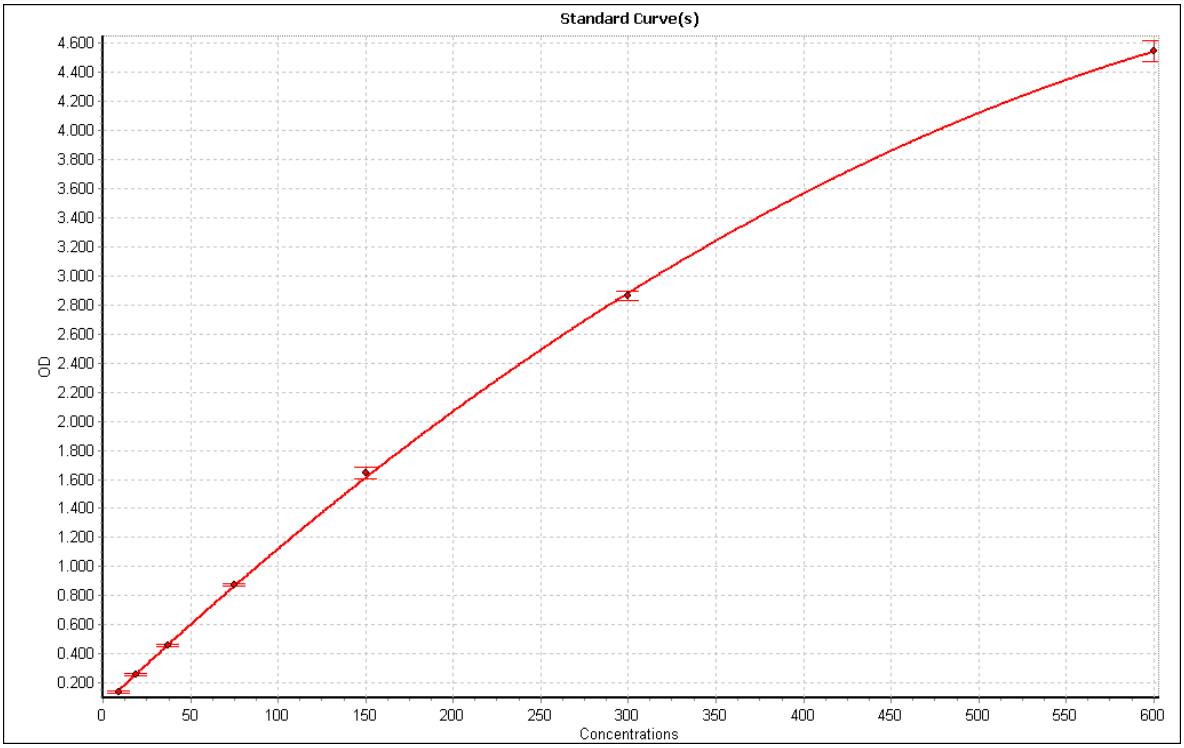

ELISA plate contained recombinant IL-6 standards (in duplicate) serial diluted in reagent diluent ranging from 600pg/mL – 9.375pg/mL and reagent diluent (in duplicate) as blank

7. Gating Strategy for phospho-p65 NF-κB flow cytometry assay